Thesis

Role of oxidative stress and calcium regulation in Duchenne muscular dystrophy: pharmacological investigations

ISMAIL, Hesham

Abstract

Duchenne Muscular Dystrophy (DMD) is the most common and most severe myopathy. Currently, no cure exists for DMD and novel pharmacotherapy holds the promise of being the fastest route for reaching the patients until a curative genetic therapy is delivered. Towards this end, three drug candidates were evaluated in DMD models. The first was doxorubicin which inhibited phospholipase A2 activity and reduced Ca2+ influx through stretch-activated channels, both reported to be overactive in dystrophic cells. Dystrophic muscles treated with doxorubicin were protected from damaging eccentric contractions. We have also tested the classical NADPH oxidase inhibitor apocynin and its synthetic dimer, diapocynin. Our in vitro and in vivo results show that diapocynin holds a superior therapeutic potential. In conclusion, the work presented in this thesis presents novel drug candidates that can be developed further as potential pharmacotherapeutic treatment for DMD. It also sheds light on the pathways involved in DMD pathogenesis.

Reference

ISMAIL, Hesham. *Role of oxidative stress and calcium regulation in Duchenne muscular dystrophy: pharmacological investigations*. Thèse de doctorat : Univ. Genève, 2013, no. Sc. 4607

URN : urn:nbn:ch:unige-321331

UNIVERSITÉ DE GENÈVE
Section de Sciences Pharmaceutiques
Pharmacologie

FACULTÉ DES SCIENCES
Professeur Urs T. Ruegg
Professeur Leonardo Scapozza

Role of oxidative stress and calcium regulation in Duchenne muscular dystrophy: Pharmacological investigations

THÈSE

présentée à la Faculté des sciences de l'Université de Genève
pour obtenir le grade de Docteur ès sciences, mention sciences pharmaceutiques

par

Hesham Mohamed Ismail HAMED

du

Caire (Egypte)

These N°: 4607

Genève

Atelier de reproduction Repromail

2013

UNIVERSITÉ
DE GENÈVE

FACULTÉ DES SCIENCES

Doctorat ès sciences
Mention sciences pharmaceutiques

Thèse de *Monsieur Hesham Mohamed Ismail HAMED*

intitulée :

" Role of oxidative stress and calcium regulation in Duchenne muscular dystrophy: Pharmacological investigations "

La Faculté des sciences, sur le préavis de Messieurs U. RUEGG, professeur honoraire et directeur de thèse (Section des sciences pharmaceutiques), L. SCAPOZZA, professeur ordinaire et co-directeur de thèse (Section des sciences pharmaceutiques), Madame N. SHIROKOVA, professeure (Department of Pharmacology & Physiology, UMDNJ – New Jersey Medical School, Newark, Etats-Unis d'Amérique), Messieurs M. T. KHAYYAL, professeur (Department of Pharmacology, Faculty of Pharmacy, Cairo University, Caire, Egypte), K.-H. KRAUSE, professeur (Département de pathologie et immunologie, Faculté de médecine), G. HOPFGARTNER, professeur (Section des sciences pharmaceutiques), et O. DORCHIES, docteur, (Département de biologie cellulaire, Section de biologie), autorise l'impression de la présente thèse, sans exprimer d'opinion sur les propositions qui y sont énoncées.

Genève, le 25 octobre 2013

Thèse - 4607 -

Le Doyen Jean-Marc TRISCONE

N.B. - La thèse doit porter la déclaration précédente et remplir les conditions énumérées dans les "Informations relatives aux thèses de doctorat à l'Université de Genève".

Acknowledgments

I would like to start my acknowledgments by expressing my sincere gratitude to Professor Urs Ruegg & Leonardo Scapozza as well as Dr. Olivier Dorchies for supervising my work.

Urs, Thank you for giving me the chance to be a part of your lab team and for the joyful atmosphere and discussions we always have. Thank you for giving me much freedom of choosing my topics, trying out new techniques and experiments and for your generosity. I would have had a lot of difficulties supervising a student like me.

Leonardo, I cannot thank you enough for accepting me as a part of your lab after Urs' retirement and for your continuous support without which most of the work in this study would not have been completed. You made me feel as one of your own team. Also thank you for your support and encouragement for my future plans and projects.

Olivier, all these results would not have existed if it was not for your help. Your remarks, pointers, discussions and suggestions redirected my work towards the better continuously. Your encouragement after every progress report I gave was very supportive. Having you in the empty lab after Urs' retirement was really fun.

I would like to thank the jury members, including Professors Natalia Shirokova, Karl Heinz Krause, and Gérard Hopfgartner for accepting to review my thesis and for their time spent in this process.

To the ex-members of the lab of pharmacology, Chiara, Colette, Dominique, George, Julie, Karin, Miriam, Olivier, Ophélie, Piter, Yoshiko and Youssef……you are the best! Thank you for the lovely times we spent together inside the lab and outside. It would not have been the same without you. And a special thank you goes to Dominique who has been my legal advisor, lawyer, translator, facilitator among many others. I would be in a mess if it weren't for you. For all of those in FABIP and the rest of the section, you really created a lovely atmosphere to work in, I enjoyed the coffee breaks , outings and courses and I hope we keep in touch even after all will go their own way.

Prof. Khayyal, I consider you more a family member than my undergraduate professor, my M.S.c. supervisor and a jury member of my PhD thesis. I thank you very much for your support and encouragement at every step of the way and I hope to live up to your expectations even further.

Finally to my family, to my mother, words cannot describe how much I am in debt to you for molding me through the years to be where I am today. Father, you lived up to be my role model, I just hope I will be close to achieving your expectations. My son Yousef whom I was blessed with during the work on this PhD thesis, thank you for finally accepting that my laptop is off limits! And Nesrin, I cannot thank you enough for supporting me not only through the ups and downs, of which there were a lot, during the work on my thesis but also throughout our marriage. Thank you for being who you are, I am truly blessed by you.

Table of Contents

List of figures and tables

Abbreviations

2OMeAO	2'-O-methyl antisense oligonucleotide
AAV	adeno-associated virus
ACh	acetylcholine
CIF	calcium influx factor
CK	creatine kinase
CRAC	Ca^{2+} release activated Ca^{2+} channels
DAPC	dystrophin associated protein complex
DGC	dystrophin glycoprotein complex
DHPR	dihydropyridine receptors
DMD	Duchenne muscular dystrophy
EDL	*extensor digitorum longus*
GsMTx-4	Grammotoxin-4
IP3R	inositol 1,4,5-trisphosphate receptors
$iPLA_2$	calcium independent form of phospholipase A_2
MAPK	mitogen-activated protein kinase
mPTP	mitochondrial permeability transition pore
NCX	Na^{+}-Ca^{2+} exchanger
NOS	nitric oxide synthase
NOX	NADPH oxidase
$O_2^{\bullet-}$	superoxide free radical
PMCA	plasma membrane Ca^{2+}-ATPase
PMO	phosphorodiamidate morpholino oligomers
ROS	reactive oxygen species
RyR	ryanodine channels
SACs	stretch activated channels
SERCA	sarco-endoplasmic reticulum ATPase
SOC	store operated Ca^{2+} channels
SOL	*soleus*
SR	sarcoplasmic reticulum

Author Bibliography

1. **Ismail HM**, Scapozza L, Ruegg UT and Dorchies OM. (2013). Diapocynin, a putative NADPH oxidase inhibitor, ameliorates the phenotype of a mouse model of Duchenne muscular dystrophy. Manuscript in preparation.

2. **Ismail HM**, Scapozza L, Ruegg UT and Dorchies OM. (2013). Diapocynin, a NADPH oxidase inhibitor, reduces ROS production and prevents force loss in eccentrically contracting dystrophic muscle. *PLos one.* In revision.

3. Shapovalov G, Sukhanova I, **Ismail HM**, Petermann O, Ruegg UT and Avdonin PV (2013). Native single-channel Orai1 activity in developing skeletal muscle. *Biophys J.* In revision.

4. **Ismail HM**, Dorchies OM, Perozzo R, Strosova MK, Scapozza L and Ruegg UT (2013). Inhibition of iPLA2$_\beta$ and of stretch-activated channels by doxorubicin alters dystrophic muscle function. *Br. J. Pharmacol.*, **169:** 1537-1550.

5. Dorchies OM, Reutenauer-Patte J, Dahmane E, **Ismail HM**, Petermann O, Patthey-Vuadens O, Comyn SA, Gayi E, Piacenza T, Handa RJ, Décosterd LA, Ruegg UT. (2013). The anticancer drug tamoxifen counteracts the pathology in a mouse model of Duchenne muscular dystrophy. *Am J Pathol.* 182: 485-504.

6. Ruegg UT, Shapovalov G, Jacobson K, Reutenauer-Patte J, **Ismail HM**, Dorchies OM, et al. (2012). Store-operated channels and Ca^{2+} handling in muscular dystrophy. *In: Store-operated Ca^{2+} entry (SOCE) pathways*, Groschner K, Graier WF, Romanin C (eds.) Vol. 1, 1st edn., pp. 449-457: Springer Verlag, Vienna.

Summary

Duchenne Muscular Dystrophy (DMD) is the most common and most severe myopathy. The disease affects 1 in 3500 male births and results in progressive muscle degradation affecting skeletal, respiratory and, finally cardiac muscles. Currently, no cure exists for DMD and hope remains highly dependent on the scientific advancement in the fields of gene and cell therapies. Pharmacotherapy holds the promise of being the fastest route for reaching the patients with the aim of ameliorating the devastating pathology and to fill the gap until a curative therapy is delivered. Deepened scientific understanding of the pathogenesis is needed to develop drugs that can adequately target relevant contributors in this disease. The current work aimed at addressing these issues by investigating already approved drugs or delivering novel therapies for DMD.

The first drug evaluated was doxorubicin. A series of publications established that doxorubicin is a potent inhibitor of the calcium-independent phospholipase A_2 ($iPLA_2$) in cardiomyocytes when it was administered either acutely or chronically in clinically relevant concentrations. This enzyme is of known contribution to DMD and is reported to mediate enhanced calcium influx in dystrophic muscle, causing its eventual death. Treating dystrophic myotubes with doxorubicin resulted in a concentration-dependent inhibition of $iPLA_2$ with a concomitant bimodal effect on reactive oxygen species (ROS) production. Doxorubicin also potently reduced Ca^{2+} influx through stretch-activated channels. This was the first report of such an effect of doxorubicin and can partly explain the cardiomyopathy seen by doxorubicin treatment. Furthermore, it also reduced Ca^{2+} uptake into the subsrcolemmal space and into the mitochondria when exposed to a hypo-osmotic shock. Dystrophic muscles treated with doxorubicin were protected from damaging eccentric contractions, to which they are normally highly sensitive. We speculated that part of the doxorubicin action is mediated by its ability to undergo redox cycling on flavo-enzymes and to modulate NADPH oxidase (NOXes) activities.

The two other drug candidates examined were the classical NOX inhibitor apocynin and its dimer, diapocynin, which was prepared synthetically. Treating dystrophic myotubes with apocynin resulted in a 6-fold increase in ROS production rather than inhibition. Diapocynin is an oxidative coupling product of apocynin, which is formed in activated immune cells and is reported to be the NOX inhibitory moiety. Administration of diapocynin to dystrophic cells resulted in an inhibition of ROS production, of $iPLA_2$ activity and of Ca^{2+} influx. In the presence of diapocynin, but not apocynin,

dystrophic muscles were more resistant to eccentric contractions and their sarcolemmal integrity was improved.

When given to dystrophic mice, both apocynin as well as diapocynin showed a protective effect; this was probably due to NOX inhibition. Diapocynin improved wheel-running capability and spontaneous locomotor activity and reached levels of non-dystrophic mice. Both treatments resulted in improved resistance to fatigue, prevention of membrane damage and improved diaphragm structure. Diapocynin has a superior pharmacokinetic profile because of its higher lipophilicity and efficacy compared to apocynin and should be considered for further development.

In conclusion, the work presented in this thesis presents novel drug candidates that can be developed further as potential pharmacotherapeutic treatment for DMD. It also sheds light on the pathways involved in DMD pathogenesis.

Résumé

La Dystrophie Musculaire de Duchenne (DMD) est parmi les plus graves et les plus fréquentes des maladies génétiques lié au chromosome X. La maladie touche 1 garçon sur 3500 naissances et se traduit par la dégradation progressive des muscles squelettiques, respiratoires et enfin cardiaque. Actuellement, il n'existe aucun remède pour la DMD et l'espoir reste très dépendant des avancées scientifiques dans le domaine de la thérapie génétique et cellulaire. La pharmacothérapie, plus rapide à mettre en œuvre, pourrait permettrede soulager les patients d'une pathologie dévastratrice en attendant qu'un traitement curatif soit developpé. Une meilleure compréhension de la pathogenèse est nécessaire pour développer des médicaments qui peuvent cibler adéquatement les acteurs spécifiques de cette maladie. Cette thèse vise à répondre à ces questions en redirigeant des médicaments déjà approuvés ou en évaluant de nouvelles pistes thérapeutiques pour la DMD.

Le premier médicament évalué dans cette étude est la doxorubicine. Une série de publications a établi que la doxorubicine est un puissant inhibiteur de la phospholipase A_2 indépendante du calcium ($iPLA_2$) dans les cellules cardiaques lorsqu'il est administré de façon aiguë ou chronique à des concentrations cliniquement pertinentes. L'enzyme $iPLA_2$ est connue de contribuer à la pathogenèse de la DMD et stimule l'influx excessif de calcium dans les cellules dystrophiques, favorisant ainsi leur mort. Un traitement des myotubes dystrophiques avec la doxorubicine a entraîné une inhibition concentration-dépendante de la $iPLA_2$ avec un effet bimodal concomitant sur la production des espèces réactives de l'oxygène (ROS). Il a également réduit puissamment l'influx de Ca^{2+} au travers des canaux activés par l'étirement. Avec ce travail, nous avons été les premiers à rapporter un tel effet avec la doxorubicine, qui pourrait expliquer, en partie, la toxicité cardiaque bien connue de cette molécule. La doxorubicine a également réduit l'entrée de Ca^{2+} dans les mitochondries après un choc hypo-osmotique. Les muscles dystrophiques traité avec la doxorubicine étaient protégés des dommages causés par des contractions excentriques auxquels ils sont normalement très sensibles. Ces résultats nous ont amené à penser qu'une partie de l'action de la doxorubicine est dépendante de sa capacité à subir un cycle redox sur des flavo-enzymes et de moduler l'activité des NADPH oxydases (NOX).

Les deux autres substances examinées ont été l'inhibiteur classique des NOX, l'apocynine, et son dimère synthétique, la diapocynine. Les myotubes dystrophiques traité avec apocynine ont subi une augmentation de 6 fois de la production de ROS plutôt que l'inhibition attendue.

La diapocynine est un dimère d'apocynine produit par couplage oxydatif dans les cellules immunitaires activées. Actuellement, on pense que la diapocynine, et non l'apocynine est le véritable inhibiteur des NOX. L'administration de diapocynine aux cellules dystrophiques a entraîné une inhibition de la production de ROS, de l'activité $iPLA_2$ et de l'influx de Ca^{2+}. En présence de la diapocynine mais pas d'apocynine, les muscles dystrophiques étaient plus résistants à des contractions excentriques et l'intégrité de leur sarcolemme s'est vue améliorée.

L'évaluation de l'apocynine et de la diapocynine *in vivo* chez des souris dystrophiques, modèles de la DMD, a révélé un effet protecteur. Le traitement par la diapocynine a complètement normalisé l'utilisation de roues d'activité et le déficit d'activité locomotrice spontanée que présentent les souris dystrophiques par rapport aux souris saines. Les deux traitements ont permis d'augmenter la résistance à la fatigue, de prévenir les dommages subis par la membrane, et d'améliorer la structure du diaphragme. Nous pensons que l'efficacité pharmacologique supérieure de la diapocynine par rapport à apocynine est liée sa plus grande lipophilicité et que le développement clinique de la diapocynine pour la DMD mérite d'être considéré.

En conclusion, le travail présenté dans cette thèse met en lumière certains mécanismes impliquées dans la pathogenèse de la DMD et traite de nouveaux candidats-médicaments qui présentent un potentiel pharmaco-thérapeutique pour la DMD.

Chapter 1: Introduction

Introduction

1.1 Skeletal Muscle

In mammals, three types of muscle exist: smooth, cardiac and skeletal muscles. They differ in their roles and organization but the major difference between skeletal muscles and the other two is the presence of a motor unit. Skeletal muscles are controlled by the central nervous system to assure maintenance and change of posture, locomotion and facial expressions.

1.1.1 Skeletal muscle organization and structure

Skeletal muscle structure is organized in a hierarchical manner, with the *whole muscle* being made up of *muscle fascicles*, which, in turn, are made up of *muscle fibres* (the elementary unit of muscle). Each muscle fibre is a single multi-nucleated cell. *Myofibrils* run longitudinally and in parallel spanning the length of the fibre; these structures have the ability to shorten, thereby causing a contraction of the muscle fibre. Each myofibril contains a regular arrangement of repeating units called *sarcomeres,* the basic contractile units of a muscle fibre, which in turn contain inter-digitating thick and thin myofilaments that produce a transverse banding ('striated') pattern, distinguishable by light microscopy. The thick myofilament is comprised predominately of the key contractile protein, myosin (the molecular motor in muscle contraction), the thin myofilament is made up of another key contractile protein, actin, and the Ca^{2+} regulatory proteins, troponin and tropomyosin (Gordon *et al.*, 2000; Schiaffino & Reggiani, 1996).

Together, myosin and actin produce movement by contraction through the sliding filament model (see section 1.1.2.1). In skeletal muscles, striations are readily observable by light microscopy as alternating light and dark bands on longitudinal sections. The light band (known as the I-band) is made up of thin filaments, whereas the dark band (known as the A-band) is made up of thick filaments. The M-line (the middle disc) bisects the A-band and the Z-line defines the lateral boundary of each sarcomeric unit. When contraction of the sarcomere occurs, the Z-lines move closer together, marking the contraction of the myofibrils. Protein assemblies known as costameres are located on the peripheral myofibrils of the myofibre, lining up with the Z-disk. Costameres physically link the sarcomeres, which produce force through contraction, with the sarcolemma and are proposed to transmit this force across the sarcolemma to the extracellular matrix and to neighbouring muscle cells.

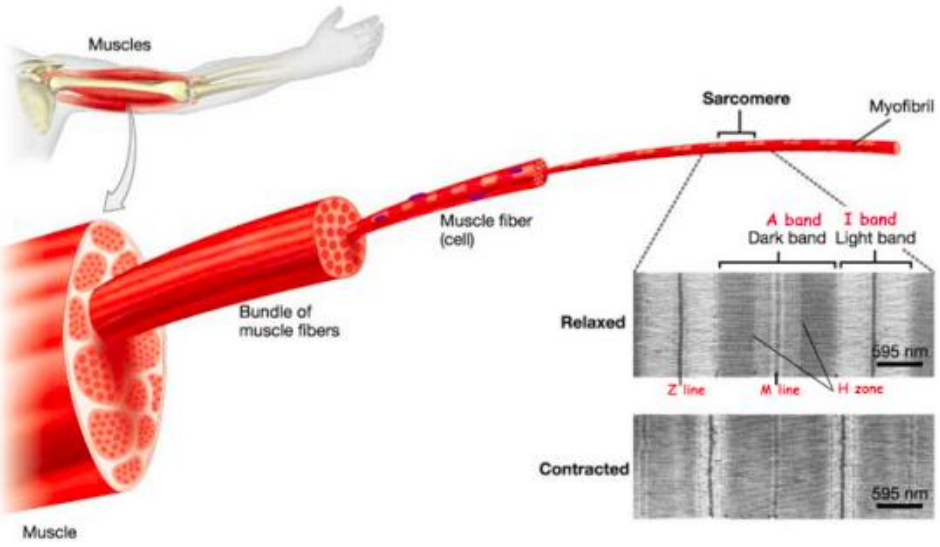

Figure 1-1, Structure of skeletal muscle

A muscle consists of bundled multinucleated muscle cells (fibres). Each fibre is constituted by myofibrils. Each myofibril is made of thick (myosin) and thin (actin) filaments aligned in contractile units called sarcomeres. This typical arrangement of myofibrils appears as alternating light and dark bands the microscope.

Skeletal muscles are classified according to structural and functional features into three main groups of fibre types: the slow-twitch fibres (type I) and the fast-twitch fibres (type IIA and IIB). Their main characteristics are summarized in table below 1.1 (Ruegg, 1992). In humans, there is no pure fast or slow muscle; the relative proportion of each fibre type determines its characteristics, while in other mammals such as mice the *soleus* (Sol) is an example of a slow twitch muscle while the *extensor digitorum longus* (EDL) is an example of a fast twitch muscle composed of 70% type 2 fibres, both of which were used in this study.

Table 1-1, Fibre types and their characteristics

(from Ruegg, 1992)

	Type I (red) SLOW-TWITCH *Ex.: soleus*	**Type II A (red) FAST-TWITCH** *Ex.: quadriceps*	**Type II B (white) FAST-TWITCH** *Ex.: EDL*
Myoglobin content	high	high	low
Contraction speed	low	high	high
Myosin ATPase activity	low	high	high
Myosin isoenzyme	slow	fast	fast
SR Ca^{2+} pumping capacity	moderate	high	high
Parvalbumin* content	absence	moderate	high
Resistance to fatigue	high	moderate	low
Number of mitochondria	high	high	low
Metabolism	oxidative	glycolytic and oxidative	glycolytic
Myofibre diameter	moderate	small	large

*Parvalbumin is a Ca^{2+}-binding protein that transports Ca^{2+} from troponin to the SERCA during muscle relaxation.

1.1.2 Skeletal muscle function

1.1.2.1 Excitation contraction coupling

Muscle fibres are excitable cells that respond to a stimulating signal coming from their motor neuron eliciting the start of a contraction. Following an action potential generated by the motor neuron, acetylcholine (ACh) is released at the neuromuscular junction and activates nicotinic receptors localized on the sarcolemma, which results in Na^+ entry and depolarization of the cell. The depolarization wave propagates along the plasma membrane and, in a few milliseconds, reaches a series of invaginations of the membrane called transverse tubular system or T-tubules, which are in close contact with the sarcoplasmic reticulum (SR), the major Ca^{2+} store in skeletal muscle cells. Upon arrival of the action potential at the t-tubule, dihydropyridine receptors (DHPR) are activated and trigger the ryanodine channels (RyR) to open causing massive SR Ca^{2+} release into the cytosol (Rios & Brum, 1987). Released Ca^{2+} interacts with the binding sites of troponin. This alters its shape and position, which in turn causes movement of attached tropomyosin molecule. Movement of tropomyosin permits the myosin head to contact actin to initiate the molecular events of contraction in what is conceived as the sliding filament theory.

1.1.2.2 The sliding filament theory

The sliding filament theory (Huxley & Niedergerke, 1954) provides the current understanding for the molecular events taking place in skeletal muscle contraction. When muscle contracts, there is a close association between actin and myosin. During contraction, the length of the filaments remains constant, yet the length of the sarcomere and band I decrease; the overlap between thick and thin filaments increases. This led to the conclusion that the 2 filaments slide on each other.

When ATP binds to the myosin head of the thick filaments, ATP is hydrolysed by myosin and disconnects actin from myosin. The energy released by the splitting of ATP is stored in the myosin molecule and represents a high-energy state; this is the predominant state at rest. Upon muscle stimulation, the inhibition of actin-myosin interaction, imposed by troponin and tropomyosin, is removed upon Ca^{2+} binding to troponin, and consequently the myosin in high-energy state binds to actin (Figure 1.2). The actin-myosin interaction triggers the release of ADP from the myosin head, resulting in movement. The energy stored in the myosin molecule

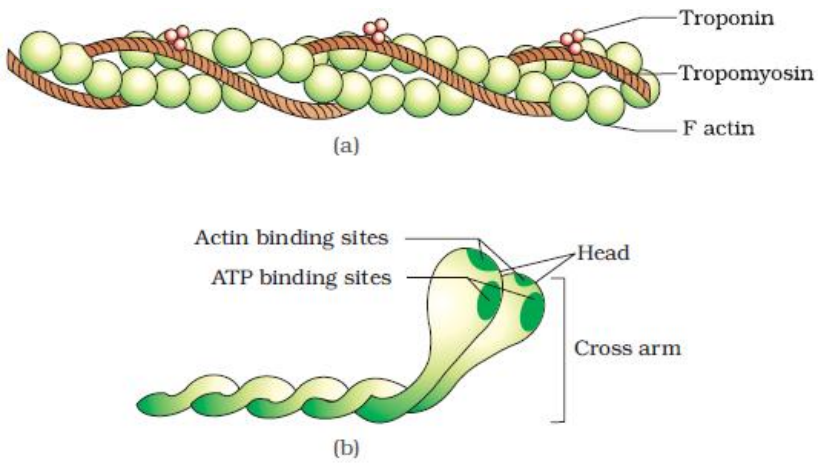

Figure 1-2, Myosin, actin and the regulatory proteins

(a) Actin filament with its inhibitory regulatory proteins. (b) Myosin myofilament showing its ATP and actin-binding site. Upon the arrival of an action potential, Ca^{2+} is released from the SR. Ca^{2+} binds to troponin changing its shape and position and leads to the removal of its inhibitory effect on cross bridge formation and the initiation of filament sliding.

triggers a conformational change in the cross-bridge between actin and myosin modifying the angle from 90° to 45°. This tilting or swivelling pulls the actin filament about 10 nm toward the centre of the sarcomere consuming the energy stored in myosin. Contraction occurs. During the swivel, the myosin head is firmly attached to actin. So, when the head swivels it pulls the actin and, therefore, the entire thin filament forward. Many myosin heads are swivelling simultaneously and their collective effort are enough to pull the entire thin filament and globally a muscle contraction. At the end of the swivel, ATP fits into to binding site on the cross-bridge and this breaks the bond between the cross-bridge (myosin) and actin. Due to the continuous presence of Ca^{2+} and removal of the inhibitory regulators, the myosin head will swivel back. As this happens, the ATP breaks down to ADP + P_i and the cross-bridge again binds to an actin molecule. As a result, the head is once again bound firmly to actin. However, because the head was not attached to actin when it swivelled back, it will bind to a different actin molecule. In the process, the myosin heads of the thick myofilament are pulling the thin myofilament. Thus, the thick and thin myofilaments are actually sliding past each other. As this occurs, the distance between the Z-lines of the sarcomere decreases and as a consequence the myofibril and entire muscle get shorter. Skeletal muscle relaxes when the nervous impulse stops. At this stage, Ca^{2+} will no longer be released out of the SR and the sarco-endoplasmic reticulum ATPase (SERCA) pump will now transport the Ca^{2+} back into the SR. In the absence of Ca^{2+}, troponin returns to its initial state and the attached tropomyosin will go into its original shape and position bringing an end to myosin and actin interaction, which terminates the muscle contraction.

1.1.2.3 Mechanics of muscle contraction

The pattern of force development that results from neural stimulation or direct activation of a muscle, motor unit or muscle fibre is determined by the number and frequency of stimulations delivered. Muscle contraction can be divided according to the frequency of the contraction into phasic twitch and tetanic contractions. It can also be categorized depending on the direction of movement during contraction into isometric, concentric and eccentric contraction.

1.1.2.3.1 Phasic twitch and tetanic contraction

A phasic twitch is the contractile response resulting from a single maximal stimulus (Figure 1.3). Several terms are commonly used to describe a phasic twitch such as:

- Peak specific force, commonly conceived as a function of the number of strongly bound cross-bridges acting in parallel.
- Time to peak twitch force; it is used as an indicator of SR Ca^{2+} release and the rise of $[Ca^{2+}]_i$.
- Half-relaxation time; it is dependent on the rate of Ca^{2+} dissociation from troponin, its uptake by the SR and cross-bridge detachment.
- Width at half-amplitude; it correlates with the time course of the Ca^{2+} transient in the muscle cell.

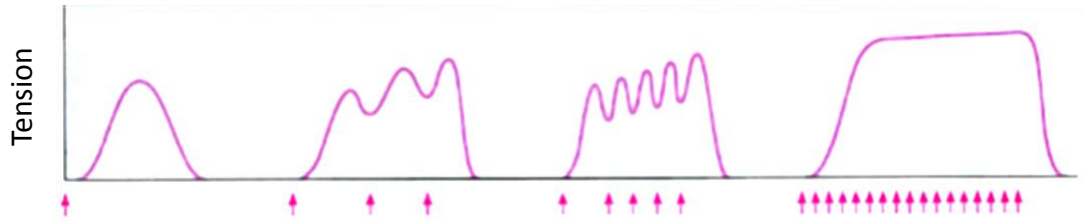

Figure 1-3, Phasic and tetanic contractions

When a muscle is exposed to a single electrical stimulus, a phasic twitch occurs (on the left). On repeating such stimulation with increasing frequencies, partial and then complete fusion occurs leading to tetanic contraction seen on the right of the illustration. Arrows point to a stimulus given to induce a contraction (Adapted from Marieb 2004).

On the other hand, if a muscle is stimulated repeatedly, such that each stimulus arrives before complete relaxation induced by the previous contraction, force summation occurs, and the force developed is greater than that of a single twitch. Several terms are used to describe tetanic contractions such as: peak specific force, peak rate of force development, half-relaxation time, peak rate of relaxation and rate of linear phase of relaxation.

1.1.2.3.2 Isometric, concentric and eccentric contraction

A muscle exerting force by shortening causes concentric contractions and these cover most of the daily body movements. A muscle producing force while being fixed constant in length leads to an isometric contraction and this kind of contraction is required to maintain posture. Finally, a muscle producing force but being pulled in an opposite direction is performing an eccentric contraction. Eccentric or stretching contractions take place at the end of activities to slow down movements and in situations when energy is being lost such as when walking down stairs or landing from a jump. Eccentric contractions are known to be the most demanding and damaging ones to skeletal muscles. Isometric and eccentric types of contractions are used in this study to evaluate muscle performance.

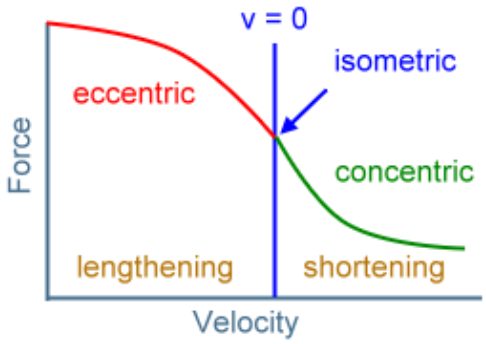

Figure 1-4, Force-velocity relationship in skeletal muscle

Movement in a positive direction of muscle force denotes a concentric contraction while in a negative direction highlights an eccentric contraction. Remaining constant in length is referred to as isometric contraction.

1.1.3 Calcium handling in skeletal muscles

Not only does Ca^{2+} play a pivotal role in the initiation, termination of muscle contraction, but it also serves as a key regulator in other cellular processes. Extensive research aiming at deciphering the complexity of the cascade regulating Ca^{2+} handling in skeletal muscle cells has been carried out during the last decades. This work led to the unveiling of several receptors, channels, transporters and carriers, which are responsible for the handling of this essential second messenger. These are discussed below.

1.1.3.1 Voltage-operated Ca^{2+} channels or dihydropyridine receptors

DHPR mediate the release of the intracellular Ca^{2+} from the SR following the depolarization wave initiated at the neuromuscular junction. Structurally, it is a complex of 5 subunits: alpha 1, alpha 2,

beta, gamma, delta (Catterall, 1991). DHPRs of fast twitch fibres were found to have 3 to 5-fold greater density than those of slow twitch fibres (Renganathan *et al.*, 1998).

1.1.3.2 Ryanodine receptors

RyRs are large, high conductance Ca^{2+} channels that control the release of Ca^{2+} from the SR. The name was derived from the plant alkaloid ryanodine, due to the receptor's ability to bind it with high affinity and specificity, which distinguishes them from another intracellular Ca^{2+} release channel family, the inositol 1,4,5-trisphosphate receptors (IP3R). Mammalian tissues express different RyRs isoforms: RyR1 is the dominant isoform in skeletal muscle, RyR2 is found in high levels in cardiac muscle, RyR3 is ubiquitously expressed, and all three isoforms are present in smooth muscles. RyRs are homotetramers constituted of 4 transmembrane helices forming a Ca^{2+} channel (Inui *et al.*, 1987) and a very large protruding cytoplasmic domain, the foot region, which allows a direct connection between the channel and the DHPR at the plasma membrane (Brini & Carafoli, 2000; Serysheva *et al.*, 2005). Interaction between DHPRs and RyRs following an action potential occurs by protein-protein interaction (Paolini *et al.*, 2004; Yin *et al.*, 2005). RyRs are regulated by protein kinases and reactive oxygen species as indicated by the presence of phosphorylation sites (Hain *et al.*, 1994), and a large number of free sulfhydryl groups, respectively (Hidalgo *et al.*, 2005).

1.1.3.3 IP3R

IP3Rs are important regulators of Ca^{2+} release from the SR in smooth and cardiac muscle (Estrada *et al.*, 2001); they are hardly expressed in skeletal muscle (Talon *et al.*, 2002). However, they have been reported to be expressed in skeletal myoblasts and myotubes in culture (Jaimovich *et al.*, 2000).

1.1.3.4 SR and sarcoplasmic reticulum Ca^{2+} ATPase

SR is the main store for Ca^{2+} in skeletal muscle with Ca^{2+} concentration as high as 1 mM at rest. SERCA utilizes ATP mostly generated by the cytosolic isoform of creatine kinase (CK) bound to the SR to pump Ca^{2+} from the cytosol back into the SR against the Ca^{2+}- concentration gradient (Korge *et al.*, 1993; Rossi *et al.*, 1990). SERCAs are encoded by three genes and alternative splicing leads to five different isoforms, the expression of which is tissue specific (Wuytack *et al.*, 1992). SERCA1 is expressed only in skeletal muscles and shows a high abundance in fast twitch fibres, whereas SERCA2a is expressed in the heart and in slow twitch fibres. SERCA density is 5-7 times higher in fast

twitch compared to slow twitch fibres, to comply with the fast kinetics of Ca^{2+} removal needed by these muscles (Leberer & Pette, 1986).

1.1.3.5 Plasma membrane Ca^{2+} - ATPase (PMCA) and Na^{+}- Ca^{2+} exchanger (NCX)

Pumping back Ca^{2+} into the SR is not the only pathway for extruding Ca^{2+} from the cytosol following contraction. Plasma membrane Ca^{2+}-ATPase (PMCA) and Na^{+}-Ca^{2+} exchanger (NCX) serve as extrusion pathways for Ca^{2+}. While PMCA uses ATP to extrude Ca^{2+}, NCX exchanges Ca^{2+} for Na^{+} (Strehler & Zacharias, 2001). However, their role is minor compared to SERCA in removing cytosolic Ca^{2+} after a contraction in healthy skeletal muscles.

1.1.3.6 Store operated Ca^{2+} channels (SOCs)

These are also referred to as capacitive Ca^{2+} entry pathways and are constituted by Ca^{2+} release activated Ca^{2+} channels (CRAC). These channels are found in most cells and are activated by SR Ca^{2+} depletion (Parekh & Putney, 2005). Abnormal function of such channels has been implicated in autoimmune diseases and inflammation. Activation of this Ca^{2+} entry pathway has been thoroughly investigated leading to the proposal of 2 mechanisms of activation. The first one is thought to occur through physical interaction between the channel-forming protein Orai1, and a sensor protein in the SR called Stim1. Upon store emptying, Stim1 oligomerises and interacts with the pore forming unit Orai1 leading to the activation of Ca^{2+} influx (Cahalan, 2009). The second one is thought to be due to release of a diffusible messenger termed calcium influx factor (CIF), which activates the Ca^{2+}-independent form of phospholipase A_2 ($iPLA_2$) by releasing the inhibitory protein calmodulin. This cascade is reported to activate SOCs through the production of lysophospholipids (Bolotina, 2008).

1.1.3.7 Stretch activated channels (SACs)

Stretch activated channels (SACs) are non-selective cationic channels that belong to the class of mechano-sensitive channels. Several members of the TRP channels have been described to be mechano-sensitive but to date the molecular identity of SAC in skeletal muscle have not been discovered (Holle & Engler, 2011). Activation of SACs is not fully understood; however, recent reports suggest the involvement of the microtubule network that conveys the mechanical signal subsequently to activate NADPH oxidases (NOXes) leading to the eventual opening of the channel (Khairallah *et al.*, 2012; Prosser *et al.*, 2012). These channels are inhibited by gadolinum ion (Gd^{3+}), streptomycin, an aminoglycoside, and the *tarantula* spider (*Grammostola spatulata)* venom, grammotoxin (GsMTx-4) (Hamill & McBride, 1996).

1.1.3.8 Mitochondrial channels and transporters

Mitochondria play an essential role not only in energy production through oxidative phosphorylation, generation of reactive oxygen species (ROS) and programmed cell death, but are also involved in Ca^{2+} homeostasis due to their Ca^{2+} buffering capability (Pozzan & Rizzuto, 2000). Ca^{2+} uptake by mitochondria is mediated by the uniporters, which is a gated channel driven by the electrochemical gradient across the inner mitochondrial membrane (Gunter *et al.*, 2000). Other pathways of Ca^{2+} entry into mitochondria include the 'rapid-mode' uptake (RaM) (Sparagna *et al.*, 1995) and the RyR1 localized to the inner membrane of mitochondria (Beutner *et al.*, 2001). On the other hand, Ca^{2+} efflux is mediated by its exchange with Na^{+} or H^{+} through the antiporters (Carafoli, 2003). Another means of extruding not only Ca^{2+}, but any molecule up to 1.5 kDa from the mitochondria is the mitochondrial permeability transition pore (mPTP). The mPTP structure has been shown recently to be formed from dimers of ATP synthase (Giorgio *et al.*, 2013). Prolonged mPTP opening causes massive swelling of mitochondria, rupture of the outer membrane and release of inter-membrane components that induce apoptosis (Rasola & Bernardi, 2007).

1.1.3.9 Ca^{2+} buffering proteins

Several Ca^{2+}-binding proteins exist in different cellular compartments such as calmodulin and parvalbumin in the cytosol, or calsequestrin and calreticulin in the SR. Most of these proteins belong to the EF-hand protein family and participate in Ca^{2+} handling by acting as Ca^{2+} buffering systems. One of the most important ones is calmodulin, which besides its ability to buffer Ca^{2+}, interacts with a variety of other proteins and regulates their function (Vetter & Leclerc, 2003). Another cytosolic protein, parvalbumin, is expressed in murine fast fibres but is absent in slow fibres and is completely absent in humans (Campbell *et al.*, 2001). Calsequestrin is the major Ca^{2+} storage protein in the SR of all striated muscles (reviewed in Yano and Zarain-Herzberg (1994)). An illustration showing the pathways involved in Ca^{2+} handling in skeletal muscles is depicted in figure 1.5.

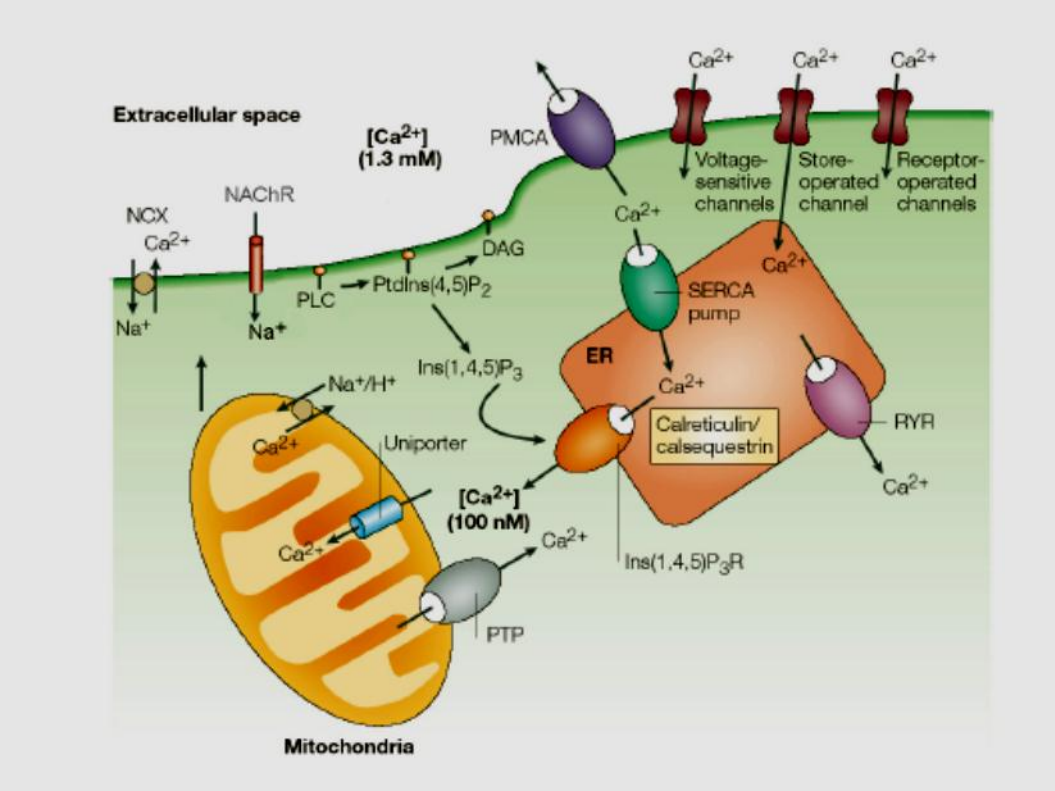

Figure 1-5, Calcium handling in skeletal muscle cells

The illustration shows different mediators of Ca^{2+} influx and extrusion pathways in skeletal muscle. The two compartments, which play a major role in Ca^{2+} buffering, the sarcoplasmic reticulum and the mitochondria, are shown in orange (adapted from Orrenius *et al.* (2003).

1.2 Duchenne muscular dystrophy (DMD)

"Muscular dystrophy" originates from the Latin word "dys", meaning difficult and the Greek work "trophe", relating to nourishment, and denotes a heterogeneous group of neuromuscular disorders. Such disorders affect skeletal muscles and are accompanied by muscle wasting and weakness of variable distribution and severity, which may also affect cardiac and smooth muscles or other tissues (Engel *et al.*, 1994). Inheritance in these disorders is either dominant or recessive, although the gene may be defective because of a *de novo* mutation (Arahata, 2000). Historically, the classification of these disorders were based on the phenotype till the early 1990's when the identification of the genes involved changed the phenotype-based classification and shed new light on the molecular pathogenesis of these disorders (Cohn & Campbell, 2000). Currently, neuromuscular disorders are subdivided into several groups: Duchenne and Becker, Emery-Dreifuss, distal, facioscapulohumeral, oculopharyngeal and limb-girdle, which is the most heterogeneous group (Emery, 2002).

1.2.1 Clinical features and genetic aspects of DMD

DMD is an X-linked neuromuscular disease that affects about 1 in 3500 males and which results in progressive muscle degeneration (Emery, 2002). DMD patients typically present clinically at 4-5 years of age, with symptoms including difficulties in standing from a seated position, climbing stairs, and keeping up with their peers during play. The muscle degeneration is progressive and replacement with fibrous/fatty tissue occurs, which ultimately results in death by cardiac or respiratory failure by the late teens to the mid-twenties. With adequate supportive treatment, life expectancy has increased into late-twenties and early thirties (reviewed in (Bushby *et al.*, 2010a, b). Severe cognitive impairments such as reduced verbal skills are seen in approximately 30% of DMD cases (Moizard *et al.*, 2000). Elevated levels of creatine kinase derived from muscle, in serum and amniotic fluid (Emery, 1977) remain the most widely used clinical markers in DMD diagnosis. Diagnosis is confirmed by mutational analysis based on DNA sequencing tests.

The disease is caused by the lack of the protein dystrophin. The dystrophin gene is a large gene of 2.5 Mb transcribed to a 14 kb mRNA and coding for a 427 kDa protein (Hoffman *et al.*, 1987). The large size of the gene, amounting to about 1% of the human X-chromosome, is a likely reason for the high rates of mutation (Hoffman & Schwartz, 1991). The gene is composed of 79 exons that map the Xp21 and occupies approximately 0.1% of the entire genome (Monaco & Kunkel, 1988). About 70% of the affected boys inherit the gene from their carrier mother; the others exhibit *de-*

novo mutations, whereas their mothers have a normal X-chromosome. Approximately 60% of dystrophin mutations are large insertions or deletions that lead to downstream frameshift errors, whereas approximately 40% are point mutations or small frameshift rearrangements (Hoffman & Dressman, 2001). This protein is localized just under the plasma membrane of muscle cells and links the extracellular matrix with the cytoskeleton. Several proteins are associated with dystrophin and are described in the following section.

1.2.2 Dystrophin and dystrophin-associated proteins complex

Dystrophin is a cytoskeletal linker protein linking F-actin to laminin-2 of the extracellular matrix. It is a rod-shaped protein consisting of four domains: an N-terminal actin-binding domain, twenty four triple helix spectrin-like repeats separated by four hinge regions, a cysteine-rich domain containing two predicted calcium binding motifs, and a unique C-terminal domain (Koenig *et al.*, 1988). Dystrophin localization is restricted to sub-sarcolemmal bands distributed along differentiated muscle fibres, where it binds F-actin at its N-terminus, and proteins such as nitric oxide synthase (NOS) via the syntrophins, the dystrobrevins, and syncoilin at its C-terminus (Suzuki *et al.*, 1994). The most important link regarding DMD is that made between the cysteine rich domain and the dystrophin glycoprotein complex (DGC) or dystrophin associated protein complex (DAPC). Dystrophin appears to coordinate a link from the actin cytoskeleton to laminin-2 of the extracellular matrix (Ahn & Kunkel, 1993; Campbell, 1995) by way of β-dystroglycan (Jung *et al.*, 1995), the sarcoglycans and sarcospan located in the sarcolemma, and α-dystroglycan on the external face of the membrane (Figure 1.6) (Ervasti & Campbell, 1991; Yoshida & Ozawa, 1990). Mutations in dystrophin or of any component of the DGC complex cause various types of muscular dystrophies (reviewed in Durbeej and Campbell (2002)). Yet the mechanism by which a protein absence causes a defined phenotype is still to be resolved awaiting a thorough knowledge of the biochemical and structural function of each member of the DGC.

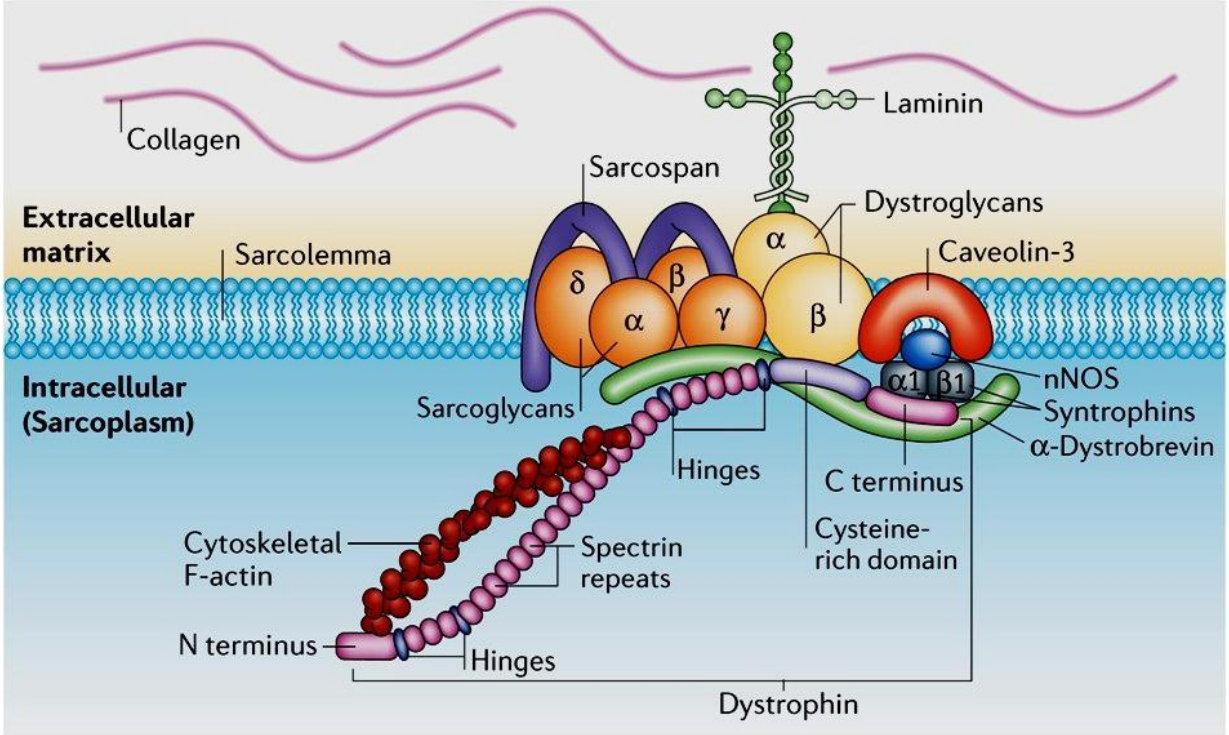

Figure 1-6, Dystrophin associated protein complex

The illustration shows the central role orchestrated by dystrophin in linking not only the cytoskeletal F-actin with laminin in the extracellular matrix, but also to other essential proteins such as nitric oxide synthase and caveolin-3 (from Davies and Nowak (2006).

1.2.3 Pathogenesis of DMD

Despite the discovery of the primary defect in DMD, the secondary molecular mechanisms leading ultimately to muscle degeneration are diverse and interconnected. Evidence established from research on DMD patients and animal models points towards a crucial role for the loss of cytoskeletal and sarcolemmal integrity, deregulation of calcium homeostasis, enhanced protease activity, increased oxidative stress and impaired energy metabolism in the pathogenesis of the disease (Blake *et al.*, 2002; Hopf *et al.*, 2007). Historically, two hypotheses were presented in the literature to explain the pathogenesis seen in DMD: The structural/mechanical hypothesis and the dystrophin associated-signalosome hypothesis, however, there is no longer a clear distinction between the two.

In normal muscle, the DGC complex confers mechanical stability to the plasma membrane during muscle contraction by linking the cytoskeleton and the extracellular matrix, yet in DMD this stabilization effect is lacking and lead to tearing of the membrane during muscle exercise (Allen *et al.*, 2005; Petrof *et al.*, 1993). Evidence for the existence of such tears came not only from the presence of muscle-specific proteins in the blood of DMD patients, such as creatine kinase, but also

from the entry of membrane impermeable dyes, like Evans blue and Procion orange into dystrophic muscle cells when these were exposed to repeated contractions. It has also been reported that Ca^{2+} would enter extensively through these tears, leading to its chronic increment that activates a variety of downstream effectors ending up in muscle cell death.

It has also been reported that dystrophin and the DGC have several signalling functions and that loss of the complex in muscular dystrophy has been associated with alterations in multiple signal transduction pathways such as the mitogen-activated protein kinase (MAPK) or the Akt signalling pathways (Dogra *et al.*, 2008). The biochemical repercussions of dystrophin absence in skeletal muscle cells are diverse, interconnected and amplify each other in viscous cycles. A description of the major downstream effectors of dystrophin absence is given below.

1.2.3.1 Ca^{2+} dysregulation

The lack of dystrophin has also been proposed to be directly responsible for enhanced Ca^{2+} entry in dystrophic muscle (Carlson, 1998; Hopf *et al.*, 2007; Turner *et al.*, 1991), because of abnormal activity of the non-selective cationic channels activated either by membrane stretch (SAC) or by Ca^{2+}-store depletion (SOC) (Ducret *et al.*, 2006; Vandebrouck *et al.*, 2006) or through membrane tears (McNeil & Khakee, 1992). Recent evidence that support the central role played by Ca^{2+} dysregulation in the pathogenesis of DMD came from overexpressing TRPC3 channels, which was sufficient to replicate muscular dystrophy to some extent (Millay *et al.*, 2009). Another study showed that the inhibition of Ca^{2+} influx by the expression of a dominant negative form of TRPV2 ameliorates muscular dystrophy in models of DMD (Iwata *et al.*, 2009).

Several studies have shown that SOC activity is increased in dystrophic fibres (Boittin *et al.*, 2006; Harisseh *et al.*, 2013). It was also reported that these channels are regulated by $iPLA_2$ in dystrophic fibres and that the increased activity of this enzyme is likely responsible for the enhanced SOC activity in dystrophin-deficient fibres (Boittin *et al.*, 2010).

SAC activity has also been reported to be increased in models of DMD. Recent studies show that activation of SAC channels is initiated by stretch that is conveyed through the microtubular network to activate NOXes, eventually activating these channels. This report established that the microtubule network is denser in mdx fibres, and that interventions antagonizing such an increment correct the increased Ca^{2+} influx through SACs (Khairallah *et al.*, 2012; Prosser *et al.*, 2012).

1.2.3.2 Protease activation

Calcium-dependent cysteine proteases, in particular μ-calpain, known to degrade a range of skeletal muscle proteins, including cytoskeletal and plasma membrane proteins, show both, elevated concentrations and activity in *mdx* muscles at the peak of muscle necrosis (Spencer *et al.*, 1995). Calpain activity has been found elevated in extracts of muscle biopsies from DMD patients (Reddy *et al.*, 1986). Despite the well-documented increase in calpain activity in DMD, and much efforts in research that have been invested, its role in the pathogenesis of muscular dystrophies is still unclear (Childers *et al.*, 2011) and is probably of little importance.

1.2.3.3 Neuronal nitric oxide synthase (nNOS)

Loss of dystrophin in DMD results not only in delocalization of nNOS from the sarcolemma to the cytosol (Brenman *et al.*, 1995), but also to a reduction of NO release from dystrophic muscle and decrement in circulating NO levels. Reduced NO levels lead to decreased superoxide scavenging and reduced vasorelaxation, local muscle ischemia and to an impairment of regeneration (Niebroj-Dobosz & Hausmanowa-Petrusewicz, 2005).

1.2.3.4 Ca^{2+} independent phospholipase A_2 ($iPLA_2$)

As stated above, $iPLA_2$ plays a role in modulating Ca^{2+} entry not only through SOC but also through SAC. The first report on the role of $iPLA_2$ in DMD came from Lindahl et *al.* on muscle biopsies in which a 10-fold increase of PLA_2 activity as compared to controls was observed (Lindahl *et al.*, 1995). Also, work from our lab showed increased expression of $iPLA_2$ in *mdx* muscles (Boittin *et al.*, 2006).

This enzyme is also known as group VIA PLA_2, and was initially purified and characterized from the P388D1 macrophage-like cell line (Ackermann *et al.*, 1994). Group VIA PLA_2 has a molecular weight of around 85 kDa, and can exist in an aggregated form. It contains multiple ankyrin repeats, which may play a role in its oligomerisation. It exhibits lysophospholipase activity as well as phospholipase A_2 activity, and is capable of hydrolysing a wide variety of phospholipid substrates. $iPLA_2$ catalyses the hydrolysis of phospholipids at the sn-2 position, releasing a free fatty and a lysophospholipid. Two isoforms are reported to be present in skeletal muscles, the short and the long isoform (Winstead *et al.*, 2000). The long isoform has a 54 amino acid insert, which disrupts the 8^{th} ankyrin repeat (figure 1.7) and is reported to mediate membrane association (Hsu *et al.*, 2009).

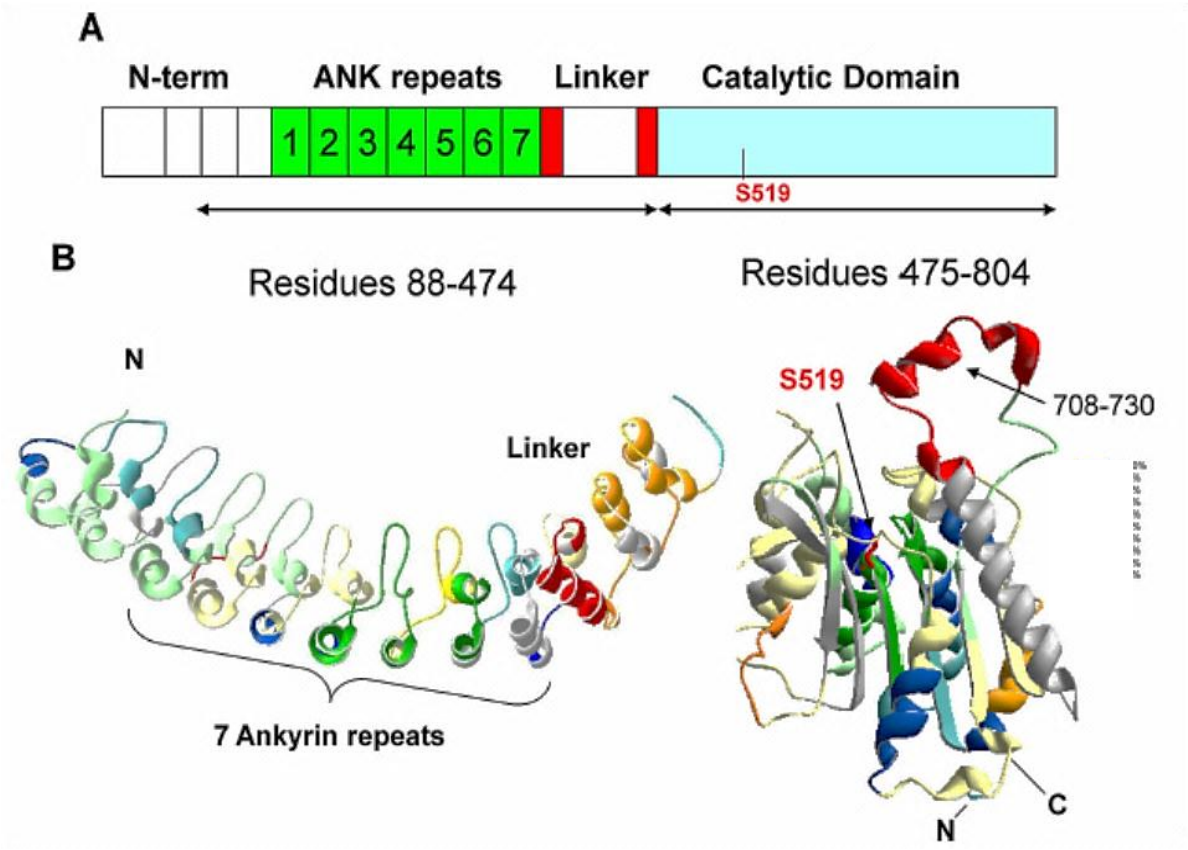

Figure 1-7, Structure of group VIA-2 phospholipase A_2

A, Schematic representation of the different domains of $iPLA_2$. B, Deuterium exchange map showing the 7 ankyrin repeats and the catalytic domain (Hsu *et al.* 2009).

1.2.3.5 Oxidative stress

Oxidative stress is generally defined as an imbalance that favours the production of ROS over cellular antioxidant defences. Early studies have suggested that increased oxidative stress contribute to muscle damage and degeneration in dystrophic muscle. Protein carbonyls and lipid peroxidation by-products, markers of oxidative stress, have been detected in muscles of DMD patients and *mdx* mice (Murphy & Kehrer, 1986; Ragusa *et al.*, 1997; Rodriguez & Tranopolsky, 2003).

The demonstration that oxidative stress is not only a secondary effect of muscle degeneration but precedes the pathologic changes of muscle dystrophy, came from the observation that lipid peroxidation products and expression of antioxidant enzymes were increased in 3-week-old *mdx* mice before the onset of the disease (Disatnik *et al.*, 1998).

Sources of oxidative stress in respiratory and locomotor muscles in DMD are thought to include mitochondria, NOXes, and infiltrating inflammatory cells, and on the other hand, reduced ROS

scavenging due to delocalization of nNOS (reviewed in Lawler (2011)). In the current overview, we will focus on mitochondria and NOXes due to their pertinent role in the oxidative stress seen in DMD.

1.2.3.5.1 Mitochondria

Mitochondria have generally been cited as the predominant source of ROS in muscle cells. Early reports suggested that 2-5% of the total oxygen consumed by mitochondria might undergo a one-electron reduction with the generation of superoxide, and that complexes I and III of the electron transport chain are the main sites of mitochondrial superoxide production (Davies *et al.*, 1982; Koren *et al.*, 1983). During exercise, a number of researchers have assumed that the increased ROS generation that occurs during contractile activity is directly related to the elevated oxygen consumption that occurs with increased mitochondrial activity. Such a correlation would imply a 50- or 100-fold increase in superoxide generation by skeletal muscle during aerobic contractions (Kanter, 1994). However, recent findings suggest that NOXes and not mitochondria are the dominant source of ROS during exercise (Sakellariou *et al.*, 2013b; Xia *et al.*, 2003).

1.2.3.5.2 NADPH oxidases

The NOX family members are transmembrane proteins that transport electrons across biological membranes to reduce oxygen to superoxide free radical ($O_2^{\bullet-}$) or H_2O_2. Historically, the first reports of its existence came from the observation of the phagocyte respiratory burst. Subsequent discoveries reported NOXes ability to produce $O_2^{\bullet-}$ and H_2O_2, and their insensitivity towards cyanide discriminated them from mitochondrial enzymes. In the late 1980s, the gene coding for the catalytic subunit of the phagocyte NADPH oxidase, originally referred to as $gp91^{phox}$, currently known as NOX2, was cloned (for a review see Bedard and Krause 2007). RNA analysis revealed the presence of both NOX2 and NOX4 in skeletal muscles (Mofarrahi *et al.*, 2008). NOX2 is the prototype NOX isoform, which most of our current understanding of NOX physiology is based upon (Figure 1.8).

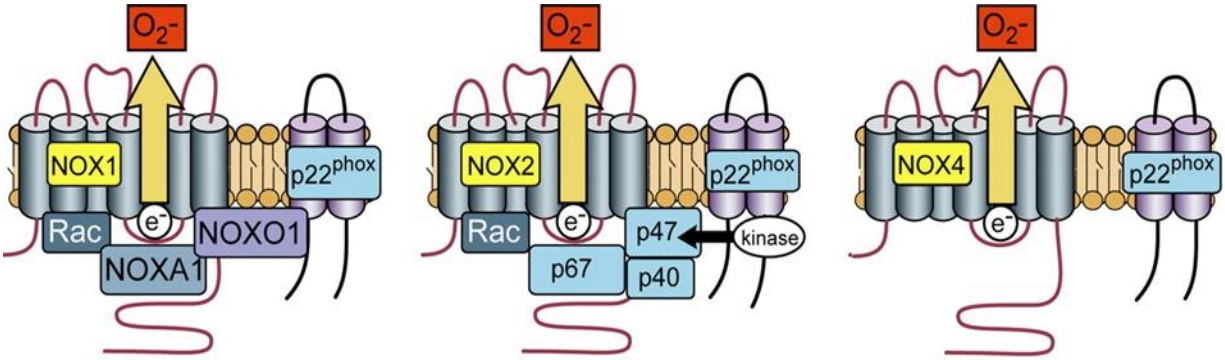

Figure 1-8, NOX isoforms expressed in skeletal muscles

NOX1, NOX2 and NOX4 seem to be the isoforms expressed in skeletal muscle (Mofarrahi et al, 2008). All isoforms require the $p22^{phox}$ subunit (from Bedard and Krause 2008).

Electron transfer in NOX2 occurs from NADPH, which binds to NOX2 at the cytosolic C-terminus via FAD, and two heme moieties (one toward the inner face and one towards the outer face of the membrane), to molecular O_2. The initiation of electron transfer requires the recruitment of the G protein Rac, the cytosolic oxidase components $p47^{phox}$, $p67^{phox}$ and $p40^{phox}$ to the cell membrane, and their association with NOX2 and the $p22^{phox}$ complex. During neutrophil activation, $p47^{phox}$ becomes phosphorylated at up to 11 sites, which relieves the auto-inhibitory interactions of $p47^{phox}$ and elicits interaction with phosphoinositides on the cell surface (Ago *et al.*, 2003; 1999). Binding of SH3 domains of $p47^{phox}$ to a proline-rich domain of $p22^{phox}$ then allows interaction of $p67^{phox}$ with NOX2 and oxidase activation. Thus, $p47^{phox}$ plays an essential role in the assembly of the oxidase complex (Figure 1.9).

On the other hand, NOX4, an isoform present in skeletal muscles, stands out from other NOX isoforms because it does not require cytosolic subunits for its activity. Another particularity is the ability to produce H_2O_2 directly and not only $O_2^{\bullet-}$ (Bedard & Krause, 2007).

Increased expression and activity of NOXes have been reported in *mdx* mice (Whitehead *et al.*, 2010). The study showed that NOX2 and all of its subunits, except $p22^{phox}$, are overexpressed in skeletal muscles of 19-day old *mdx* mice, just before the onset of necrosis. Another study showed that NOX4 mRNA is increased 5-fold in the left ventricles from 9-10 months old *mdx* mice (Spurney *et al.*, 2008). These data, together with those mentioned above, suggest a central role of NOXes in the early stages of the pathogenesis of DMD.

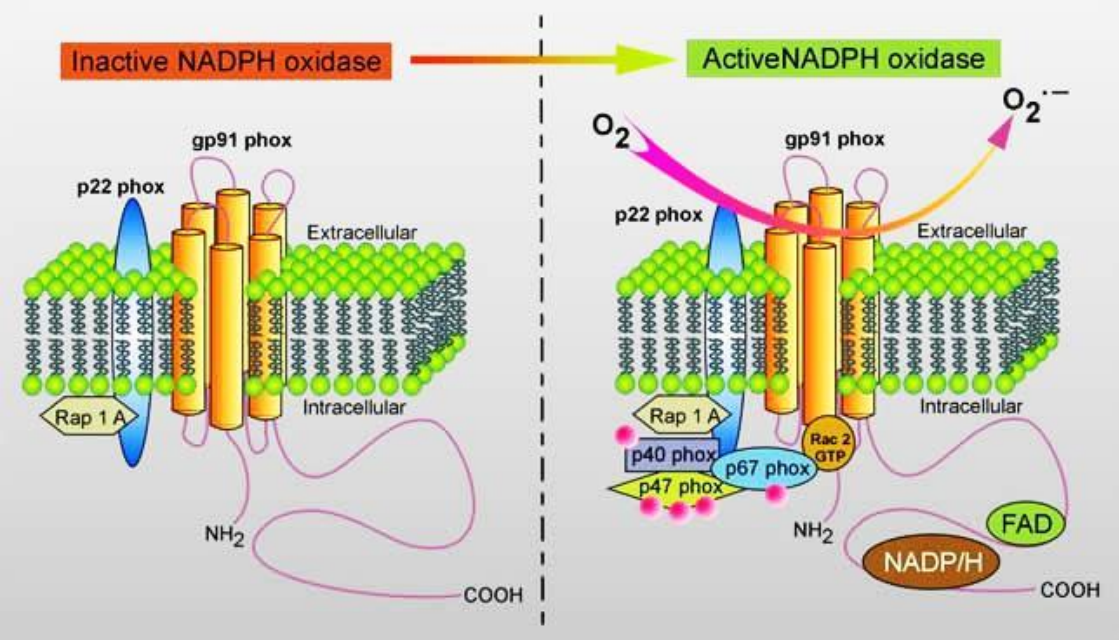

Figure 1-9, NOX2 and its assembly upon activation

When stimulated, NOX2 assembly starts by the phosphorylation of the p47^{phox}, which elicits its interaction with phosphoinositides on the cell surface bringing the cytosolic subunits into contact with the membrane unit gp91^{phox} and the p22^{phox} subunit. Electron transfer commences from NADPH bound at the C-terminus through the FAD and the heme moieties to the extracellular oxygen generating $O_2^{\bullet-}$ (from www.genkyotex.com)

1.2.4 Therapeutic approaches for DMD

Therapeutic interventions in DMD aim at re-expressing or replacing the functional elements of the dystrophin protein in muscle or ameliorating the condition. These therapies can be grouped into gene therapies, cell therapies and pharmacological therapies.

1.2.4.1 Gene therapy

Gene therapy-based approaches seek to artificially introduce DNA sequences into diseased tissues, aiming at achieving tissue-specific expression of normal or modified host-derived protein sequences to fulfil, or partially fulfil functions of the absent protein. Several strategies are employed to achieve this goal, an overview of which is listed below.

1.2.4.1.1 Gene replacement

Although considerable progress has been made in gene therapy constructs, multiple hurdles remain to be resolved before such a treatment will become available. Viral vectors proved to be an efficient tool for delivering the missing gene into the host tissue; however, they exhibit several limitations, including difficulties to produce sufficient quantities of vector, cellular tropism of the vectors, ectopic gene expression, the need to achieve whole-body delivery and the potential immune response to the vector and/or the transgene (Odom *et al.*, 2007).

One of the largest obstacles in DMD gene therapy is the large size of the gene. To fit dystrophin gene into an efficacious viral vector, one has to keep its size by deleting about 70% of the gene. Several mini-dystrophins have been developed and recently successful gene delivery using an adeno-associated virus (AAV9) viral vector to muscles of dogs has been achieved and resulted in reduced inflammation and fibrosis and improved muscle strength (Shin *et al.*, 2013).

1.2.4.1.2 Gene correction

Although the name of this sub-group suggests gene therapy, most compounds used in this class are small molecules and belong to the class of the pharmacological treatments.

Read through agents Approximately 15% of the mutations that cause DMD are due to point mutations in the coding sequence that create a stop codon and cause the premature termination of transcription, leading to a truncated, non-functional protein product. Many of the mutations that cause DMD are due to deletions or premature stop codons within the dystrophin gene affecting the rod-spectrin repeat domain of the protein. The first drug to produce such an effect was the aminoglycoside gentamicin, which induced a read-through of these premature stop codons to produce a nearly intact dystrophin having about 10-20% of normal function (Barton-Davis *et al.*, 1999). A novel molecule, PTC124, that was shown to induce dystrophin expression and to improve functional endpoints in *mdx* mice (Welch *et al.*, 2007), is now in clinical trials in DMD.

Exon skipping Dystrophin pre-mRNA is composed of 79 exons that undergo splicing to become the dystrophin-encoding mRNA in skeletal muscle. Since alternative splicing for dystrophin exists and depends upon recognition of exon boundaries, it is possible to manipulate the normal gene splicing machinery in order to prevent the transcription of the mutation-containing exon that otherwise would generate a non-functional dystrophin protein. Targeted skipping of mutation-containing exons could theoretically benefit 60-75% of DMD patients, yet it has to be tailored to the exon containing the mutation (Aartsma-Rus *et al.*, 2002; Béroud *et al.*, 2007). Skipping exons in the rod-spectrin repeat domain of dystrophin converts a severe DMD to a milder Becker muscular dystrophy phenotype.

To achieve exon skipping, a mutation-specific antisense oligonucleotide or small nuclear RNA is used to mask each mutation-containing exon. Novel anti-oligonucleotides such as 2'-O-methyl antisense oligonucleotide (2OMeAO) or phosphorodiamidate morpholino oligomers (PMO) have proven efficacious in partially restoring dystrophin expression and reversing the *mdx* phenotype

(Alter *et al.*, 2006; Doran *et al.*, 2009). Currently, two compounds are in clinical trials for exon skipping in DMD, AVI-4658 and drisapersen, both aimed to skip exon 51. These compounds showed a good tolerability, safety profile and led to an increase in dystrophin expression (Anthony *et al.*, 2012; Hammond & Wood, 2010). Recently, the U.S. Food and Drug Administration have granted drisapersen, a "breakthrough therapy" status. This classification will allow the drug to be ushered through clinical trials with quicker FDA review than usual (see figure 1.10).

Small nuclear RNAs (snRNA) have also been utilized as vectors for stable antisense expression. U1 and U7 snRNA-derived antisense molecules have been shown to be effective in inducing exon skipping and dystrophin rescue, both, in human DMD myoblasts and in the *mdx* mouse (Danos, 2008; Wilton & Fletcher, 2008). The major limitation of the exon skipping approach is the need to periodically re-administer the treatments to maintain physiologically relevant levels of dystrophin throughout a patients' life.

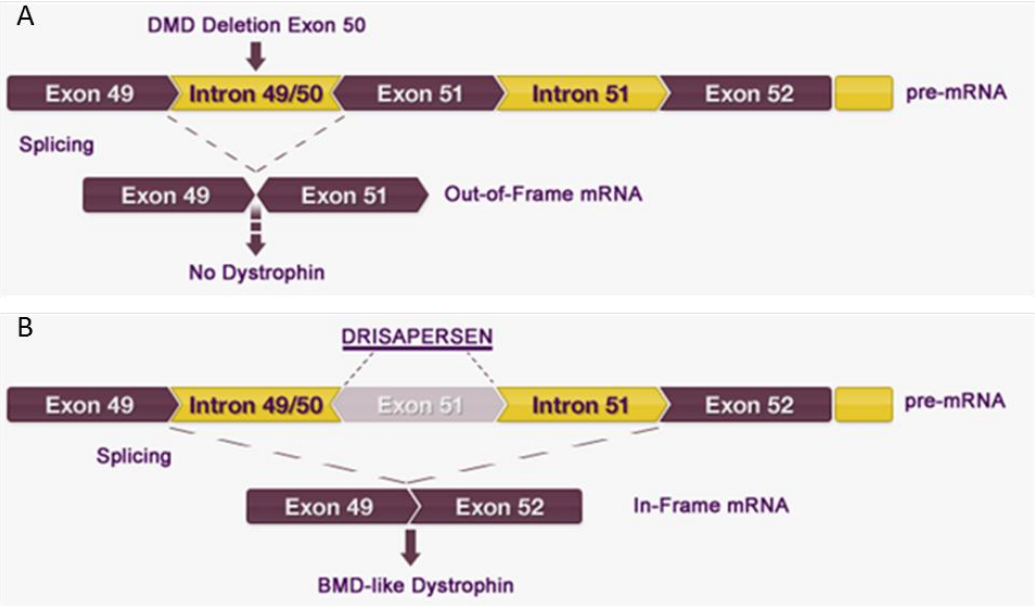

Figure 1-10, Exon skipping technology in DMD

(A) Pre-mRNA in DMD shows an out-of-frame shift that leads to the complete absence of dystrophin in these patients. (B) Exon skipping induced by drisapersen, which aims at skipping exon 51 and the conversion of the severe Duchenne phenotype to a milder Becker muscular dystrophy (from www.prosensa.eu).

1.2.4.2 Cell therapy

Cell-based therapies are based upon delivering a population of normal cells that has the ability to proliferate, fuse and repopulate dystrophic muscle. Such an approach proved to be beneficial when a normal Sol from a 1-day old normal mouse was grafted into a 20-day old dystrophic recipient

muscle. The results of this study showed nearly normal contractile properties after transplantation of a muscle graft (Law & Yap, 1979).

This technique was developed by the introduction of myoblast transfer, a procedure that involves injecting or transplanting muscle precursor cells (myoblasts) into a dystrophic host. Injection of myoblasts into *mdx* mouse muscle resulted in its fusion with the host *mdx* myofibers and in dystrophin expression at 30-40% of normal levels (Partridge *et al.*, 1989). Clinical trials using this approach failed due to immune rejection and limited survival in the host tissue (Gussoni *et al.*, 1992; Mendell *et al.*, 1995).

Subsequent studies revealed a plethora of cell types and to date, more than a dozen populations of myogenic precursor/facilitator cells have been reported to offer potential therapeutic benefit for muscular dystrophy (for recent reviews see (Konieczny *et al.*, 2013; Meregalli *et al.*, 2010)).

Despite the hurdles facing cell therapy techniques, it remains one of the most promising therapeutic approaches in DMD, especially in combination with gene therapy and pharmacological treatments. One example of such an approach is called autologous transfer, in which patient's own cells are genetically corrected *in vitro* with lentiviral vectors and then re-implanted to allow the re-expression of functional dystrophin protein.

1.2.4.3 Pharmacological therapy

Currently, there is no cure for DMD, all present therapeutic interventions aim at ameliorating the progression of the disease, support of the patient and improving the quality of life. Corticosteroid treatment is the only approved pharmacological intervention. We will provide in the following section a non-exhaustive description of investigated pharmacological agents with shown efficiency in DMD animal models and/or in a clinical setting.

Corticosteroids These are currently the only approved therapy used in clinics for DMD. They act to delay the loss of independent ambulation, delay the onset of cardiac and respiratory failure, and to prolong muscle function. Their mechanism of action is still debated and was attributed to reduction in all inflammatory cell populations, promotion of muscle-specific gene expression, correction of Ca^{2+} dysregulation (Leijendekker *et al.*, 1996; Metzinger *et al.*, 1995), and activation of the calcineurin pathway (St-Pierre *et al.*, 2004). However, corticosteroid treatment is accompanied by a variety of side effects including hyperactivity, excessive weight gain, hypertension and susceptibility to diabetes mellitus. In contrast, the prednisone derivative deflazacort appears to provide a better

alternative with less severe side effects (Bonifati *et al.*, 2000; Mesa *et al.*, 1991). This observation is highly disputed and is reflected in a recent study that shows the lack of a standardized treatment protocol within clinics, specialized in DMD treatment (Griggs *et al.*, 2013).

A novel approach to overcome the side effect of glucocorticoid therapy is the use of glucocorticoid receptor modulators. The detrimental effects of corticosteroid treatment result from direct glucocorticoid receptor homodimer interactions with glucocorticoid response elements of the relevant genes. A recent report provided evidence that Compound A, a non-steroidal selective glucocorticoid receptor modulator, is capable of transrepression of these genes without transactivation (Huynh *et al.*, 2013). The authors of this study showed *in vitro* NF-κB inhibitory activity of Compound A in *mdx* myoblasts and myotubes, and demonstrated improvements in the disease phenotype of *mdx* mice.

Myostatin inhibition and enhancement of muscle growth Myostatin is a member of the transforming growth factor-beta family of cytokines expressed predominantly in muscle (Patel & Amthor, 2005). The rationale for therapeutic development based upon growth factor modulation is that myostatin inhibition is known to enhance muscle regeneration (Wagner *et al.*, 2005) and regulate skeletal muscle fibrosis (Li *et al.*, 2008). Injection of myostatin antibodies or knock-down of myostatin in *mdx* mice resulted in increased body weight and muscle mass. It also decreased fibrosis and fat infiltration, however, no change in central nucleation was observed. On the other hand, it has also been reported that lack of myostatin compromises force production (Amthor *et al.*, 2007). Other approaches for increasing muscle size include the use of insulin like growth factor-1 and beta-agonists. However the use of the latter showed limited improvement and increased side effects.

Gentamycin The aminoglycoside antibiotic gentamycin has been examined in *mdx* muscle as aminoglycosides can cause suppression of stop codons by extensive misreading of RNA codes (Barton-Davis *et al.*, 1999) and insertion of alternative amino acids in place of the stop codon (see section 1.2.4.1.2). This treatment revealed an increased sarcolemmal expression of dystrophin, restoration of some components of the dystrophin complex and offered a degree of protection to the sarcolemma against mechanical stress (Barton-Davis *et al.*, 1999). Although only 10-20% of dystrophin levels were restored, this level was enough to protect the muscles from contraction-induced damage. Unfortunately, results have not been promising in clinical trials (Wagner *et al.*,

2001). Another aspect in the use of this class of molecules is its efficacy in blocking SACs, which seem to contribute to the pathology seen in DMD.

Selective estrogen receptor modulators In a recent publication, Dorchies et *al.* suggested that tamoxifen is one of the most promising pharmacological agents used in *mdx* mice. It is commonly used as an anti-estrogen in cases of breast cancer among other indications, but it was shown to have pro-estrogenic effects in muscles. A long-term treatment from 3 weeks to 15 months resulted in remarkable improvements of muscle force and of diaphragm and cardiac structure in the *mdx* mice. It stabilized myofibre membranes, normalized whole body force, and increased force production and resistance to repeated contractions of the triceps muscle above normal values. Tamoxifen improved the structure of leg muscles and diminished cardiac fibrosis by about 50%. It also reduced fibrosis in the diaphragm, while increasing its thickness, myofibre count, and myofibre diameter, thereby augmenting by 72% the amount of contractile tissue available for respiratory function. Tamoxifen also normalized the relative abundance of ERβ isoform, which was found to be several times more abundant in dystrophic than in normal muscles (Dorchies *et al.*, 2013).

Another study published just afterwards showed a beneficial effect of androgen receptor modulators as well in *mdx* mice. GLPG0492 significantly increased strength, increased diaphragm force, decreased the non-muscle area and markers of fibrosis and increased the resistance to fatigue (Cozzoli *et al.*, 2013).

Nutritional supplementation Nutritional supplements are being used more frequently either in conjunction with medications or on their own. In *mdx* mice, administration of creatine, a metabolite known to function as a muscle energy reserve, improved cellular energetics, corrected Ca^{2+} overload in myotubes, improved survival rates, decreased necrotic lesions and improved Ca^{2+} buffering capacity (Louis *et al.*, 2004; Passaquin *et al.*, 2002; 1998). However, when creatine was administered to DMD patients, improvement of only certain parameters of muscle function was observed (Louis *et al.*, 2004; Tarnopolsky *et al.*, 1997).

Several other supplements are commonly used; these include green tea polyphenols (Dorchies *et al.*, 2006), nitric oxide donors, such as L-arginine (Hnia *et al.*, 2008) and co-enzyme Q10 as antioxidant (Spurney *et al.*, 2011).

Proteolysis inhibitors Calpain inhibition holds minor therapeutic potential in DMD (refer to section 1.2.3.2). The endogenous calpain inhibitor (Spencer & Mellgren, 2002), calpastatin, or the non-

specific inhibitor, leupeptin (Badalamente & Stracher, 2000), reduced necrosis and disease severity in *mdx* mice. A novel approach aiming at inhibiting not only calpains but also the 20S proteasome in *mdx* mice showed clear histological improvements (Briguet *et al.*, 2008).

Reducing inflammation and immunosuppression NF-κB inhibitors such as curcumin (Pan *et al.*, 2008), TNF-α antibodies (Grounds & Torrisi, 2004; Radley *et al.*, 2008) and mast cell degranulation inhibitors such as oxatomide (Buyse *et al.*, 2007) have all shown amelioration of the dystrophic phenotype. This indicates the important role played by inflammation in DMD pathology. Immunosuppression and desensitization of the mPTP using cyclosporin A (De Luca *et al.*, 2005) showed a beneficial effect in *mdx* mice but clinical results with 154 DMD patients receiving CsA indicated absence of positive effects (Kirschner *et al.*, 2010).

Targeting Ca^{2+} dysregulation Due to the central role played by chronic elevation of cytosolic Ca^{2+} in DMD, several attempts at reducing such an increment took place over the past 30 years. There were several trials using Ca^{2+} channel blockers such as flunarizine, nifedipine, verapamil and diltiazem (Bertorini *et al.*, 1988; Dick *et al.*, 1986; Emery *et al.*, 1982; Moxley *et al.*, 1987), yet these failed to show any beneficial effect. Another approach to prevent the increased Ca^{2+} influx through tears induced by activity used the membrane sealant poloxamer 188, which seals sarcolemmal injury and prevents Ca^{2+} influx through such tears. The use of poloxamer 188 prevented and reversed the progression of cardiomyopathy and heart failure seen in *mdx* mice (Yasuda *et al.*, 2005). Also the use of streptomycin, a SAC blocker, led to clear benefits, both on isolated muscles and in *mdx* mice (Whitehead *et al.*, 2006). We also show evidence for the benefit provided by doxorubicin treatment of isolated muscle and of dystrophic myotubes (see chapter 2). Doxorubicin is an anthracycline chemotherapeutic agent reported to inhibit $iPLA_2$ in clinically relevant concentrations. Through its inhibition of this enzyme, it also modulates Ca^{2+} influx through SAC, which seems to prevent force loss in eccentrically contracting dystrophic muscle (Ismail *et al.*, 2013a).

Antioxidants The use of antioxidants to counteract oxidative stress ameliorates skeletal muscle structure and function of dystrophic mice. Among these molecules are green tea extract including (-)-epigallocatechin gallate (Buetler *et al.*, 2002; Dorchies *et al.*, 2009; 2006), melatonin (Hibaoui *et al.*, 2011; 2009), *N*-acetylcysteine (Whitehead *et al.*, 2008) and the superoxide/catalase mimetic EUK-134 (Kim & Lawler, 2012). However, the use of such non-selective anti-oxidant interventions

was of minimal clinical benefit and even resulted in deterioration in some cases (Kim *et al.*, 2013). In the current work, we present a novel approach using a NOX inhibitor, diapocynin, to decrease excessive ROS production without globally scavenging ROS (see chapters 3 and 4). Diapocynin showed beneficial effects not only on ROS production, but also on Ca^{2+} handling and $iPLA_2$ activity. It also showed clear benefits in an *in vivo* treatment protocol in *mdx* mice.

Other Intensive research is carried out to deliver new agents into the field of muscular dystrophy therapeutics. Examples of such agents include compounds that drive overexpression of utrophin, pentoxifylline and other vascular therapies, lansoprazol as a proton pump inhibitor, MG53 as a membrane repair agent, Debio025 for desensitizing the mPTP, halofuginone as an anti-fibrotic and several others (for a recent review see (Ruegg, 2013). Such new discoveries aim not only at providing agents with clinical significance for DMD, but also at deepening our knowledge of the pathophysiology of the disease.

Aim of the work

Although the genetic defect in DMD has been discovered more than 25 years ago, no cure to date exists for this debilitating disorder. Patients' hope remains highly in the quick development of cell therapy approaches combined with genetic approaches for correcting the defective gene. Looking at the most successful candidates currently undergoing clinical trials, first estimates for their availability, if successful, would be 3-20 years. Another issue is the patient population to which these new therapeutics aim. Exon skipping technologies, available so far, are focused at skipping exon 51, which would be of benefit to a population of about 13% of DMD patients. These facts highlight the urgent need to increase our battery of pharmacological interventions that should serve to ameliorate the condition and to improve the quality of life DMD patients.

In the current work, we focused on Ca^{2+} dysregulation and aberrant ROS production due to their central role in the pathophysiology seen in DMD. We selected two compounds to be tested on models of DMD, namely doxorubicin and diapocynin.

The anthracycline antibiotic doxorubicin is a chemotherapeutic agent used in the treatment of various malignancies. Reports in the literature highlighted the efficacy of doxorubicin to target specifically $iPLA_2$, inhibiting its activity not only on enzymatic systems but also clinically in chronic anthracycline treatment regimens. This enzyme is reported to modulate the enhanced Ca^{2+} influx through SOCs and SACs reported to be major mediators of the enhanced Ca^{2+} entry in DMD. The aims of this project were to assess if doxorubicin inhibits $iPLA_2$ in skeletal muscle cells, to investigate its consequences on Ca^{2+} handling, and to evaluate if these effects would convey an improvement of dystrophic skeletal muscle function.

The second compound investigated in this study, diapocynin, is a dimer of apocynin, a classical NOX inhibitor. Several reports have shown the lack of ROS inhibitory effect of the often-used apocynin in non-phagocytic cells and even a ROS promoting effect (Vejrazka *et al.*, 2005). Apocynin seems to act as a prodrug that is metabolised into diapocynin, the active NOX inhibitory moiety in phagocytic cells. The aims of this project were to synthesize diapocynin, evaluate its ROS inhibitory effects, investigate the biochemical consequences of such an inhibition and finally to evaluate its usefulness in an *in vivo* treatment protocol in *mdx* mice.

Chapter 2: Inhibition of iPLA$_2$β and of stretch-activated channels by doxorubicin alters dystrophic muscle function

Published in the *British Journal of Pharmacology*, 2013 Aug; 169(7):1537-50.

Inhibition of iPLA$_2$β and of stretch-activated channels by doxorubicin alters dystrophic muscle function

H M Ismail[1,2], O M Dorchies[1,3], R Perozzo[2], M K Strosova[1], L Scapozza[2] and U T Ruegg[1]

[1]Pharmacology; [2]Pharmaceutical Biochemistry, Geneva-Lausanne School of Pharmaceutical Sciences, University of Geneva and University of Lausanne, 30 Quai Ernest-Ansermet, Geneva 4, Switzerland; [3]Department of Cell Biology, University of Geneva, 30 Quai Ernest-Ansermet, Geneva 4, Switzerland.

Corresponding author: Urs T. Ruegg, Urs.ruegg@unige.ch

Summary

Background and purpose

Chronic elevation in intracellular Ca^{2+} concentration participates in death of skeletal muscle from mdx mice, a model for Duchenne muscular dystrophy (DMD). Candidate pathways mediating this Ca^{2+} overload involve store-operated channels (SOC) and stretch-activated channels (SAC), which are modulated by the Ca^{2+}-independent form of phospholipase A_2 ($iPLA_2$). We investigated the effect of doxorubicin (Dox), a chemotherapeutic agent reported to inhibit $iPLA_2$ in other systems, on the activity of this enzyme and on the consequences on Ca^{2+} handling and muscle function in mdx mice.

Experimental approach

Effects of Dox on PLA_2 activity, ROS production, and on Ca^{2+} influx were investigated in C2C12 and mdx myotubes. The mechanism of Dox-mediated $iPLA_2$ inhibition was evaluated using purified 6x His-tagged enzyme. Aequorin technology was used to assess Ca^{2+} concentrations underneath the plasma membrane. Isolated muscles were exposed to fatigue protocols and eccentric contractions to evaluate the effects of Dox on muscle function.

Key results

Dox at 1-30 µM inhibited $iPLA_2$ activity in cells and of the purified enzyme. Dox also inhibited SAC- but not SOC-mediated Ca^{2+} influx in myotubes. Stimulated elevations of Ca^{2+} concentrations below the plasmalemma were also blocked. Exposure of excised muscle to Dox was not deleterious to force production and promoted recovery from eccentric contractions.

Conclusions and implications

Dox showed efficacy against targets known to play a role in the pathology of DMD, namely $iPLA_2$ and SAC. The potent SAC inhibitory effect of Dox is a novel finding that can explain partly the cardiomyopathy seen in chronic anthracycline treatment.

Keywords

Dystrophin, mdx, doxorubicin, muscle, calcium, phospholipase A_2, stretch-activated channels, store-operated channels, aequorin, reactive oxygen species

Abbreviations

$AACOCF_3$, arachidonyl trifluoromethyl ketone; DMD, Duchenne muscular dystrophy; DMEM, Dulbecco's modified minimal essential medium; Dox, doxorubicin; EDL, extensor digitorum longus muscle; $iPLA_2$, Ca^{2+} independent phospholipase A_2; L_0, optimum length; MAFP, methyl arachidonyl fluorophosphonate; NOX, NADPH oxidases; PSS, physiological salt solution; ROS, reactive oxygen species; SAC, stretch-activated channels; ; BEL, bromoenol lactone; SOC, store-operated channels; SOL, soleus muscle.

Introduction

Duchenne muscular dystrophy (DMD) represents the most frequent muscular dystrophy and affects 1 in approximately 4000 male births. Mutations in the dystrophin gene on chromosome Xp21 result in the absence of the 427 kD protein dystrophin, a key component in a complex of proteins that connects the cytoskeleton to the extracellular matrix. The lack of dystrophin leads to mechanical instability of the cell membrane (Gailly, 2002) and renders it more susceptible to rupture (Petrof *et al.*, 1993) causing elevated Ca^{2+} influx and increased susceptibility to oxidative stress (Lawler, 2011), which activate each other in a vicious cycle that contributes to DMD pathogenesis. Several studies have suggested that the rise in intracellular Ca^{2+} is an important initiating event in the pathogenesis of dystrophic muscle (Hopf *et al.*, 2007; Millay *et al.*, 2009; Whitehead *et al.*, 2006). The increased Ca^{2+} entry occurring during activity, in particular during eccentric exercise, may lead to local proteolytic activation of cationic channels, and result in a further increase of Ca^{2+} entry (Alderton & Steinhardt, 2000). Stretch-activated channels (SAC) and store-operated channels (SOC) are regarded as candidates for this excessive Ca^{2+} influx (Ruegg *et al.*, 2012). Physiological and pharmacological data indicate that these channels belong to the same channel population or share common constituents (Ducret *et al.*, 2006). Earlier work from our lab and others showed that SOCs and SACs are regulated, at least in part, by the Ca^{2+} independent form of phospholipase A_2 ($iPLA_2\beta$) (Boittin *et al.*, 2006; Bolotina, 2008; Burkholder, 2009). PLA_2 activity has been shown to be up to 10-fold higher in muscles from DMD patients compared to normal controls (Lindahl *et al.*, 1995). Muscles from mdx^{5Cv} mice, a mouse model for DMD, also showed increased $iPLA_2$ expression (Boittin *et al.*, 2006). All these findings led to the hypothesis that inhibition of $iPLA_2$ would reduce the excessive Ca^{2+} entry and ameliorate the pathogenesis of DMD.

The anthracycline antibiotic doxorubicin (Dox), and its congener, daunorubicin, have been used since the 1970s to treat a variety of malignancies, including leukaemias, lymphomas and solid tumours (Gaitanis & Staal, 2010). Their antitumor effect has been attributed to intercalation between DNA strands (Jung & Reszka, 2001). The use of Dox and its analogues is limited by their cardiac toxicity. Swift and collaborators linked this to their ability to inhibit $iPLA_2$ (McHowat *et al.*, 2001; 2004; Swift *et al.*, 2003, 2007). Dox showed selectivity towards $iPLA_2$, the same enzyme that activates the Ca^{2+} channels thought to be involved in DMD pathogenesis. Dox-mediated inhibition of $iPLA_2$ was evident both *in vivo* and *in vitro* at clinically relevant concentrations as low as 100 nM.

We demonstrate here that Dox directly inhibits purified $iPLA_2$. Furthermore, Dox potently inhibits $iPLA_2$ activity in dystrophic myotubes and blocks SAC- but not SOC-mediated Ca^{2+} influx, affecting Ca^{2+} handling and production of reactive oxygen species (ROS). Using isolated fast and slow dystrophic muscles, we found that Dox was not deleterious to force production and promoted recovery from eccentric contractions.

Methods

Cell culture

Myotubes were prepared from EDL-MDX-2 myoblasts as described previously (Basset *et al.*, 2004; Wagner *et al.*, 2003). Briefly, myoblasts were plated on collagen-treated Petri dishes (Falcon, Becton Dickinson) in a proliferation medium containing a 1:1 mixture of Dulbecco's modified minimal essential medium (DMEM, Invitrogen) with 4.5 g/L glucose and MCBD202 (supplemented with $NaHCO_3$ and 1% v/v Glutamax II x100; Gibco), 10% foetal bovine serum (Invitrogen), 1% Ultroser SF (Biosepra), and 10 µg/mL ciprofloxacin (Bayer). The myoblasts were cultured on a feeder layer of 10T½ fibroblasts to support the growth and viability of the muscle cells (Pinset *et al.*, 1991). Briefly, the 10T½ fibroblasts were inactivated for 4 hours with mitomycin C (2 µg/mL; Sigma) in DMEM containing 10% foetal bovine serum and 10µg/mL ciprofloxacin. Cells were then seeded in the same proliferation medium as above at densities of 40,000 EDL-MDX-2 myoblasts and 30,000 inactivated fibroblasts per well in 24-well plates coated with 1 µg/cm^2 Matrigel (Becton Dickinson). After 2 days, myotube formation was induced by changing the medium to a differentiation medium consisting of 1:1 v/v DMEM and MCDB202 medium, supplemented with 1.7% foetal bovine serum, 3.3 % horse serum (Invitrogen), 10 µg/mL insulin (Sigma) and 10 µg/mL ciprofloxacin. After 3-4 days, mature contracting myotubes were obtained.

C2C12 myoblasts were plated in 24-well plates at a density of 30,000 cells per well in DMEM supplemented with 10% foetal bovine serum, and 10 µg/mL ciprofloxacin. When 60-80% confluent, myotube formation was induced by switching to differentiation medium (DMEM containing 2% horse serum and ciprofloxacin as above). Four days later, the cultures were used for the experiments.

Determination of PLA_2 activity

PLA_2 activity was measured using a cell-permeant fluorescent probe, PED-6 (Invitrogen). PED-6 is cleaved by PLA_2, to release BODIPY, a green fluorescent compound. The measured fluorescence is proportional to PLA_2 activity. Briefly, EDL-MDX-2 myotubes on a layer of 10T½ fibroblasts or C2C12 myotubes, were washed with a calcium-free physiological salt solution (PSS-; composition in mM: HEPES, 5; KCl, 5; $MgCl_2$, 1; NaCl, 145; glucose, 10 and EGTA, 0.2) to promote activation of $iPLA_2$. PED-6 (1 µM) was added and the fluorescence increment was measured over a period of 30 min at 37°C using a FLUOStar Galaxy fluorimeter (BMG Laboratories, Offenburg, Germany) set for measurements every 15s with an excitation wavelength of 488 nm, and emission at 520 nm (Reutenauer-Patte *et al.*, 2012).

Cloning of mouse $iPLA_2\beta$ into expression plasmid

A pCMV6-Kan/Neo vector containing the mouse $iPLA_2\beta$ transcript variant 1 (Ref. MC202080, TrueClone, Origene) was used for cloning the full-length mouse $iPLA_2\beta$ cDNA and inserting 6xHis tags in a pAAV-CMV-MCS expression vector (Ref. VPK-410-SER2, Cell Biolabs). Briefly, the full-length mouse $iPLA_2\beta$ cDNA was amplified by PCR using the high-fidelity Phusion DNA polymerase (New England Biolabs) and primers (Microsynth) designed for inserting SalI and BglII restriction sites as well as a 6xHis tag with a short flexible Gly-Ser linker at either the N-terminus (primers 372Fwd + 372Rev) or the C-terminus (primers 373Fwd + 373Rev): primer 372Fwd: 5'-ATG CAG TCG ACA TGC ATC ATC ACC ATC ACC ACG GCA GCC AGT TCT TCG GAC GCC TCG-3'; primer 372Rev: 5'-ATG CAA GAT CTT CAG GGA GAC AGC AGC AGC TGG-3'; primers 373Fwd: 5'-ATG CAG TCG ACA TGC AGT TCT TCG GAC GCC T-3'; primers 373Rev: 5'-ATG CAA GAT CTT CAC TAG TGG TGA TGG TGA TGA TGG CTG CCG GGA GAC AGC AGC AGC TGG-3'. The SalI-BglII-digested PCR products were gel-purified and ligated into dephosphorylated SalI-BglII-digested pAAV-CMV-β-globin intron-MCS expression vector. Competent *E coli* were transformed, positive clones selected, and sequence identity verified (Fasteris) by classical procedures. The vectors pITER #63 (pAAV-CMV-N_{His}-$iPLA_2\beta$) and pITER #64 (pAAV-CMV-C_{His}-$iPLA_2\beta$) were selected for further expression and purification steps.

Expression and purification of recombinant mouse $iPLA_2\beta$

HEK293 cells cultured in 6-well plates were transfected when about 60% confluent with pITER #63 or pITER #64 using Lipofectamine 2000 (Life Technologies) according to the provider's recommendations. HEK293 cells transfected with pITER#10 (pAAV-CMV vector expressing the red

fluorescent reporter DsRedExpress2) were used to monitor the efficacy of the transfection. About 44 h post-transfection, the supernatant was discarded, cells were gently scrapped in ice-cold lysis buffer (20 mM sodium phosphate, 10% glycerol, pH 7.8), 800 µL per well. Cells were broken by passing them 10 times through a 26-G needle, and the suspension was sonicated. After centrifugation at 10000 *g* for 20 min at 4°C, the clarified supernatants were loaded onto a 1 mL HisTrap FF column (GE Healthcare Life Sciences) loaded with nickel, washed with buffer A (20 mM sodium phosphate, 500 mM NaCl, 10% glycerol, pH 7.8) containing 4% buffer B (20 mM sodium phosphate, 500 mM NaCl, 500 mM imidazole, 10% glycerol, pH 7.8), and finally eluted using a gradient of 4 to 100% buffer B (10 column volumes) with a flow rate of 1 mL/min. The PLA$_2$ activity in the fractions was assayed using PED6 as above. The fractions showing the highest activity were pooled. Aliquots of the homogenates and of the fractions collected during the purification process were resolved by SDS-PAGE using gradient gels containing 6% acrylamide and 0% glycerol (top) to 11% acrylamide and 10% glycerol (bottom) and with 10 mM 2-mercaptoethanol in the cathode chamber. Coomassie Blue staining and immunoblotting with a rabbit polyclonal antibody raised against iPLA$_2$β (Cayman Chemical) were performed according to classical procedures to check the purity and identity of N_{His}-iPLA$_2$β and C_{His}-iPLA$_2$β.

Determination of ROS production

Oxidative stress was measured using DCFH-DA (Invitrogen), a probe for ROS that readily enters cells, becomes deacetylated into the non-fluorescent membrane impermeant DCFH, which can react with a variety of reactive oxygen/nitrogen species such as hydrogen peroxide, superoxide and peroxynitrite to yield dichlorofluorescin (DCF^-), a fluorescent compound. Following our procedure (Dorchies *et al.*, 2009), cells were washed twice with PSS- and incubated with 20µM of DCFH-DA in PSS- for 1 h to allow sufficient loading of the cells. Subsequently, compounds to be tested were added and the development of the fluorescent signal was monitored with a FLUOStar Galaxy fluorimeter, as described above.

$^{45}Ca^{2+}$ influx under conditions of store depletion and hypo-osmotic shock

$^{45}Ca^{2+}$uptake was recorded as described by Passaquin and colleagues (Passaquin *et al.*, 1998) with minor modifications. To quantify SAC activity, myotube cultures were washed twice with PSS containing 1.2 mM Ca^{2+} (PSS+), pre-incubated at 37°C for 15 min with test compounds and then exposed to a hypo-osmotic PSS+ (100 mOsm obtained by decreasing the NaCl concentration from

145 to 25mM) containing 1µCi/mL of $^{45}Ca^{2+}$. Such a procedure has been shown to cause myotube swelling, distension of the plasma membrane, and opening of SAC (Fanchaouy *et al.*, 2009). Ca^{2+} influx was stopped by placing the cultures on ice and washing four times with 0.5 mL of ice-cold PSS-. Cells were subsequently lysed with 0.5 mL of 1N NaOH, and the radioactivity in the lysates was determined by scintillation counting (Ultima Gold, Packard, Groningen, NL) using a beta-counter (LKB Wallac 1217 Rackbeta, Turku, Finland).

To study SOC activity, a protocol similar to that used on isolated fibres (Boittin *et al.*, 2006) was employed with slight modifications. Briefly, myotube cultures were washed twice with PSS-, pre-incubated for 15 min at 37°C in 200 µL PSS-, and finally exposed for 15 min to PSS- containing the test compounds and 5µM thapsigargin to ensure complete depletion of the intracellular Ca^{2+} stores. Calcium influx was initiated by switching to PSS+ containing 1 µCi/mL $^{45}Ca^{2+}$ and the test compounds. After 10 min, cells were washed, lysed and the radioactivity was determined as above.

Measurement of subsarcolemmal Ca^{2+} concentrations

Myoblasts were transfected with plasmids allowing targeted expression of the Ca^{2+}-sensitive photoprotein aequorin at the plasma membrane , as described previously (Basset *et al.*, 2004). Briefly, 80,000 EDL-MDX-2 myoblasts were seeded on 13-mm diameter Thermanox coverslips (Nalge Nunc International) in four-well plates. When 80-90% confluent, growth medium was removed and transfection was carried out as described above. On the next day, the cells were placed in differentiation medium to induce myotube formation as above. The plasmids were pcDNAI expression vectors containing the wild-type aequorin coding sequence fused with the plasma membrane-targeting sequence from SNAP-25 for measurements of subsarcolemmal Ca^{2+}concentrations (Rizzuto *et al.*, 1992). Subsarcolemmal Ca^{2+} concentrations were determined after 3-4 days of differentiation. Briefly, myotubes were exposed to 5 µM coelenterazine (Calbiochem) for 1 h, and then superfused at a rate of 3 mL/min in a custom-made 0.5 mL chamber at 37°C (MecaTest, Geneva, Switzerland). Emitted luminescence was recorded every second with single photon-counting tubes (EMI 9789A, Electron Tubes Ltd., UK) using a computer with a photon-counting board (EMI C660). Signal calibration was done by permeabilizing cells with 100 µM digitonin in the presence of 10 mM $CaCl_2$ in order to consume all remaining aequorin. The increment in maximum amplitude upon exposure to hypo-osmotic shock was calculated in the presence and absence of Dox, or *S*-bromoenol lactone (*S*-BEL), a selective inhibitor of $iPLA_2$.

Isolated muscle experiments

To evaluate whether Dox affects skeletal muscle performance, a modification of the method described by Brooks and Faulkner (Brooks & Faulkner, 1988) was used. Dystrophic (mdx^{5Cv}) and wild type (C57BL/6J) mice were maintained in the animal facility of the School of Pharmaceutical Sciences and used in compliance with the local rules on animal experimentation and welfare (Authorization #106/3626/0 delivered by the Cantonal Veterinary Office of Geneva and approved by the Swiss Veterinary Office). Mice between 8 and 12 weeks of age were anesthetized, the extensor digitorum longus muscle (EDL) and soleus (SOL) muscles were exposed, and their proximal and distal tendons tied with silk sutures. The proximal tendons were tied to an isometric force transducer (Hugo Sachs Elektronik, March-Hugstetten, Germany), and the distal tendons fixed to a pin in vertical incubation chambers (Radnoti, Monrovia, CA, USA) filled with a physiological Ringer solution (composition in mM: NaCl 137; $NaHCO_3$ 24; glucose 11; KCl 5; $CaCl_2$ 2; $MgSO_4$ 1; NaH_2PO_4 1; and d-tubocurarine chloride 0.025) continuously bubbled with 95% O_2-5% CO_2. Muscles were stimulated by 0.2 ms square wave pulses generated by a Grass S88X stimulator (Grass Technologies, West Warwick, RI, USA), delivered via platinum electrodes on both sides of the muscles. After setting the optimum stimulating voltage and the optimum length (L_0), muscles were divided into two experimental groups. The first group served to evaluate the force and kinetics of contraction and relaxation before and after treatment with test compounds: After addition of vehicle to the bathing solution, a series of 3 phasic twitches was recorded. Then, the force-frequency dependency was established by delivering 500 ms-long pulses of increasing frequency (50, 100, and 150 Hz). Finally, after incubation with the compounds for 20 min, the procedure was repeated. The phasic twitch traces were used to determine the absolute phasic tension, the time-to-twitch-peak tension and the time for half-relaxation from the twitch peak. Muscles in the second group were exposed to vehicle or test compounds for 20 min prior to being subjected to two stimulation protocols of different intensity aimed at inducing two types of fatigue: The “mild intensity protocol” consisted of 20 tetanic stimuli at 100 Hz for a duration of 200 ms with 30s rest between contractions, and the “high intensity protocol” consisted of 60 tetanic stimuli at 80 Hz (EDL), or 60 Hz (SOL), for a duration of 1s every 4s. The change in muscle tension as the stimulations were repeatedly delivered was expressed as a percentage of the tension generated by the first stimulation. In another set of experiments, EDL muscles were placed in a 10 mL horizontal chamber in an eccentric muscle test system, Model 305C-LR (Aurora Scientific Inc., Ontario, Canada). The optimum stimulating voltage

and L_0 were set and EDL muscles were exposed to 10 contractions of 400 ms each at 100 Hz, 30s apart. One hundred and fifty ms after the initiation of each contraction, the muscle was stretched by a value of 9% of L_0 over a period of 100 ms at a speed of 0.9 L_0/s and maintained at that level for another 100 ms before returning to the original length at the end of the stimulation. Force loss and recovery after 20 min of rest were expressed for every muscle.

Statistics

Results are reported as mean ± S.E.M. Comparisons within each experiment were analysed by 1-way ANOVA followed by Dunnett's multiple comparison post-tests using the GraphPad Prism software, version 5. Differences were considered significant at values of $P \leq 0.05$.

Results

We tested the hypothesis that Dox inhibits $iPLA_2$ in normal and dystrophic skeletal muscle cells, and explored the consequences of Dox treatment on intracellular Ca^{2+} handling and muscle performance.

Doxorubicin inhibits PLA_2 activity in C2C12 and dystrophic myotubes

C2C12 cells grown into myotubes were used to evaluate the inhibitory effect of Dox on PLA_2. Experiments were done in the absence of Ca^{2+} and in the presence of 0.2 mM EGTA (PSS-) to chelate Ca^{2+} and maximize the contribution of $iPLA_2$ over other Ca^{2+} dependent isoforms (Reutenauer-Patte, 2012). Dox showed a concentration-dependent inhibition starting at 1 µM, and reaching a value of 33.0 ± 3.2% of non-treated cells at 60 µM as depicted in Figure 1. Dox was as potent as the most commonly used inhibitor for $iPLA_2$, *S*-BEL, at the same concentration of 30 µM. The inhibition exerted by the general PLA_2 inhibitor MAFP was greater than that of the $iPLA_2$-specific inhibitor *S*-BEL and the $cPLA_2$ selective inhibitor $AACOCF_3$. Thus, our results suggest that Dox preferentially inhibits $iPLA_2$, in accordance with previous data (Swift *et al.*, 2007).

We obtained similar results using EDL-MDX-2 dystrophic myotubes, our model cells for Duchenne muscular dystrophy. Dox at concentrations of 1 to 60 µM resulted in a reduction of the PED-6 signal down to 50.6 ± 9.5% of control activity (n=5-9). Again, when compared with *S*-BEL and $AACOCF_3$, Dox at 30 µM showed similar potency (Figure 1C).

Doxorubicin inhibits purified iPLA$_2$β through a direct interaction

Transfection of HEK293 cells with pITER #63 or pITER #64 resulted in overexpression of the N_{His}-iPLA$_2$β or C_{His}-iPLA$_2$β, respectively, to levels comparable to that of the control reporter gene DsRedExpress2 (Figure 2A, B). After lysis, both 6x His-tagged iPLA$_2$β enzymes present in the soluble fraction were nickel-affinity purified yieliding pure enzyme (Figure 2A, B). Using the pure C_{His}-iPLA$_2$β, Dox showed a concentration dependent inhibition with an IC_{50} value of around 16.5 µM (Figure 2C, 2D). Dox at 30 µM was as potent as the classical inhibitors *S*-BEL and MAFP used in the same concentration range.

Although the method described here resulted in the production of pure enzymes from the soluble fractions, the majority of the overexpressed iPLA$_2$β was found in the insoluble fractions of the homogenates, likely because of iPLA$_2$β aggregation through their ankyrin repeats (Hsu *et al.*, 2009). In an attempt to recover the iPLA$_2$β protein, the pellets were washed with a buffer containing 20 mM sodium phosphate, 134 mM NaCl, 10% glycerol and 1% n-octyl-β-D-glucopyranoside at pH 7.8, which removed most contaminants. After centrifugation as above, the resulting pellets were resuspended in lysis buffer and analysis revealed nearly-pure iPLA$_2$β (Figure 2A, 2B). Both the pellet-purified and the soluble fraction-purified C_{His}-iPLA$_2$β showed the same sensitivity to Dox and to PLA$_2$ inhibitors (not shown).

Doxorubicin exhibits a biphasic effect on ROS production in dystrophic myotubes

We investigated whether Dox affects ROS production in dystrophic skeletal muscle cells under conditions that maximize iPLA$_2$ activity. Dox caused a concentration-dependent increase in ROS production, amounting to 2-fold at 30 µM in the first 10 minutes. This rise was followed by an inhibition of the activity down to 77.0 ± 5.1% of control activity over the following 20 minutes (Figure 3). *S*-BEL had no effect, suggesting that iPLA$_2$β did not affect ROS production.

Doxorubicin inhibits $^{45}Ca^{2+}$ influx through SAC but not SOC

To study a potential effect of Dox on SAC, differentiated myotubes were subjected to a hypo-osmotic buffer, a procedure used to induce swelling and subsequent opening of SAC. After 5 minutes under hypo-osmotic conditions, $^{45}Ca^{2+}$ influx increased to a value of 252.6 ± 14.0% when compared to myotubes kept in an isotonic buffer. Dox at a concentration as low as 1 µM inhibited stretch-induced influx to an extent similar to that of 300 µM streptomycin or 30 µM of the spider

venom peptide GsMTx4, the most commonly used and specific SAC inhibitors (Whitehead *et al.*, 2006) or to 30 µM *S*-BEL (Figure 4A).

$^{45}Ca^{2+}$ influx via thapsigargin-stimulated SOC was increased to a value of 354.6 ± 26.3% compared to controls. Dox at concentrations up to 30 µM had no significant effect on SOC influx. Treating the cells with *S*-BEL or with the SOC blocker, BTP2 (Boittin *et al.*, 2006; Zitt *et al.*, 2004) resulted in about 90% inhibition (Figure 4B).

Dox alters subsarcolemmal Ca^{2+} under hypo-osmotic conditions

Muscle fibers or cultured myotubes prepared from dystrophic mice have been shown to display a 4- to 10-fold increase of $[Ca^{2+}]$ in the narrow space underneath the sarcolemma, as compared to wild-type cells, when analysed using the Ca^{2+}-sensitive photoprotein aequorin targeted to this space (Basset *et al.*, 2004). We used transfected muscle cells expressing aequorin restricted to this space.

Superfusing the myotubes with a hypo-osmotic buffer resulted in an increase of the maximum amplitude of subsarcolemmal $[Ca^{2+}]$ with a value of 3.01 ± 0.23 µM, while myotubes in normo-osmotic PSS+ remained at around 1.5 µM (Figure 5). Incubation with 10 or 30 µM Dox prior and during the hypo-osmotic shock limited this increase to a value of 1.66 ± 0.35 and 1.47 ± 0.13 µM, respectively, corresponding to about a 50% reduction of the stretch-induced $[Ca^{2+}]$ elevation in the sub-sarcolemmal space. Interestingly, *S*-BEL produced no significant effect.

Dox affects fatigability and recovery from eccentric contraction but not force production of isolated muscles

In experiments using isolated muscle, a concentration of 30 µM Dox was used, as this concentration showed efficacy on PLA_2 activity, ROS production and Ca^{2+} handling in cellular assays. To investigate the acute Dox effects on dystrophic muscle contraction parameters, we chose the EDL and the SOL muscles as models for the fast-contracting, fatigue sensitive muscles, and slow-contracting, fatigue insensitive muscles, respectively.

Acute treatment of EDL and SOL muscles with 30 µM Dox had no effect on either absolute phasic or tetanic forces (Figure 6). Neither did Dox have any effect on the kinetics of contraction, as evaluated by the time to peak and the time for half-relaxation from the peak.

In order to investigate the effects of Dox on fatigue, EDL and SOL muscles were consecutively exposed to two regimens of repeated tetanizations. When exposed to the mild-intensity protocol, SOL muscles did not lose force up to the 20th cycle, whereas the force of the dystrophic EDL muscles declined to 88.5 ± 2.0% of the initial values. This muscle fatigue was completely recuperated after 5 minutes of rest. Treating the EDL or SOL dystrophic muscle with 30 µM Dox did not affect their fatigability, whereas *S*-BEL treatment (30 µM) almost doubled the rate of force loss, yielding a force of 77.4 ± 3.7% of the initial values after only 20 mild contractions (Figure 7A).

Dystrophic EDL muscle exposed to the high intensity fatigue protocol showed a primary phase of potentiation of the force to a value of 30% above the initial force during the first 10 contractions before the force loss phase commenced. Treatment of the muscles with either Dox or *S*-BEL abolished the potentiation phase (Figure 7B). When SOL muscles were exposed to drastic fatigue, they displayed a pattern resembling that of mildly fatigued EDL. Non-treated dystrophic SOL muscles showed a decline of force to a value of 68.9 ± 2.8% of the initial values. Dox treatment caused a deterioration of muscle performance reaching a value of 60.6 ± 5.8% of initial values, similar to *S*-BEL, which attained a value of 60.8 ± 5.1% (Figure 7C).

To further explore the effects of Dox on muscle function, EDL muscles were exposed to a series of 10 eccentric contractions, i.e. tetanic contractions during which the muscles were stretched in a direction opposite to the contraction. Such lengthening contractions are known to be particularly deleterious to dystrophic muscles. In this assay, wild-type EDL muscle lost 30% of its initial force while dystrophic EDL lost around 40% (Figure 8A). Dox treatment did not cause further loss of force in dystrophic muscles. *S*-BEL, however, showed a significant deleterious effect since the force declined down to 42.2 ± 5.7%. After a 20-minute recovery period, wild-type muscles showed a marked recovery of 13.47 ± 1.0% of their pre-contraction value, while dystrophic muscle recuperated only slightly (by 2.7 ± 2.6%). Dox treated muscles recovered with a value of 11.6 ± 2.6%, while those treated with *S*-BEL displayed further deterioration of force during the recovery period, losing an additional 6.8 ± 3.7% (Figure 8B).

Discussion

In the current study, we report that Dox inhibits iPLA$_2$ activity in both wild-type and dystrophic skeletal muscle cells. Moreover, using the purified recombinant enzyme, we demonstrated, for the

first time, that Dox is able to directly inhibit iPLA$_2$β activity. Using a combination of assays, we also demonstrated the ability of Dox to inhibit Ca^{2+} influx though SAC but not SOC, to modulate ROS production, to alter fatigability, and to ameliorate the post-traumatic recovery of dystrophic muscles. Overall, our findings suggest that these effects resulted from both direct and indirect inhibition of iPLA$_2$β by Dox. A possible model showing the sites of action of Dox on these pathways is shown in Figure 9.

The ability of Dox to inhibit iPLA$_2$ activity in skeletal muscle cells is in accordance with earlier reports on cardiomyocytes (McHowat *et al.*, 2001; Swift *et al.*, 2003, 2007). Dox showed a similar potency towards iPLA$_2$ as *S*-BEL, currently the most potent and selective inhibitor of this enzyme. BEL is a suicide inhibitor, which covalently binds and irreversibly inhibits iPLA$_2$ (Hazen *et al.*, 1991). To evaluate if Dox inhibited the enzyme directly, we cloned the full length mouse iPLA$_2$β and introduced a histidine tag to allow affinity purification. Dox inhibited the purified iPLA$_2$β in our assays with an IC_{50} of about 16.5 µM indicating direct mode of inhibition. Nevertheless, this finding does not rule out other indirect interactions that could take place in intact cells.

A well-known consequence of Dox action in cells is a reduction of the ATP pool. In fact, Dox has been shown to inhibit key metabolic enzymes, such as glyceraldehyde-3-phosphate dehydrogenase and glucose-6-phosphate dehydrogenase, resulting in lowered ATP levels (Wolf & Baynes, 2006). iPLA$_2$β possesses an ATP binding pocket that is important for the enzymatic activity (Ackermann *et al.*, 1994) and ATP has been shown to stabilize the enzyme during purification (Balboa *et al.*, 1997). Therefore, one such indirect effect of Dox on iPLA$_2$β could be due to lowered ATP levels.

What are the molecular bases for Dox mediated alteration of ROS production?

We examined whether the reported effects of Dox on increasing ROS production in cardiac cells were also valid in skeletal muscle cells. Using DCFH-DA as a probe, we found that Dox had a biphasic effect on ROS production. A concentration-dependent increase in ROS production was evident immediately after adding Dox to the myotubes; it continued for 10 minutes. Thereafter, a slight apparent concentration-dependent inhibition of ROS production was observed (Figure 2).

The structure of Dox plays a major role to play in ROS production. Its quinone moiety undergoes redox cycling on flavoenzymes by electron transfer from these to Dox, thus reducing the quinone to the semiquinone. Subsequent electron transfer from this to oxygen results in the formation of superoxide and hydrogen peroxide, thereby reverting the semiquinone to quinone. This redox

cycling continues until the system becomes anaerobic, at which point oxygen radical production decreases and semiquinone begins to accumulate (Gutierrez, 2000). This phenomenon was reported to occur in mitochondria (Davies & Doroshow, 1986), to be associated with nitric oxide synthase (Fu *et al.*, 2004) or with cytochrome P450 (Bartoszek, 2002). ROS could also originate from a reduction of Dox by ferric ion of the heme moieties of nitric oxide synthase or NADPH oxidases (NOX). This was demonstrated to occur by the reversal of this effect using NOX inhibitors, and from the protection of mice deficient in gp^{91phox}, the core protein of NOX2, from Dox-induced cardiotoxicity (Gilliam & St Clair, 2011). In relation to redox-generated ROS, the group of Sarvazyan postulated that Dox-mediated inhibition of iPLA$_2$ was due to oxidation of cysteine residues on the enzyme (McHowat *et al.*, 2001).

All of the above mentioned mechanisms are likely to contribute to the increased ROS production seen in the early phase, while decreased ROS production in the late phase could be attributed to the system becoming anaerobic, or to depletion of co-factors.

Why does Dox cause SAC but not SOC inhibition?

The present report shows that Dox potently and completely inhibited Ca^{2+} influx through SAC but not SOC. In the past years, it has been established that SOC activity is mostly dependent on STIM1-Orai interactions (Cahalan, 2009), and that iPLA$_2$β plays a role in modulating SOC activity (Boittin *et al.*, 2006). The mechanisms by which iPLA$_2$β controls SOC are not fully clarified (Bolotina, 2008); however, we have shown earlier that in certain paradigms its role may be prominent (Boittin *et al.*, 2006). Also, further data from our lab using various pharmacological compounds such as NOX inhibitors and lipoxygenase inhibitors confirm a good correlation between iPLA$_2$ inhibition and SOC blockade in muscle cell cultures (Ismail *et al.*, manuscript in preparation; Dorchies *et al.*, unpublished data). On the other hand, other structurally unrelated compounds under testing in our lab, such as raloxifene and calmidazolium, failed to block SOC while reducing iPLA$_2$ activity as reported here for Dox (Dorchies *et al.*, unpublished data). The causes behind the apparent discrepancy between the fatty acid-releasing activity of iPLA$_2$, measured here by PED-6, and SOC inhibition might be the following: (i) the Dox-sensitive fatty acid-releasing activity of iPLA$_2$β might be independent from the ability of iPLA$_2$β to inhibit SOC; (ii) besides blocking iPLA$_2$β, Dox could have additional effects that compensate for iPLA$_2$-dependent SOC inhibition; (iii) the cross talk between

the two pathways involved in SOC influx could compensate for the incomplete $iPLA_2\beta$ inhibition seen in this work (Gwozdz *et al.*, 2012).

Besides the ability of Dox to inhibit $iPLA_2\beta$, our investigation reveals for the first time that Dox is a SAC inhibitor. This was evident at concentrations as low as 1 μM, and the effect was similar in extent to that produced by 300 μM streptomycin, a prototype SAC blocker or by 30 μM GsMTx4, the most selective SAC blocker reported in the literature (Whitehead *et al.*, 2006).

Although the mechano-sensing process leading to SAC opening has not yet been clearly identified, TRP channels have received much attention (Holle & Engler, 2011). Lysophospholipids produced by PLA_2 have been shown to activate some members of this family, such as TRPV2 (Monet *et al.*, 2009) and TRPCs (Beech *et al.*, 2009). Hence, by inhibiting lysophospholipid formation by $iPLA_2$, Dox could inhibit activation of these channels.

The following cascade mechanism has also been suggested to activate SACs: Membrane stretch stimulates NOX, the resulting increase in ROS (as $O_2\bullet^-$) leads to activation of c-Src kinase, causing opening of SAC and Ca^{2+} influx (Allen *et al.*, 2010). Dox by binding to ferric ion in NOX (Gilliam & St Clair, 2011), or by modulating c-Src kinase activity could possibly inhibit this cascade. In a recent report, Khairallah *et al.* showed that the microtubule network is responsible for the transmission of the mechano-transduction signal induced by muscle stretch to NOX (Khairallah *et al.*, 2012). Disruptors of the microtubule network, such as colchicine, resulted in ROS inhibition and subsequently failure of SAC activation. Dox has also been reported to cause disruptions in the microtubules system in cardiomyocytes (Rabkin & Sunga, 1987). This could possibly be another explanation for the Dox-mediated SAC inhibitory effect observed here.

Mechanical stress, such as the one due to stretching contractions, causes Ca^{2+} influx into the muscle not only through SAC but also through membrane tears (Allen *et al.*, 2010; McNeil & Khakee, 1992). Using an ionophore to increase intracellular Ca^{2+} levels, membrane damage occurred and protection was provided by PLA_2 inhibitors as well as by ROS scavengers (Duncan & Jackson, 1987; Howl & Publicover, 1990). Thus, the increased activity of $iPLA_2$, known to be present in dystrophic muscle (Boittin *et al.*, 2006; Lindahl *et al.*, 1995), would render the membrane more susceptible to mechanical damage, and hence increase Ca^{2+} influx through tears. Dox could counteract this effect by inhibition of $iPLA_2$.

To investigate the consequences of Dox action on SAC, and on the downstream local Ca^{2+} levels, targeted aequorin expression to the subsarcolemmal space was used. Dox also showed an inhibitory effect, which could not be attributed to iPLA$_2$ inhibition alone since *S*-BEL failed to do so. Indeed, our findings reveal that the concentration of Dox required for achieving full inhibition of iPLA$_2$β (30 µM) is much higher than that required for blocking SAC activity (1 µM), which strongly suggest that Dox-mediated SAC inhibition is not primarily the consequence of iPLA$_2$β inhibition.

To our knowledge, this is the first report demonstrating the ability of Dox to inhibit Ca^{2+} influx through SAC. We suggest that this effect is of clinical relevance to the cardiomyopathy induced by Dox in patients undergoing chemotherapy. SAC play a role in heart adaptation to increased perfusion pressure. One of the heart's mechanisms to adapt to this is by increasing the force of contraction through activation of SAC (Calaghan & White, 2004). Dox, by inhibiting stretch-induced Ca^{2+} influx, would reduce this compensatory mechanism. This is consistent with an observation that was made in mice chronically treated with streptomycin: Treatment led to improved skeletal muscle function and quality, whereas the cardiac muscle deteriorated (Jorgensen *et al.*, 2011).

Dox effects on isolated muscles

Isolated EDL and SOL muscles were used to assess functional effects. Dox neither affected force production nor contraction kinetics. High concentrations of Dox (up to 175 µM) were reported to reduce force and accelerate fatigue (Van Norren *et al.*, 2009), but this was not observed at clinically relevant concentrations (1 to 5 µM) (Gilliam *et al.*, 2009). Treatment of EDL muscles with Dox did not alter fatigability in the mild fatigue protocol.

S-BEL caused a rapid decline of force under repeated tetanic contractions. This is very likely due to an inhibition of SOC and impaired refilling of the Ca^{2+} stores, essential for maintaining force. Alternatively, this decline could be due to the ability of *S*-BEL to inhibit voltage-gated Ca^{2+} channels as has been shown in smooth muscle (Chakraborty *et al.*, 2011), causing reduced excitation-contraction coupling and leading to force loss.

When the high intensity protocol was used to induce fatigue, post-tetanic potentiation was observed in EDL, but not in the SOL, muscles. This was abolished in Dox and *S*-BEL treated EDL muscles. Post-tetanic potentiation is commonly seen when muscles are exposed to repeated submaximal contractions leading to an augmented force production before fatigue takes over. It is prevalent in fast twitch muscles, such as the EDL, almost absent in slow twitch muscles, such as the

SOL (Hamada *et al.*, 2000), is due to phosphorylation of myosin light chains by the Ca^{2+}/calmodulin-dependent myosin light chain kinase (Zhi *et al.*, 2005), and corresponds with our results. Our finding that Dox and *S*-BEL abolished this post-tetanic potentiation in EDL muscle strongly supports the idea that these compounds interfere with key mediators, such as Ca^{2+} signalling, phosphorylation status, and ATP availability, leading to the disappearance of the initial potentiation phase and, ultimately, to acceleration of fatigue, which was also observed (Figure 7B). As mentioned above, other factors likely involved in these effects are Dox-mediated inhibition of SERCA (data not shown) and *S*-BEL-mediated inhibition of SOC; both of which would prevent proper refilling of the SR and eventually facilitate the loss of force as seen in EDL and SOL muscle.

Exposure of EDL muscles from mdx^{5Cv} mice to eccentric contractions resulted in greater force loss and reduced recuperation when compared with wild-type EDL muscles (Figure 8A). This has been attributed to an increased Ca^{2+} influx through either SAC or membrane tears, and subsequent activation of calpains causing protein degradation (Zhang *et al.*, 2012; 2008). In the current study, Dox, which strongly blocked SAC, did not prevent the loss of force induced by eccentric contractions, but normalized post-injury recovery of the EDL muscle (Figure 8). In contrast, *S*-BEL, which inhibits both SAC and SOC activity, caused a dramatic loss of force that was further aggravated after cessation of the eccentric contractions (Figure 8). We propose that the impaired response of EDL muscles treated with S-BEL is due to SOC inhibition. This is not observed with Dox as it blocks SAC but not SOC.

What could be the links between Dox-mediated modulation of ROS, PLA_2 activity and muscle fragility?

Besides the role of $iPLA_2$ in modulating Ca^{2+} entry, it can also contribute to maintaining membrane homeostasis (Balboa & Balsinde, 2002). In fact, when ROS levels are elevated, membrane phospholipids become oxidized, and the resulting peroxides are preferentially cleaved by PLA_2 (Balboa & Balsinde, 2002). The $iPLA_2$ inhibitor *S*-BEL would disrupt this homeostatic mechanism, lead to a more vulnerable membrane, and contribute to the diminished muscle resistance observed here. Since both Dox and *S*-BEL inhibit $iPLA_2\beta$, one may suggest that a similar response to eccentric contractions should be seen after Dox or *S*-BEL treatment. However, our findings on recovery from eccentric contractions (Figure 8) show that this was not the case. The fact that Dox does not cause the same dramatic effects as *S*-BEL after eccentric contractions although both compounds inhibit $iPLA_2\beta$ directly may result from their differential ability (i) to accumulate into biological membranes,

to generate ROS, or to promote the formation of lipid peroxides, (ii) to inhibit SOC and other targets, and (iii) to alter calcium handling and downstream calcium-dependent pathways through reduction of mitochondrial Ca^{2+} uptake and of SERCA pump activity (Ismail *et al.*, unpublished data). Eventually, these differential properties of Dox and *S*-BEL would define specific sensitivities to stretch or tears upon damaging muscle contraction, resulting in toxicity with *S*-BEL but enhanced recovery with Dox.

Conclusion

Increased activity of $iPLA_2$ in muscle from Duchenne muscular dystrophy patients was reported over 15 years ago (Lindahl *et al.*, 1995); yet to date its role has not been fully clarified. In this study, we demonstrated the ability of Dox to inhibit $iPLA_2$ activity in cell cultures prepared from dystrophic and wild-type muscle and of the purified enzyme. For the first time, we report that Dox inhibits SAC. We also show that Dox was not detrimental to skeletal muscle function, but facilitated force recovery after damaging contractions.

Acknowledgments

This work was supported by grants from the Swiss National Science Foundation, the Association Française contre les myopathies (AFM, France) and the Duchenne Parent Project-The Netherlands (DPP-NL).

Conflicts of interest

None.

References

Ackermann EJ, Kempner ES, Dennis EA (1994). Calcium independent cytosolic phospholipase A_2 from macrophage-like P338D_1 cells - isolation and characterization. *J Biol Chem* 269(12): 9227-9233.

Alderton JM, Steinhardt RA (2000). Calcium influx through calcium leak channels is responsible for the elevated levels of calcium-dependent proteolysis in dystrophic myotubes. *J Biol Chem* 275(13): 9452-9460.

Allen DG, Gervasio OL, Yeung EW, Whitehead NP (2010). Calcium and the damage pathways in muscular dystrophy. *Can J Physiol Pharmacol* 88(2): 83-91.

Balboa MA, Balsinde J (2002). Involvement of calcium-independent phospholipase A_2 in hydrogen peroxide-induced accumulation of free fatty acids in human U937 cells. *J Biol Chem* 277(43): 40384-40389.

Balboa MA, Balsinde J, Jones SS, Dennis EA (1997). Identity between the Ca^{2+}-independent phospholipase A_2 enzymes from P388D_1 macrophages and Chinese hamster ovary cells. *J Biol Chem* 272(13): 8576-8580.

Bartoszek A (2002). Metabolic activation of adriamycin by NADPH-cytochrome P450 reductase; overview of its biological and biochemical effects. *Acta Biochimica Polonica* 49(2): 323-331.

Basset O, Boittin FX, Dorchies OM, Chatton JY, van Breemen C, Ruegg UT (2004). Involvement of inositol 1,4,5-trisphosphate in nicotinic calcium responses in dystrophic myotubes assessed by near-plasma membrane calcium measurement. *J Biol Chem* 279(45): 47092-47100.

Beech DJ, Bahnasi YM, Dedman AM, Al-Shawaf E (2009). TRPC channel lipid specificity and mechanisms of lipid regulation. *Cell Calcium* 45(6): 583-588.

Boittin FX, Petermann O, Hirn C, Mittaud P, Dorchies OM, Roulet E*, et al.* (2006). Ca^{2+}-independent phospholipase A_2 enhances store-operated Ca^{2+} entry in dystrophic skeletal muscle fibers. *J Cell Sci* 119(18): 3733-3742.

Bolotina VM (2008). Orai, STIM1 and iPLA$_2$beta: a view from a different perspective. *J Physiol* 586(13): 3035-3042.

Brooks SV, Faulkner JA (1988). Contractile properties of skeletal-muscles from young, adult and aged mice. *J Physiol* 404: 71-82.

Burkholder TJ (2009). Stretch-induced ERK2 phosphorylation requires PLA_2 activity in skeletal myotubes. *Biochem Biophys Res Commun* 386(1): 60-64.

Cahalan MD (2009). STIMulating store-operated Ca^{2+} entry. *Nat Cell Biol* 11(6): 669-677.

Calaghan S, White E (2004). Activation of Na^+-H^+ exchange and stretch-activated channels underlies the slow inotropic response to stretch in myocytes and muscle from the rat heart. *J Physiol* 559(1): 205-214.

Chakraborty S, Berwick ZC, Bartlett PJ, Kumar S, Thomas AP, Sturek M*, et al.* (2011). Bromoenol lactone inhibits voltage-gated Ca^{2+} and transient receptor potential canonical channels. *J Pharmacol Exp Ther* 339(2): 329-340.

Davies KJ, Doroshow JH (1986). Redox cycling of anthracyclines by cardiac mitochondria. I. Anthracycline radical formation by NADH dehydrogenase. *J Biol Chem* 261(7): 3060-3067.

Dorchies OM, Wagner S, Buetler TM, Ruegg UT (2009). Protection of dystrophic muscle cells with polyphenols from green tea correlates with improved glutathione balance and increased expression of 67LR, a receptor for (-)-epigallocatechin gallate. *Biofactors* 35(3): 279-294.

Ducret T, Vandebrouck C, Cao ML, Lebacq J, Gailly P (2006). Functional role of store-operated and stretch-activated channels in murine adult skeletal muscle fibres. *J Physiol* 575(Pt 3): 913-924.

Duncan CJ, Jackson MJ (1987). Different mechanisms mediate structural-changes and intracellular enzyme efflux following damage to skeletal-muscle. *J Cell Sci* 87: 183-188.

Fanchaouy M, Polakova E, Jung C, Ogrodnik J, Shirokova N, Niggli E (2009). Pathways of abnormal stress-induced Ca^{2+} influx into dystrophic mdx cardiomyocytes. *Cell Calcium* 46(2): 114-121.

Fu J, Yamamoto K, Guan ZW, Kimura S, Iyanagi T (2004). Human neuronal nitric oxide synthase one-electron reduction of adriamycin: role can catalyze of flavin domain. *Arch Biochem Biophys* 427(2): 180-187.

Gailly P (2002). New aspects of calcium signaling in skeletal muscle cells: implications in Duchenne muscular dystrophy. *Biochim Biophys Acta - Proteins & Proteomics* 1600(1-2): 38-44.

Gaitanis A, Staal S (2010). Liposomal doxorubicin and nab-paclitaxel: nanoparticle cancer chemotherapy in current clinical use. *Methods Mol Biol* 624: 385-392.

Gilliam LAA, Ferreira LF, Bruton JD, Moylan JS, Westerblad H, Clair DKS*, et al.* (2009). Doxorubicin acts through tumor necrosis factor receptor subtype 1 to cause dysfunction of murine skeletal muscle. *J Appl Physiol* 107(6): 1935-1942.

Gilliam LAA, St Clair DK (2011). Chemotherapy-induced weakness and fatigue in skeletal muscle: The role of oxidative stress. *Antioxid Redox Sign* 15(9): 2543-2563.

Gutierrez PL (2000). The metabolism of quinone-containing alkylating agents: Free radical production and measurement. *Front Biosci* 5: D629-D638.

Gwozdz T, Dutko-Gwozdz J, Schafer C, Bolotina VM (2012). Overexpression of Orai1 and STIM1 proteins alters regulation of store-operated Ca^{2+} entry by endogenous mediators. *J Biol Chem* 287(27): 22865-22872.

Hamada T, Sale DG, MacDougall JD, Tarnopolsky MA (2000). Postactivation potentiation, fiber type, and twitch contraction time in human knee extensor muscles. *J Appl Physiol* 88(6): 2131-2137.

Hazen SL, Zupan LA, Weiss RH, Getman DP, Gross RW (1991). Suicide inhibition of canine myocardial cytosolic calcium-independent phospholipase A_2. Mechanism-based discrimination between calcium-dependent and -independent phospholipases A_2. *J Biol Chem* 266(11): 7227-7232.

Holle AW, Engler AJ (2011). More than a feeling: discovering, understanding, and influencing mechanosensing pathways. *Curr Opin Biotech* 22(5): 648-654.

Hopf FW, Turner PR, Steinhardt RA (2007). Calcium misregulation and the pathogenesis of muscular dystrophy. *Sub-Cell Biochem* 45: 429-464.

Howl JD, Publicover SJ (1990). Permeabilzation of the sarcolemmal in mouse diaphragm exposed to BAY-K-8644 in vitro- time course, dependence on Ca^{2+} and effects of enzyme-inhibitors. *Acta Neuropathologica* 79(4): 438-443.

Hsu YH, Burke JE, Li S, Woods VL, Jr., Dennis EA (2009). Localizing the membrane binding region of Group VIA Ca^{2+}-independent phospholipase A_2 using peptide amide hydrogen/deuterium exchange mass spectrometry. *J Biol Chem* **284**(35)**:** 23652-23661.

Jorgensen LH, Blain A, Greally E, Laval SH, Blamire AM, Davison BJ*, et al.* (2011). Long-term blocking of calcium channels in mdx mice results in differential effects on heart and skeletal muscle. *Am J Pathol* 178(1): 273-283.

Jung K, Reszka R (2001). Mitochondria as subcellular targets for clinically useful anthracyclines. *Adv Drug Deliver Rev* 49(1-2): 87-105.

Khairallah RJ, Shi G, Sbrana F, Prosser BL, Borroto C, Mazaitis MJ*, et al.* (2012). Microtubules underlie dysfunction in duchenne muscular dystrophy. *Sci Signal* 5(236): ra56.

Lawler JM (2011). Exacerbation of pathology by oxidative stress in respiratory and locomotor muscles with Duchenne muscular dystrophy. *J Physiol* 589(Pt 9): 2161-2170.

Lindahl M, Backman E, Henriksson KG, Gorospe JR, Hoffman EP (1995). Phospolipase A_2 activity in dystrophinopathies. *Neuromuscular Disord* 5(3): 193-199.

McHowat J, Swift LM, Arutunyan A, Sarvazyan N (2001). Clinical concentrations of doxorubicin inhibit activity of myocardial membrane-associated, calcium-independent phospholipase A_2. *Cancer Res* 61(10): 4024-4029.

McHowat J, Swift LM, Crown KN, Sarvazyan NA (2004). Changes in phospholipid content and myocardial calcium-independent phospholipase A_2 activity during chronic anthracycline administration. *J Pharmacol Exp Ther* 311(2): 736-741.

McNeil PL, Khakee R (1992). Disruptions of muscle fiber plasma membranes. Role in exercise-induced damage. *Am J Pathol* 140(5): 1097-1109.

Millay DP, Goonasekera SA, Sargent MA, Maillet M, Aronow BJ, Molkentin JD (2009). Calcium influx is sufficient to induce muscular dystrophy through a TRPC-dependent mechanism. *Proc Natl Acad Sci USA* 106(45): 19023-19028.

Monet M, Gkika D, Lehen'kyi V, Pourtier A, Vanden Abeele F, Bidaux G*, et al.* (2009). Lysophospholipids stimulate prostate cancer cell migration via TRPV2 channel activation. *Biochim Biophys Acta* 1793(3): 528-539.

Passaquin AC, Lhote P, Ruegg UT (1998). Calcium influx inhibition by steroids and analogs in C2C12 skeletal muscle cells. *Brit J Pharmacol* 124(8): 1751-1759.

Petrof BJ, Shrager JB, Stedman HH, Kelly AM, Sweeney HL (1993). Dystrophin protects the sarcolemma from stresses developed during muscle contraction. *Proc Natl Acad Sci USA* 90(8): 3710-3714.

Pinset C, Mulle C, Benoit P, Changeux JP, Chelly J, Gros F*, et al.* (1991). Functional adult acetylcholine receptor develops independently of motor innervation in Sol 8 mouse muscle cell line. *Embo J* 10(9): 2411-2418.

Rabkin SW, Sunga P (1987). The effect of doxorubicin (adriamycin) on cytoplasmic microtubule system in cardiac cells. *J Mol Cell Cardiol* 19(11): 1073-1083.

Reutenauer-Patte J, Boittin FX, Patthey-Vuadens O, Ruegg UT, Dorchies OM (2012). Urocortins improve dystrophic skeletal muscle structure and function through both PKA- and Epac-dependent pathways. *Am J Pathol* 180(2): 749-762.

Rizzuto R, Simpson AW, Brini M, Pozzan T (1992). Rapid changes of mitochondrial Ca^{2+} revealed by specifically targeted recombinant aequorin. *Nature* 358(6384): 325-327.

Ruegg UT, Shapovalov G, Jacobson K, Reutenauer-Patte J, Ismail H, Dorchies OM*, et al.* (2012). Store-operated channels and Ca^{2+} handling in muscular dystrophy. In: *Store-operated Ca^{2+} entry (SOCE) pathways*, Groschner K, Graier WF, Romanin C (eds) Vol. 1, 1 edn, pp 449-457: SpringerWien.

Swift L, McHowat J, Sarvazyan N (2007). Anthracycline-induced phospholipase A_2 inhibition. *Cardiovasc Toxicol* 7(2): 86-91.

Swift L, McHowat J, Sarvazyan N (2003). Inhibition of membrane-associated calcium-independent phospholipase A_2 as a potential culprit of anthracycline cardiotoxicity. *Cancer Res* 63(18): 5992-5998.

Van Norren K, van Helvoort A, Argiles JM, van Tuijl S, Arts K, Gorselink M*, et al.* (2009). Direct effects of doxorubicin on skeletal muscle contribute to fatigue. *Brit J Cancer* 100(2): 311-314.

Wagner S, Dorchies OM, Stoeckel H, Warter JM, Poindron P, Takeda K (2003). Functional maturation of nicotinic acetylcholine receptors as an indicator of murine muscular differentiation in a new nerve-muscle co-culture system. *Pflugers Arch* 447(1): 14-22.

Whitehead NP, Streamer M, Lusambili LI, Sachs F, Allen DG (2006). Streptomycin reduces stretch-induced membrane permeability in muscles from mdx mice. *Neuromuscular Disord* 16(12): 845-854.

Wolf MB, Baynes JW (2006). The anti-cancer drug, doxorubicin, causes oxidant stress-induced endothelial dysfunction. *Biochim Biophys Acta* 1760(2): 267-271.

Zhang BT, Whitehead NP, Gervasio OL, Reardon TF, Vale M, Fatkin D*, et al.* (2012). Pathways of Ca^{2+} entry and cytoskeletal damage following eccentric contractions in mouse skeletal muscle. *J Appl Physiol* 112(12): 2077-2086.

Zhang BT, Yeung SS, Allen DG, Qin L, Yeung EW (2008). Role of the calcium-calpain pathway in cytoskeletal damage after eccentric contractions. *J Appl Physiol* 105(1): 352-357.

Zhi G, Ryder JW, Huang J, Ding P, Chen Y, Zhao Y*, et al.* (2005). Myosin light chain kinase and myosin phosphorylation effect frequency-dependent potentiation of skeletal muscle contraction. *Proc Natl Acad Sci USA* 102(48): 17519-17524.

Zitt C, Strauss B, Schwarz EC, Spaeth N, Rast G, Hatzelmann A*, et al.* (2004). Potent inhibition of Ca^{2+} release-activated Ca^{2+} channels and T-lymphocyte activation by the pyrazole derivative BTP2. *J Biol Chem* 279(13): 12427-12437.

Legend to figures and figures

Figure 1

Assessment of Dox effect on $iPLA_2$ activity in normal and dystrophic myotubes

PED-6 was used to measure the activity of PLA_2 in C2C12 and EDL-MDX-2 myotubes. Measurements were made in PSS devoid of Ca^{2+} and in the presence of 0.2 mM EGTA (PSS-) in order to chelate Ca^{2+} and maximize the contribution of $iPLA_2$ over other isoforms. Cells were incubated with test compounds at the indicated concentrations (µM) for 20 minutes prior to the measurements (n=3-14). The inhibitory effect was compared with the one of the selective $iPLA_2$ inhibitor *S*-BEL (30 µM), a selective $cPLA_2$ inhibitor $AACOCF_3$ (AA, 50 µM), and with the global PLA_2 inhibitor MAFP (25 µM). (A) Representative traces in C2C12 myotubes showing fluorescence increments over time resulting from the cleavage of PED-6 by cellular PLA_2 and its inhibition by increasing concentration of Dox (µM). (B) PLA_2 activity in C2C12 myotubes. (C) PLA_2 activity in EDL-MDX-2 myotubes. * $P \leq 0.05$, ** $P \leq 0.01$, *** $P \leq 0.001$.

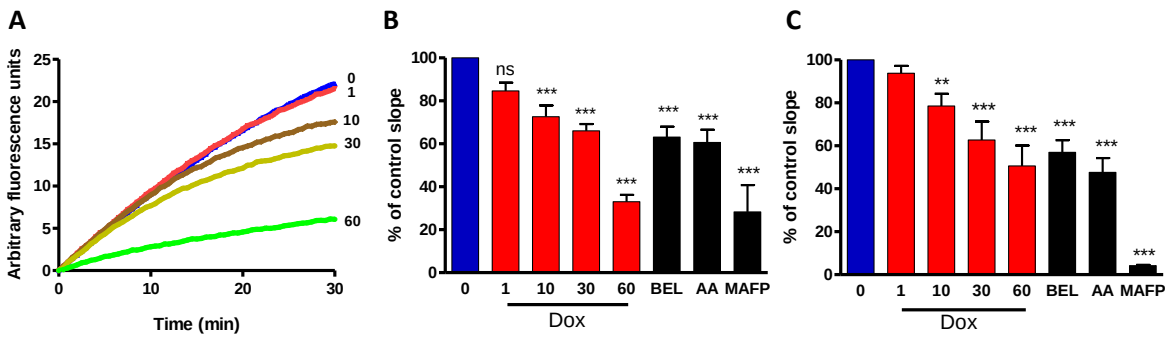
A
Arbitrary fluorescence units
25
20
15
10
5
0
0
10
20
30
Time (min)
0
1
10
30
60
B
% of control slope
100
80
60
40
20
0
ns
***
***
***
***
***
***
0
1
10
30
60
BEL
AA
MAFP
Dox
C
% of control slope
100
80
60
40
20
0
**
***
***
***
***
***
0
1
10
30
60
BEL
AA
MAFP
Dox

Figure 1

Figure 2

Inhibitory action of Dox on purified recombinant mouse iPLA$_2$β

Histidine-tagged iPLA$_2$β was overexpressed in HEK293 cells, purified by nickel affinity chromatography, and used to assay the ability of Dox to inhibit iPLA$_2$β activity through direct interaction. (A) Coomassie-stained gels, (B) Western-blot detection of iPLA$_2$β. Molecular weight markers (lane 1; in kDa). Homogenates from non-transfected cells (lane 2), cells overexpressing DsRedExpress2 (lane 3), or cells overexpressing C_{His}-iPLA$_2$β (lane 4) were prepared in lysis buffer. The overexpressed DsRedExpress2 and C_{His}-iPLA$_2$β are shown by arrows at around 25 kDa and 80 kDa, respectively. After centrifugation, the soluble fraction of the C_{His}-iPLA$_2$β-overexpressing cell lysate (lane 5) was loaded on a nickel column. The flow-through (lane 6) was depleted from C_{His}-iPLA$_2$β, and pure C_{His}-iPLA$_2$β was eluted from the nickel column (lane 7). The insoluble fraction (pellet) still contained most of the overexpressed C_{His}-iPLA$_2$β (lane 8). Washing the pellet with n-octyl-β-D-glucopyranoside removed most contaminants (lane 9) and yielded nearly-pure C_{His}-iPLA$_2$β that was readily recovered by centrifugation (lane 10). Protein obtained from the purified pellet was active and displayed the same sensitivity to Dox and classical PLA$_2$ inhibitors as the enzyme purified from the soluble fraction. (C) Traces (average of 4-8 determinations) showing the inhibition of pure C_{His}-iPLA$_2$β by increasing concentrations of Dox (μM) and by *S*-BEL (30 μM) using the fluorogenic substrate PED-6 which was added at the time indicated by the arrow. (D) Quantification of the inhibitory effect of the tested compounds at the indicated concentrations (μM) on C_{His}-iPLA$_2$β activity (n=4-8) and its comparison to the classical inhibitors MAFP (25 μM) and AACOCF$_3$ (AA, 50μM). *** P≤0.001. See text for details.

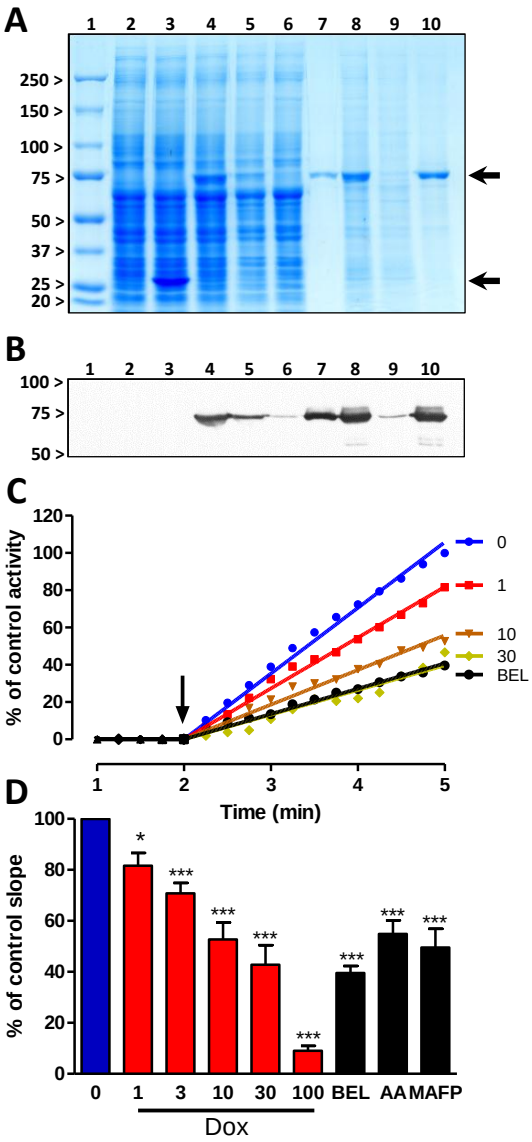
A
1 2 3 4 5 6 7 8 9 10
250 >
150 >
100 >
75 >
50 >
37 >
25 >
20 >
B
1 2 3 4 5 6 7 8 9 10
100 >
75 >
50 >
C
% of control activity
120
100
80
60
40
20
0
0
1
10
30
BEL
1 2 3 4 5
Time (min)
D
% of control slope
100
80
60
40
20
0
*
***
***
***
***
***
***
***
0 1 3 10 30 100 BEL AA MAFP
Dox

Figure 2

Figure 3

Modulation of ROS production by Dox in dystrophic myotubes

The probe DCFH-DA was used to monitor ROS production in EDL-MDX-2 myotubes. Cells were incubated with the probe for 1 hour prior to measurement in order to allow deacetylation and trapping of the probe. Test compounds were added at the indicated concentrations (µM) and fluorescence increments monitored over 30 minutes. (A) Representative traces in EDL-MDX-2 myotubes showing fluorescence increment over time resulting from the oxidation of DCFH by free radicals and its inhibition by increasing concentrations of Dox (µM). (B) Early phase (0-10 min) effect of Dox compared to control and 30 µM *S*-BEL. (C) Late phase (20-30 min), n=6-8 for B and C. * P≤0.05, ** P≤0.01, *** P≤0.001.

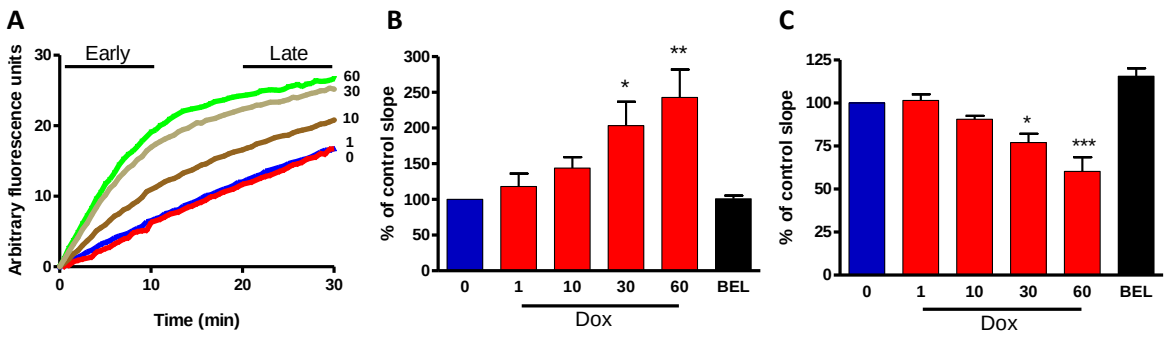
A
Early
Late
Arbitrary fluorescence units
Time (min)
60
30
10
1
0
B
% of control slope
Dox
BEL
C
% of control slope
Dox
BEL

Figure 3

Figure 4

Effect of Dox on hypo-osmotic and thapsigargin induced $^{45}Ca^{2+}$ influx

$^{45}Ca^{2+}$ was used to measure influx under conditions of hypo-osmotic shock (A) or in the presence of 5 µM thapsigargin (B) in EDL-MDX-2 myotubes. Cells were treated with 300 µM of streptomycin or 30 µM GsMTx4 (GsM), inhibitors of SAC, 10µM BTP2, an inhibitor of SOC, 30 µM *S*-BEL, an inhibitor of $iPLA_2\beta$ or Dox at the indicated concentrations in µM (n=3-15). * P≤0.05, **P≤0.01, *** P≤0.001.

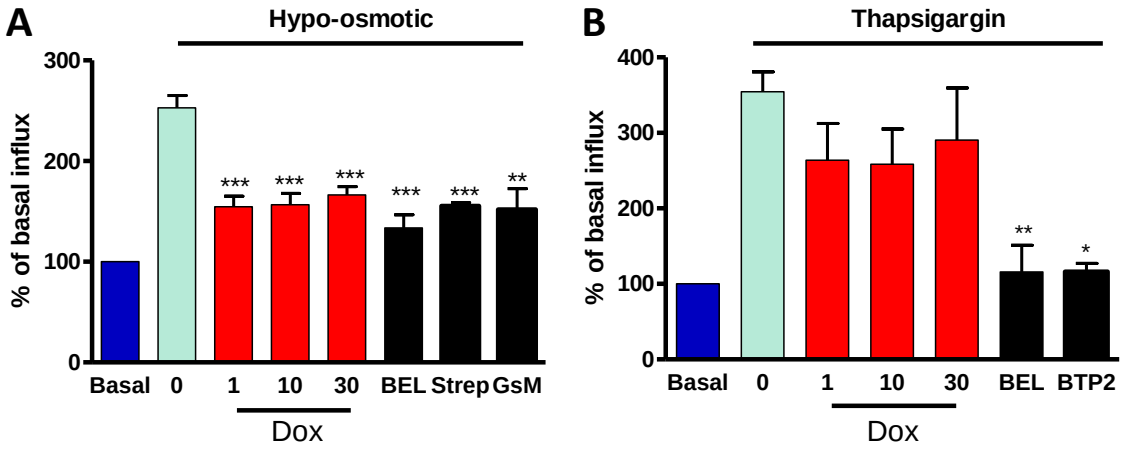
A
Hypo-osmotic
% of basal influx
300
200
100
0
***
***
***
***
***
**
Basal
0
1
10
30
BEL
Strep
GsM
Dox
B
Thapsigargin
% of basal influx
400
300
200
100
0
**
*
Basal
0
1
10
30
BEL
BTP2
Dox

Figure 4

Figure 5

Effect of Dox on subsarcolemmal Ca^{2+} in response to hypo-osmotic shock

The bioluminescent protein aequorin was targeted to the subsarcolemmal space in order to measure the responses to hypo-osmotic shock. (A) Representative traces showing responses to hypo-osmotic shock of EDL-MDX-2 myotubes transfected with SNAP-25 aequorin, treated or untreated with 30 µM Dox. (B) Difference between maximal amplitudes reached in myotubes treated with vehicle, Dox or *S*-BEL (30 µM). *P≤0.05, **P≤0.01, ***P≤0.001.

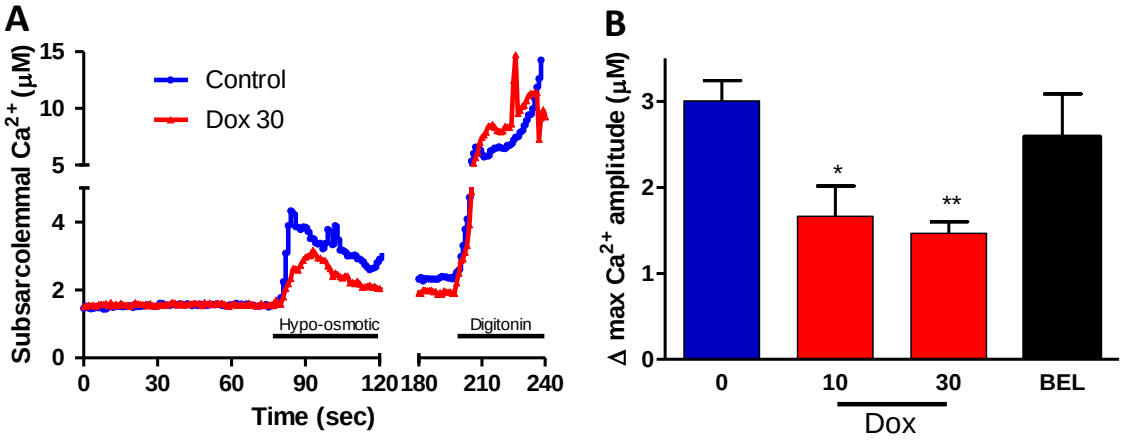
A
Subsarcolemmal Ca2+ (µM)
15
10
5
4
2
0
Control
Dox 30
Hypo-osmotic
Digitonin
0
30
60
90
120
180
210
240
Time (sec)
B
Δ max Ca2+ amplitude (µM)
3
2
1
0
*
**
0
10
30
BEL
Dox

Figure 5

Figure 6

Dox does not affect force production in isolated dystrophic EDL muscle

EDL muscles were isolated from 8-12 week old mdx^{5Cv} mice and maintained at their optimal length in oxygenated physiological buffer. A force-frequency relationship was established by electrical stimulation at 50, 100 and 150 Hz before, and 20 minutes after treatment with 30 µM Dox (n=5). Phasic twitches produced by single stimulation are shown for comparison.

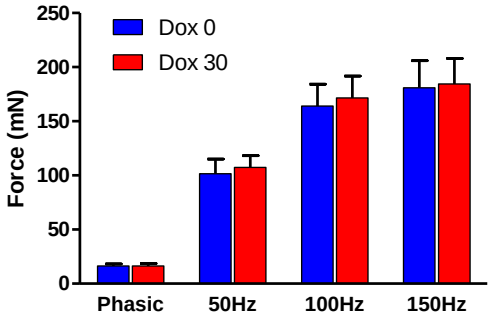
Dox 0
Dox 30
Force (mN)
250
200
150
100
50
0
Phasic
50Hz
100Hz
150Hz

Figure 6

Figure 7

Treatment with Dox or *S*-BEL affects fatigue in isometrically contracting EDL and SOL dystrophic muscle

Isolated EDL and SOL muscles were fatigued using low and high intensity fatigue procedures. (A) Low intensity fatigue in EDL muscles consisted of 20 contractions of 200 ms at 100 Hz, 30s apart (n=6-8). (B) High intensity fatigue in EDL muscles consisted of 60 contractions of 1s each at 80 Hz, repeated every 4 s (n=5-11). (C) High intensity fatigue in SOL muscle was carried out in the same manner as in EDL, but using 60 Hz instead of 80 Hz stimulations (n=5).

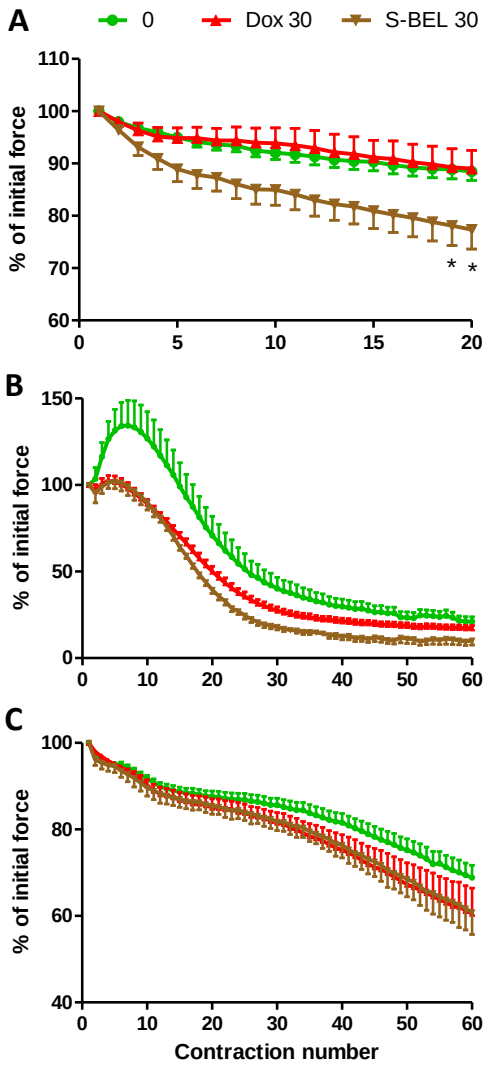
A
0
Dox 30
S-BEL 30
% of initial force
110
100
90
80
70
60
0
5
10
15
20
* *
B
% of initial force
150
100
50
0
0
10
20
30
40
50
60
C
% of initial force
100
80
60
40
0
10
20
30
40
50
60
Contraction number

Figure 7

Figure 8

Eccentric contractions of EDL muscles reveal different responses to Dox and *S*-BEL

EDL muscles were exposed to 10 eccentric contractions of 400 ms at 100 Hz, 30s apart. During each contraction the muscle was stretched to 109% of its optimum length. (A) Responses of dystrophic, wild-type (B6), Dox (30 µM), and *S*-BEL (30 µM)-treated EDL muscles. Upper and lower lines show statistical significances between dystrophic and wild-type, dystrophic and *S*-BEL-treated EDL muscles, respectively. (B) Force recovered as % of pre-contraction force after a 20 min rest period showing enhanced recovery of wild-type muscles, restoration of normal recovery with Dox and further deterioration in muscles treated with *S*-BEL (n=6-12). *P≤0.05, **P≤0.01, ***P≤0.001.

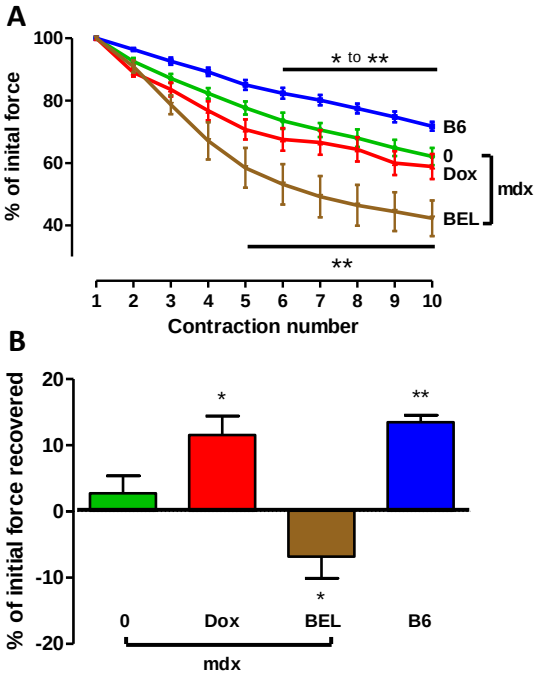
A
100
80
60
40
% of inital force
* to **
B6
0
Dox
BEL
mdx
**
1 2 3 4 5 6 7 8 9 10
Contraction number
B
20
10
0
-10
-20
% of initial force recovered
*
**
*
0
Dox
BEL
B6
mdx

Figure 8

Figure 9

A possible model for the effects of Dox on iPLA$_2$β, SAC, SOC, and fatigue in dystrophic muscle

In muscle cells, plasma membrane (PM) depolarisation (ΔΨ) triggers opening of the ryanodine receptors (RyR) and release of Ca^{2+} from the sarcoplasmic reticulum (SR) into the cytosol, initiating muscle contraction that is terminated after Ca^{2+} re-uptake by the sarco/endoplasmic reticulum calcium ATPase (SERCA) pump. Sustained contractile activity causes Ca^{2+} depletion from the intracellular stores, which triggers Ca^{2+} entry directly via STIM1-mediated formation of store-operated channels (SOC) as well as indirectly via activation of iPLA$_2$β and release of lysophospholipids (LPL). Contractile activity also stimulates Ca^{2+} entry through mechanosensitive stretch-activated channels (SAC), which also respond to iPLA$_2$β-derived LPL. In dystrophic cells, the activity of SAC, SOC, iPLA$_2$β, and NOX2 (a superoxide-generating enzyme) are reported to be enhanced, resulting in an excessive susceptibility to damages mediated by contraction, Ca^{2+} overload, oxidative stress and increased muscle fatigability. The present report describes the effects of Dox on several targets involved in dystrophic pathogenesis (the concentrations of Dox required for significant effects are shown in parentheses). We found that Dox (1-30 µM) inhibited iPLA$_2$β directly and probably also indirectly (see text for details). Dox (1 µM) was also very efficacious for preventing SAC influx. In addition, we observed that Dox (1-30 µM) slightly inhibited SERCA activity and decreased mitochondrial Ca^{2+} uptake under condition that activate SAC (data not shown). As a result of these actions, and although Dox can produce superoxide through redox cycling, the net effect of Dox was to enhance recovery of muscle from eccentric contractions.

Key. Plain arrows: direct mechanism of action, ion flux, or enzymatic reaction. Dashed arrows: Indirect mechanism of action. ⊕: Stimulatory action. Red blunt arrows: Dox-mediated inhibition.

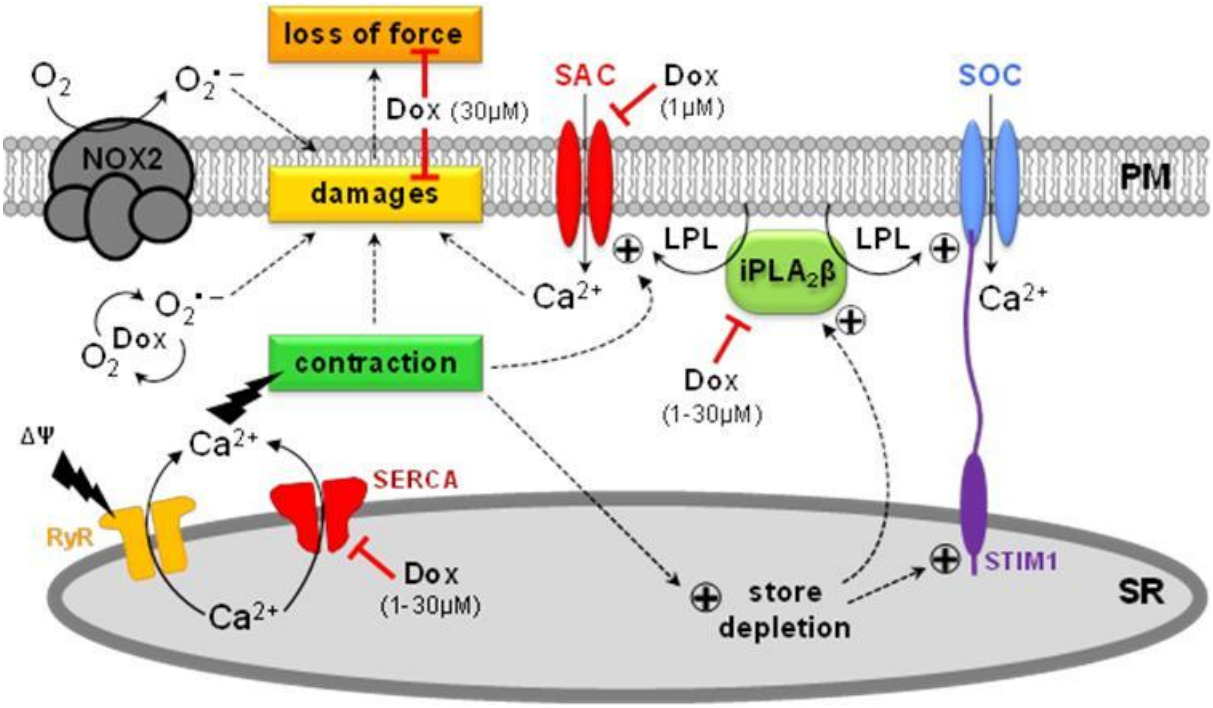
loss of force
Dox (30μM)
damages
NOX2
SAC
Dox
(1μM)
SOC
PM
LPL
iPLA2β
LPL
Ca2+
Ca2+
Dox
(1-30μM)
contraction
ΔΨ
Ca2+
SERCA
RyR
Dox
(1-30μM)
Ca2+
store
depletion
STIM1
SR

Figure 9

Chapter 3: Diapocynin, a NADPH oxidase inhibitor, reduces ROS production and prevents force loss in eccentrically contracting dystrophic muscle

In revision in PLoS One, September 2013

Diapocynin, a NADPH oxidase inhibitor, reduces ROS production and prevents force loss in eccentrically contracting dystrophic muscle

Hesham M Ismail[1,2], Leonardo Scapozza[2], Urs T Ruegg[1], Olivier M Dorchies[1,3]

[1]Pharmacology; [2]Pharmaceutical Biochemistry, Geneva-Lausanne School of Pharmaceutical Sciences, University of Geneva and University of Lausanne, 30 Quai Ernest-Ansermet, Geneva 4, Switzerland; [3]Department of Cell Biology, University of Geneva, 30 Quai Ernest-Ansermet, Geneva 4, Switzerland.

Corresponding author: Urs T. Ruegg, Urs.ruegg@unige.ch

Abstract

Elevation of intracellular Ca^{2+}, excessive ROS production and increased phospholipase A_2 activity contribute to the pathology in dystrophin-deficient muscle. Moreover, Ca^{2+}, ROS and phospholipase A_2, in particular $iPLA_2$, are thought to potentiate each other in positive feedback loops. NADPH oxidases (NOX) have been considered as a major source of ROS in muscle and have been reported to be overexpressed in muscles of mdx mice.

We report here on our investigations regarding the effect of diapocynin, a dimer of the commonly used NOX inhibitor apocynin, on the activity of $iPLA_2$, Ca^{2+} handling and ROS generation in dystrophic myotubes. We also examined the effects of diapocynin on force production and recovery ability of isolated EDL muscles exposed to eccentric contractions *in vitro*, a damaging procedure to which dystrophic muscle is extremely sensitive.

In dystrophic myotubes, diapocynin inhibited ROS production, abolished $iPLA_2$ activity and reduced Ca^{2+} influx through stretch-activated and store-operated channels, two major pathways responsible for excessive Ca^{2+} entry in dystrophic muscle. Diapocynin also prevented force loss induced by eccentric contractions of mdx muscle close to the value of wild-type muscle and reduced membrane damage as seen by Procion orange dye uptake. These findings highlight the central roles played by NOX, ROS, $iPLA_2$ and Ca^{2+} in the pathogenic cascade leading to muscular dystrophy and might be helpful for future therapeutic approaches.

Keywords

Apocynin, diapocynin, Duchenne muscular dystrophy, eccentric contractions, mdx, muscle, NADPH oxidase, phospholipase A2, reactive oxygen species, stretch activated channels, store operated channels

Abbreviations

BEL: Bromoenol lactone

DCFH-DA: 2',7'-dichlorohydrofluorescein diacetate

DMD: Duchenne muscular dystrophy

DPI: Diphenylene iodonium chloride

GsMTx-4: grammotoxin

$iPLA_2$: calcium-independent phospholipase A_2

NOX: NADPH oxidase

PBS: phosphate buffered saline

ROS: reactive oxygen species

SAC: stretch-activated channel

SOC: store-operated channel

Introduction

Duchenne muscular dystrophy (DMD) is a very severe muscle disease characterized by progressive skeletal muscle wasting. It is provoked by mutations in the gene encoding the protein dystrophin, leading to its absence in skeletal muscles of DMD patients (Koenig *et al.*, 1987), and causing loss of the dystrophin-glycoprotein complex and improper mechano-transduction. Dystrophin-deficient myofibres are more susceptible to contraction-induced injury, leading to necrosis, muscle wasting and premature death (De Luca, 2012).

There are numerous consequences of the absence of dystrophin on cellular signalling affecting muscle function and homeostasis of the myofibre. Of primary concern is the upregulated influx of Ca^{2+} through channels and transient breaks in the membrane (Hoffman & Dressman, 2001). Indeed, a number of studies have reported chronic elevation in intracellular Ca^{2+} concentrations in skeletal muscle fibres or in cultured myotubes from DMD patients and mdx mice, a mouse model for DMD. Stretch-activated channels (SACs) and store-operated channels (SOCs) are considered as candidates for mediating such an influx (Ducret *et al.*, 2006). Another consequence of the lack of dystrophin is increased activity of the calcium-independent isoform of phospholipase A_2 ($iPLA_2$), observed in biopsies from DMD patients (Lindahl *et al.*, 1995) and mdx mice (Boittin *et al.*, 2006). This enzyme has been reported to activate SOCs and SACs as evidenced by $iPLA_2$ inhibition (Ruegg *et al.*, 2012).

Another downstream consequence of the lack of dystrophin is increased reactive oxygen species (ROS) production. Markers of oxidative stress and lipid peroxidation are elevated in dystrophic muscles, even before the first symptoms of the disease appear (reviewed in Tidball and Wehling-Henricks (2007)). Furthermore, ROS have been proposed as possible mediators of dystrophic muscle damage as they can activate several Ca^{2+} channels and promote lipid peroxidation, resulting in sarcolemmal fragility and subsequent Ca^{2+} influx through micro-ruptures, seen in dystrophic muscle (Hoffman & Dressman, 2001). In fact, reciprocal amplification of Ca^{2+} influx and ROS production results in a vicious cycle that appears to be central in the dystrophic pathology (Shkryl *et al.*, 2009; Whitehead *et al.*, 2008). Several studies over the past decade were conducted in mdx mice to evaluate the effectiveness of anti-oxidants in ameliorating the pathological process, all of which showed benefit on selected parameters (Buetler *et al.*, 2002; Dorchies *et al.*, 2006; Hibaoui *et al.*, 2011; Nakae *et al.*, 2012; Whitehead *et al.*, 2008). On the other hand, clinical trials conducted with anti-oxidants did not show an improvement and some even resulted in deterioration of the

condition, which was attributed to lack of selectivity of the chosen anti-oxidant interventions against a defined target (Kim *et al.*, 2013).

For a long time mitochondria have been considered the main source of ROS production in skeletal muscle during exercise. NADPH oxidases (NOXes), lipoxygenases, monoamine oxidase and xanthine oxidase have been proposed as other relevant sources of ROS in muscle cells (reviewed in (Barbieri & Sestili, 2012)). It was recently shown that NOXes contribute to ROS production in skeletal muscle to a larger extent than mitochondria (Sakellariou *et al.*, 2013b; Shkryl *et al.*, 2009; Xia *et al.*, 2003), which makes NOXes attractive targets to treat DMD.

The NOX family members are transmembrane proteins that transport electrons across biological membranes to reduce oxygen to superoxide or H_2O_2 (Bedard & Krause, 2007). Total mRNA from skeletal muscle contains NOX4 and NOX2. NOX4 is a constitutively active monomeric enzyme, whereas NOX2 requires the translocation of several regulatory subunits ($p22^{phox}$, $p47^{phox}$ and $p67^{phox}$) to the membrane-spanning subunit $gp91^{phox}$ to be active (Bedard & Krause, 2007). NOX2 and all of its subunits, except p22, are overexpressed in skeletal muscles from 19-day old mice, just before the onset of necrosis, suggesting an early involvement of NOX in the pathology seen in DMD (Whitehead *et al.*, 2010). Another study showed that NOX4 mRNA is increased 5-fold in the left ventricles from 9-10 months old mdx mice (Spurney *et al.*, 2008).

In view of the importance of NOXes in various pathologies, a search for potent, efficacious, selective and non-toxic NOX inhibitors has been started. Several classes of compounds such as pyrazolopyridine, pyrazolopyrimidine, triazolopyrimidine, tetrahydroindole, fulvalene analogues have been shown to inhibit NOX activity (for a review see Kim *et al.* (2011)), and the synthetic peptide gp91ds-*tat* has also been shown to potently inhibit NOX (Rey *et al.*, 2001). However, the most commonly used experimental NOX inhibitor to date is apocynin. Apocynin was found to inhibit ROS production by NOXes in phagocytic cells whereas it failed to do so and even promoted ROS production in non-phagocytic cells (Vejrazka *et al.*, 2005). One explanation for this discrepancy is that phagocytic cells efficiently convert inactive apocynin monomers into active diapocynin through a peroxidase-mediated dimerization that is not operating in other cell types (Kanegae *et al.*, 2010; Vejrazka *et al.*, 2005).

In the current study, we synthetized diapocynin and evaluated its effect on key mediators in the pathogenesis of DMD, namely ROS production, $iPLA_2$ activity and Ca^{2+} influx through SOC and SAC in dystrophic skeletal muscle cells. We also investigated its effect on force loss induced by eccentric contractions of isolated dystrophic fast twitch muscles. Not only did diapocynin inhibit ROS production in dystrophic myotubes, but also $iPLA_2$ activity and Ca^{2+} influx. In addition, it reduced force loss induced by eccentric contractions to near-control values.

Materials and Methods

Pharmacological treatments

The present investigations used a combination of pharmacology, cell biology, and functional assays. In preliminary experiments, diapocynin showed significant alterations of the readouts at concentrations of 100 and 300 µM and were selected for further evaluation. For comparison purposes, apocynin was tested at a concentration 300 µM. The other compounds (BEL, BTP2, colchicine, DPI, GsMTx-4, streptomycin) were used at concentrations commonly reported in previous investigations in the field. These concentrations are around 3-10 times the IC_{50} of the targets in order to ensure maximum inhibitory effects (Ismail *et al.*, 2013a; Khairallah *et al.*, 2012; Whitehead *et al.*, 2006; 2010).

Diapocynin synthesis and characterization

Diapocynin was synthetized from apocynin (Sigma, Buchs, Switzerland) through an oxidative coupling reaction in the presence of ferrous sulfate and sodium persulfate as described (Wang *et al.*, 2008). The brown precipitate formed after this reaction was dissolved in 3N ammonia, re-crystallized in 6N HCl and washed 3 times with boiling water to yield pure diapocynin, as verified by NMR and mass spectrometry.

Cell culture

Myotubes were prepared from EDL-MDX-2 myoblasts co-cultured on a feeder layer of 10T½ fibroblasts as described previously (Basset *et al.*, 2004; Ismail *et al.*, 2013a). Briefly, EDL-MDX-2 and 10T½ were propagated on collagen-treated and on uncoated Petri dishes (Falcon, Becton Dickinson), respectively, in high-mitogen proliferation media. Cells were detached with trypsin and suspensions containing 80,000 EDL-MDX-2 myoblasts and 60,000 mitomycin C-inactivated 10T½

fibroblasts per ml were seeded in 24-well plates coated with 1 µg/cm^2 Matrigel (Becton Dickinson), 0.5 ml per well. After 2 days, myotube formation was induced by changing the proliferation medium to a low-mitogen differentiation medium. After 3-4 days contracting myotubes were obtained.

Determination of ROS production

ROS production was measured using 2',7' dichlorohydrofluorescein diacetate (DCFH-DA, Invitrogen, Zug, Switzerland), a probe that readily enters cells, which, upon de-acetylation by cellular esterases reacts with a variety of reactive oxygen/nitrogen species to yield fluorescent 2',7'-dichlorofluorescein (DCF). To perform these experiments, myotube cultures were washed twice with Ca^{2+}-free physiological salt solution (PSS-; composition in mM: HEPES 5, KCl 5, $MgCl_2$ 1, NaCl 145, glucose 10, EGTA 0.2) and incubated with 20 µM of DCFH-DA for 1h to allow sufficient loading of the cells. Subsequently, compounds to be tested were added and the development of the fluorescent signal was monitored with a FLUOStar Galaxy fluorimeter (BMG Laboratories, Offenburg, Germany) as described (Boittin *et al.*, 2006).

Determination of PLA_2 activity

PLA_2 activity was measured using the probe PED-6 (Invitrogen), which is cleaved by PLA_2 to release BODIPY, a green fluorescent compound. Briefly, EDL-MDX-2 myotube cultures were washed twice with PSS- and incubated with test compounds for 20 min. Subsequently, PED-6 (1 µM) was added and the fluorescence increment was measured over a period of 30 min at 37°C as described (Reutenauer-Patte *et al.*, 2012).

$^{45}Ca^{2+}$ influx triggered by store depletion and hypo-osmotic shock

$^{45}Ca^{2+}$uptake was quantified as described by Ismail *et al.* (2013a). To measure the activity of SACs, myotube cultures were washed twice with PSS containing 1.2 mM Ca^{2+} (PSS+), pre-incubated at 37°C for 15 min with test compounds and then exposed to 200 µl/well of a hypo-osmotic PSS+ (100 mOsm obtained by decreasing the NaCl concentration from 145 to 25 mM) containing 1 µCi/ml of $^{45}Ca^{2+}$. Plates were then placed on ice, and cultures were washed 4 times with ice-cold PSS- to remove remaining extracellular $^{45}Ca^{2+}$ before being lysed with 0.5 ml of 1N NaOH. The radioactivity in the lysates was determined by scintillation counting (Ultima Gold, Packard, Groningen, NL) using a beta-counter (LKB Wallac 1217 Rackbeta, Turku, Finland).

To study the activity of SOCs, the cultures were washed twice with PSS+, pre-incubated for 15 min at 37°C with test compounds in 200 µl Ca^{2+}-free PSS, and further exposed to 5 µM thapsigargin to deplete intracellular Ca^{2+} stores in the presence of test compounds. After 10 min, PSS+ containing 1 µCi/ml $^{45}Ca^{2+}$ was added and uptake was measured after another 10 min. $^{45}Ca^{2+}$ was quantified as above.

Isolated muscle experiments

To evaluate whether diapocynin modulates force loss in eccentrically contracting muscles, a method described earlier (Ismail *et al.*, 2013a) was used. Dystrophic (mdx^{5Cv}) and wild type (C57BL/6J) mice were maintained in the animal facility of the Geneva-Lausanne School of Pharmaceutical Sciences and used in compliance with the local rules on animal experimentation and welfare (Authorization #106/3626/0 delivered by the Cantonal Veterinary Office of Geneva and approved by the Swiss Veterinary Office). Mice between 8 and 12 weeks of age were anesthetized, the *extensor digitorum longus* (EDL) muscles were exposed, and their proximal and distal tendons were tied with silk sutures. Then EDL muscles were excised and transferred to a 10 ml horizontal chamber of a muscle-testing device designed for delivering eccentric contractions (model 305C-LR, Aurora Scientific Inc., Ontario, Canada). The muscle chamber was filled with a physiological Ringer solution (composition in mM: NaCl 137, $NaHCO_3$ 24, glucose 11, KCl 5, $CaCl_2$ 2, $MgSO_4$ 1, NaH_2PO_4 1, pH 7.4) that contained 25 µM D-tubocurarine chloride and was continuously bubbled with 95% O_2-5% CO_2. Muscles were stimulated by 0.2 ms square wave pulses generated by a Grass S88X stimulator (Grass Technologies, West Warwick, RI, USA), delivered via platinum electrodes on both sides of the muscles. The optimum stimulating voltage and optimal muscle length (L_0) were set and muscles were exposed to 10 contractions of 400 ms each at 100 Hz, 30s apart. One hundred and fifty ms after the initiation of each contraction, muscles were stretched by 9% of L_0 over a period of 100 ms at a speed of 0.9 L_0/s and maintained at that level for another 100 ms before returning to the original length. Force loss during the eccentric contraction procedure as well as recovery after 20 min of rest were expressed for every muscle. Test compounds or vehicle were added to the bath 20 min before initiation of the contraction protocol.

In experiments designed to assess membrane permeability, Procion orange (0.2%, w/v) was added to the bath 5 min before the eccentric contraction procedure. After performing the full protocol described above, muscles were briefly washed twice in Ringer solution, blotted, quickly embedded

in 5% Tragacanth gum and snap frozen in isopentane cooled in liquid nitrogen. Twenty µm thick sections were cut around the mid-belly of each muscle, fixed in acetone at -20°C, and incubated with wheat germ agglutinin conjugated to AlexaFluor 488 (WGA-AF_{488}, Invitrogen), 1 µg/ml in PBS for 1 hour as described to label the extracellular matrix (Dorchies *et al.*, 2013). The amount of Procion orange positive fibers was expressed as a percentage of the total number of fibers, determined from the WGA-AF_{488} counterstain.

Data presentation and statistical analyses

Results are reported as mean ± S.E.M. Statistical differences between groups were assessed by 1-way ANOVA followed by Dunnett's multiple comparison post-tests using the GraphPad Prism software, version 6. Experiments on excised muscles were compared using unpaired *t*-tests. Differences were considered significant at values of $P \leq 0.05$. For consistency, all the graphs show the untreated dystrophic and wild-type values as black and light grey columns, respectively. Values obtained with diapocynin, apocynin and blockers of specific pathways appear in green, red and blue, respectively.

Results

Diapocynin but not apocynin inhibits ROS production in dystrophic myotubes

Treating EDL-MDX-2 myotubes with 100 or 300 µM of diapocynin resulted in a reduction of the total ROS produced. Diapocynin at 300 µM reduced ROS by 36.9 ± 9.6%, a value that was indistinguishable from that of DPI, a potent non-selective NOX inhibitor (Figure 1). By contrast, apocynin caused a 6-fold increase of ROS production.

Diapocynin but not DPI potently inhibits $iPLA_2$ in dystrophic myotubes

In order to minimize the contribution of Ca^{2+}-dependent isoforms of PLA_2, measurements were made on EDL-MDX-2 myotubes in a Ca^{2+}-free buffer (PSS-). Diapocynin treatment resulted in an inhibition of the PED-6 signal, amounting to 31.2 ± 5.25% of the control values at 100 µM (Figure 2). At 300 µM, the inhibition reached a level of about 75%, similar to that obtained by 30 µM BEL, a specific $iPLA_2$ inhibitor. Interestingly, DPI failed to show a significant inhibition of PLA_2 (Figure 2).

Diapocynin affects $^{45}Ca^{2+}$ influx through SAC and SOC

Due to the central role of Ca^{2+} influx in the pathology in DMD, we evaluated the effect of diapocynin on Ca^{2+} influx through SAC and SOC. Treating the myotubes with 100 or 300 µM of

diapocynin resulted in a small but significant inhibition of SAC influx with a value of 25.6 ± 12.9% and 32.8 ± 3.6% of control values, respectively (Figure 3). DPI, however, led to an almost complete inhibition of the influx. The classical SAC inhibitors, streptomycin and grammotoxin (GsMTx-4, a peptide isolated from the venom of the tarantula spider *Grammostola spatulata*), as well as the microtubule disruptor, colchicine, inhibited about 70% of the SAC influx (Figure 3).

When SOC influx was studied using thapsigargin, similar patterns of inhibition were observed with the test compounds. Diapocynin at 300 µM inhibited about 34% of the induced influx while DPI inhibited it to a level of un-stimulated cells (Figure 4). Similarly, a reference SOC blocker, BTP2, and the $iPLA_2$ inhibitor, BEL, efficaciously blocked the induced influx down to basal levels (Figure 4).

Diapocynin prevents eccentric contraction-induced damage

Exposing dystrophic EDL muscle to 10 repeated eccentric contractions resulted in a greater force loss compared to wild-type counterparts. Incubation of the muscles with 300 µM of diapocynin prior to the contractions normalized force loss to near wild-type levels (Figure 5A). However, such a protective effect was not observed in the groups treated with streptomycin or the SOC blocker BTP2 (Figure 5A). In accordance with our previous results (Ismail *et al.*, 2013a), BEL was deleterious with respect to muscle function in this assay.

In another read-out of this assay, muscles were allowed to recover from the damaging protocol for 20 minutes and the force was measured subsequently. Again, wild-type muscles recovered almost two times better than dystrophic ones: the force recovered was about 15% of pre-exercise values (Figure 5B). Streptomycin-treated muscles displayed a striking recovery compared to dystrophic and wild-type controls (Figure 5B). All other treatments did not result in enhanced recovery and BEL caused a further deterioration of force production after the 20 minute rest period, in agreement with our previous results (Ismail *et al.*, 2013a).

To investigate sarcolemmal integrity after damaging contractions, experiments were performed in the presence of the vital dye Procion orange. Exposing dystrophic EDL muscles to 10 eccentric contractions resulted in a 4-fold increased dye uptake compared to wild-type muscles (Figure 6). Diapocynin reduced this uptake to the value of non-dystrophic muscle, whereas apocynin had no significant effect. The SAC blocker, streptomycin, also had a protective effect, rendering the

sarcolemma more resilient to stretch-induced damage whereas BEL caused deterioration as evidenced by augmented dye uptake (Figure 6).

Discussion

Our study demonstrates the ability of diapocynin, but not apocynin, to inhibit ROS production in skeletal muscle cells. We also show that diapocynin inhibits $iPLA_2$, reduces Ca^{2+} influx through SOC and SAC and protects muscle from eccentric contraction-induced force loss.

There is a lack of selective, non-toxic NOX inhibitors, the best known being apocynin. It was first isolated from the roots of *Apocynum cannabinum* by Schmiedeberg in 1883, but it was only in the 1990's that apocynin was found to inhibit NOX-dependent ROS production (for a review see (Kleniewska *et al.*, 2012)). Apocynin's ability to reduce NOX-mediated ROS generation results from both altered translocation of regulatory subunits to the membranes and prevention of their proper assembly with the transmembrane core protein $gp91^{phox}$ (Simons *et al.*, 1990). This inhibition was observed only in activated phagocytic cells but was completely lacking in other cell types and even had a ROS-promoting effect in non-phagocytic cells (Vejrazka *et al.*, 2005). In attempts to explain these findings, apocynin was proposed to act as a pro-drug undergoing two different metabolic pathways, namely oxidative dimerization by myeloperoxidases in activated phagocytic cells to form diapocynin, which is thought to be the active moiety inhibiting the enzyme (Johnson *et al.*, 2002), or generation of a transient pro-oxidant apocynin radical that can subsequently oxidize sensitive sulfhydryl groups of NOXes (Kanegae *et al.*, 2007). Diapocynin was found to be superior to apocynin in inhibiting not only NOX activity, but also $gp91^{phox}$ expression, TNF-α and IL-10 production in response to LPS challenge in non-phagocytic cells (Kanegae *et al.*, 2010).

Diapocynin inhibited ROS production in skeletal muscle myotubes while apocynin showed a 6-fold increase in ROS output (Figure 1). This finding is in accordance with another report on non-phagocytic cells (Vejrazka *et al.*, 2005). The pro-oxidant activity of apocynin depends on its prior oxidation to transient free radicals, such as apocynin radicals (Kanegae *et al.*, 2007). Such radicals have been reported to cause a 7-fold increase in glutathione oxidation and an even 100-fold increase in NADPH oxidation (Castor *et al.*, 2010). These results reinforce previous reports that diapocynin is the active species inhibiting NOX and that apocynin primarily serves as pro-drug of its oxidized dimer (Johnson *et al.*, 2002).

Both diapocynin and DPI inhibited ROS production in our cellular model to a similar extent (Figure 1). DPI is not a selective NOX inhibitor but a wide-spectrum flavo-enzyme inhibitor causing also inhibition of CytP450, nitric oxide synthases and xanthine oxidase (Wind *et al.*, 2010). The similar extent of inhibition of ROS production (about 40%) exhibited DPI and diapocynin in myotube cultures is consistent with the fact that NOXes are major ROS contributors in skeletal muscle tissue (Sakellariou *et al.*, 2013b; Xia *et al.*, 2003). A docking model for apocynin and analogues into the complex $p67^{phox}$-$p47^{phox}$ was recently proposed; it was shown that diapocynin had the highest affinity score of all tested compounds (Jiang *et al.*, 2013). This supports earlier reports that diapocynin and apocynin might have the same inhibitory mechanism on NOX, namely binding to $p47^{phox}$, thus preventing the assembly of the subunits required for NOX2 activity (Johnson *et al.*, 2002). Whether diapocynin inhibits NOX4, which does not require translocation of subunits, remains to be investigated.

We have shown previously the involvement of $iPLA_2$ in modulating Ca^{2+} entry into dystrophic myotubes and fibres and that pharmacological inhibition of $iPLA_2$ blocks the enhanced Ca^{2+} entry (Basset *et al.*, 2004; Boittin *et al.*, 2006). Diapocynin treatment fully inhibited $iPLA_2$ in our dystrophic myotubes to levels indistinguishable from those elicited by the suicide $iPLA_2$ inhibitor BEL (Figure 2). Likely targets of diapocynin could be NOXes, located in close proximity of the sarcolemma. Their inhibition would lead not only to decreased superoxide anion radical ($O_2^{\cdot -}$) formation, but also to a lower production of lipid peroxides. Such peroxides are known to be superior substrates for $iPLA_2$ compared to native phospholipids (Balboa & Balsinde, 2002). Alternatively, a direct inhibition of $iPLA_2$ by diapocynin cannot be ruled out. One important consideration in the effect of diapocynin on its targets is lipophilicity. Diapocynin is 13 times more lipophilic than apocynin (Luchtefeld *et al.*, 2008), enabling it to cross membranes freely. Such a characteristic can lead to membrane accumulation, which could bring the compound into close vicinity of its targets. By contrast, the lack of $iPLA_2$ inhibition by DPI might be attributed to its reduced ability to accumulate into biological membranes and therefore the lack of potent inhibitory action in this specific cellular compartment. Also, DPI is known to be a “dirty” compound, therefore, non-specific actions of DPI on other targets may ultimately mitigate the cellular response (Riganti *et al.*, 2004; Weir *et al.*, 1994).

Diapocynin inhibited calcium influx through SAC to a lesser extent than the classical inhibitors streptomycin and GsMTx-4 (Figure 3). In an elegant series of papers, Lederer and colleagues showed that membrane stretch activates NOXes to produce ROS, which subsequently activate SAC (Khairallah *et al.*, 2012; Prosser *et al.*, 2012). Diapocynin, through its ability to inhibit NOX2, would lead to the disruption of this cascade and eventually block cation influx through SAC. The same authors also proposed the microtubular network to convey the mechanical stretch to NOX and that colchicine, a microtubule disruptor, leads to the inhibition of SAC influx in dystrophic FDB fibres (Khairallah *et al.*, 2012). Our present results confirm these findings in dystrophic myotubes, as colchicine inhibited SAC influx to the same extent as streptomycin or GsMTx-4 (Figure 3).

SOC influx using thapsigargin as a trigger revealed that diapocynin partially inhibited this influx but this inhibition became significant only at 300 µM (Figure 4). This can be attributed to $iPLA_2$ inhibition as evidenced by the inhibition of the influx by BEL and is in line with our previous report (Boittin *et al.*, 2010). Of note, BEL does not only inhibit SOC as an $iPLA_2$ inhibitor, but it also inhibits directly several TRP channels, an effect that might contribute to its full blockade seen here as well as previously in our hands (Chakraborty *et al.*, 2011). This can explain why BEL appeared to be more efficacious than diapocynin in preventing SOC-mediated Ca^{2+} influx in our hands.

DPI caused full inhibition of both SAC and SOC, exceeding the levels reached by the most selective inhibitors of the targeted channel types, namely GsMTx-4 and BTP2, respectively (Figures 3 and 4). This cannot be explained by the sole ability of DPI to inhibit flavo-enzymes such as NOXes. In earlier work, in which patch-clamp techniques were used on isolated pulmonary smooth muscles, it was reported that DPI inhibited both Ca^{2+} and K^+ channels with at concentrations of 3 and 10 µM, independent of its NOX modulating activity (Weir *et al.*, 1994). Since the concentrations used in this study are 3-10 times higher than those reported to have channel modulating activity, such an inhibition of other channels might well play a role. To the best of our knowledge, this is the first report showing that DPI has such a potent inhibitory effect on Ca^{2+}-influx stimulated by membrane stretch and by internal store emptying. However, considering the effect of DPI on SAC and SOC influx, and its broad inhibitory profile on flavo-enzymes, we suggest that DPI should not be used as an experimental tool for blocking NOXes in a similar context.

Exposing isolated EDL muscles to 10 repeated eccentric contractions resulted in an increased force loss in dystrophic muscle compared to wild-type counterparts. This has been first reported 20 years

ago by Petrof *et al.*, who also showed enhanced membrane disruption and dye uptake as a consequence of such contractions (Petrof *et al.*, 1993). Numerous attempts were carried out to investigate the mechanisms causing this force loss and led to the notion that the two major determinants involved are disruption of Ca^{2+} homeostasis and myofibrillar disorganization (Reggiani, 2008). In line with an increased Ca^{2+} influx, SAC blockers, such as streptomycin or GsMTx-4, or removal of extracellular Ca^{2+} have been shown to be beneficial in promoting force recovery following eccentric contractions (Whitehead *et al.*, 2006; Yeung *et al.*, 2005). Recently, ROS came into play as mediators carrying an essentially cytotoxic message, as evidenced by increased resistance to eccentric damage in mdx mice by *N*-acetylcysteine treatment or by transgenic overexpression of catalase (Selsby, 2011; Whitehead *et al.*, 2008). A recent study has also shown that DPI decreased force loss induced by eccentric contractions in isolated FDB fibres (Whitehead *et al.*, 2010). In the current study, we show that diapocynin was the only compound that abolished force loss occurring during eccentric contractions, whereas streptomycin failed to do so (Figure 5). However, when measured after 20 minutes of recovery, streptomycin-treated muscles recovered to an extent similar to the one of diapocynin. All other treatments failed to show any significant improvement. Using the same assay, we have shown before that BEL treatment resulted in aggravated force loss and reduced recovery after damage (Ismail *et al.*, 2013a). These results support earlier findings that both SAC and ROS contribute to the force loss induced by eccentric contractions in dystrophic muscles, however, their specific roles in the different stages of force loss and recovery might be different. In support to this, it has been convincingly proposed recently that ROS production by NOXes precedes SAC activation seen in stretching conditions (Khairallah *et al.*, 2012; Prosser *et al.*, 2012). This can explain our findings that diapocynin prevented force loss whereas streptomycin promoted the recovery after the contractions. Gervasio *et al.* showed that increased levels of pro-oxidants, such as H_2O_2, lead to autophosphorylation of Src kinase and subsequent activation of SAC and that the anti-oxidant tiron or the Src kinase inhibitor PP2 inhibited increased Ca^{2+} influx after eccentric contractions (Gervasio *et al.*, 2008). Another study showed that addition of SAC blockers just after eccentric contractions was sufficient to obtain a protective effect (Yeung *et al.*, 2005). Taken together, these findings point towards increased ROS production in eccentrically contracting muscle having dual role, the first one promoting force loss by increasing ROS above the levels that are required for optimal force production (Reid, 2001), and the second one activating Ca^{2+} influx through SAC, promoting membrane damage and finally

enhancing dye uptake. NOX inhibitors would prevent the first step of the cascade while SAC blockers would inhibit the final step. This is illustrated in Figure 7. Our results with Procion orange dye uptake re-enforces these finding and shows that both diapocynin, and to a lesser extent streptomycin, protected the muscles form membrane damage induced by stretching contractions.

ROS contribute to normal cellular homeostasis and fine tuning of metabolic processes (Buetler *et al.*, 2004). Many anti-oxidants tested so far in dystrophic mice are global ROS scavengers that do not discriminate between different sources of ROS. Their ability to alter the cells redox status instead of targeting a specific source of ROS might explain why such anti-oxidant therapies showed only limited improvement of the dystrophic condition. Targeting overactive NOXes with diapocynin might confer higher experimental and therapeutic potential compared to global anti-oxidants. A recent study showed that diapocynin has a good pharmacokinetic profile when administered orally and that such a treatment resulted in a neuroprotective effect in models of Parkinson's disease (Ghosh *et al.*, 2012). Another study revealed that diapocynin has a powerful anti-inflammatory activity independent of its ROS modulating capability (Houser *et al.*, 2012).

Altogether, our results and data by others suggest that diapocynin is a promising compound with potential for treating dystrophic muscle diseases and is worthy of further evaluation. Towards this goal we currently are performing an *in vivo* investigation of diapocynin in mdx mice.

Acknowledgments

This work was supported by grants from the Swiss National Science Foundation, the Association Française contre les myopathies (AFM, France), the Duchenne Parent Project-The Netherlands (DPP-NL) and the Parent Project Muscular Dystrophy (PPMD, USA). We would also like to thank Dr. Andreas Nievergelt and Prof. Muriel Cuendet for their help in diapocynin synthesis and purification.

Conflict of interest

None.

References

Balboa MA, Balsinde J (2002). Involvement of calcium-independent phospholipase A_2 in hydrogen peroxide-induced accumulation of free fatty acids in human U937 cells. *J Biol Chem* **277**(43)**:** 40384-40389.

Barbieri E, Sestili P (2012). Reactive oxygen species in skeletal muscle signaling. *J Sig Transd* **2012:** 982794.

Basset O, Boittin FX, Dorchies OM, Chatton JY, van Breemen C, Ruegg UT (2004). Involvement of inositol 1,4,5-trisphosphate in nicotinic calcium responses in dystrophic myotubes assessed by near-plasma membrane calcium measurement. *J Biol Chem* **279**(45)**:** 47092-47100.

Bedard K, Krause KH (2007). The NOX family of ROS-generating NADPH oxidases: physiology and pathophysiology. *Physiol Rev* **87**(1)**:** 245-313.

Boittin FX, Petermann O, Hirn C, Mittaud P, Dorchies OM, Roulet E*, et al.* (2006). Ca^{2+}-independent phospholipase A_2 enhances store-operated Ca^{2+} entry in dystrophic skeletal muscle fibers. *J Cell Sci* **119**(18)**:** 3733-3742.

Boittin FX, Shapovalov G, Hirn C, Ruegg UT (2010). Phospholipase A2-derived lysophosphatidylcholine triggers Ca^{2+} entry in dystrophic skeletal muscle fibers. *Biochem Biophys Res Commun* **391**(1)**:** 401-406.

Buetler TM, Krauskopf A, Ruegg UT (2004). Role of superoxide as a signaling molecule. *News Physiol Sci* **19:** 120-123.

Buetler TM, Renard M, Offord EA, Schneider H, Ruegg UT (2002). Green tea extract decreases muscle necrosis in mdx mice and protects against reactive oxygen species. *Am J Clin Nutr* **75**(4)**:** 749-753.

Castor LR, Locatelli KA, Ximenes VF (2010). Pro-oxidant activity of apocynin radical. *Free Radic Biol Med* **48**(12)**:** 1636-1643.

Chakraborty S, Berwick ZC, Bartlett PJ, Kumar S, Thomas AP, Sturek M*, et al.* (2011). Bromoenol lactone inhibits voltage-gated Ca^{2+} and transient receptor potential canonical channels. *J Pharmacol Exp Ther* **339**(2)**:** 329-340.

De Luca A (2012). Pre-clinical drug tests in the mdx mouse as a model of dystrophinopathies: an overview. *Acta Myol* **31**(1)**:** 40-47.

Dorchies OM, Reutenauer-Patte J, Dahmane E, Ismail HM, Petermann O, Patthey- Vuadens O*, et al.* (2013). The anticancer drug tamoxifen counteracts the pathology in a mouse model of duchenne muscular dystrophy. *Am J Pathol* **182**(2)**:** 485-504.

Dorchies OM, Wagner S, Vuadens O, Waldhauser K, Buetler TM, Kucera P*, et al.* (2006). Green tea extract and its major polyphenol (-)-epigallocatechin gallate improve muscle function in a mouse model for Duchenne muscular dystrophy. *Am J Physiol-Cell Ph* **290**(2)**:** C616-C625.

Ducret T, Vandebrouck C, Cao ML, Lebacq J, Gailly P (2006). Functional role of store-operated and stretch-activated channels in murine adult skeletal muscle fibres. *J Physiol* **575**(Pt 3)**:** 913-924.

Gervasio OL, Whitehead NP, Yeung EW, Phillips WD, Allen DG (2008). TRPC1 binds to caveolin-3 and is regulated by Src kinase - role in Duchenne muscular dystrophy. *J Cell Sci* **121**(Pt 13)**:** 2246-2255.

Ghosh A, Kanthasamy A, Joseph J, Anantharam V, Srivastava P, Dranka BP*, et al.* (2012). Anti-inflammatory and neuroprotective effects of an orally active apocynin derivative in pre-clinical models of Parkinson's disease. *J Neuroinflamm* **9:** 241.

Hibaoui Y, Reutenauer-Patte J, Patthey-Vuadens O, Ruegg UT, Dorchies OM (2011). Melatonin improves muscle function of the dystrophic mdx5Cv mouse, a model for Duchenne muscular dystrophy. *J Pineal Res* **51**(2)**:** 163-171.

Hoffman EP, Dressman D (2001). Molecular pathophysiology and targeted therapeutics for muscular dystrophy. *Trends Pharmacol Sci* **22**(9)**:** 465-470.

Houser KR, Johnson DK, Ishmael FT (2012). Anti-inflammatory effects of methoxyphenolic compounds on human airway cells. *J Inflamm (Lond)* **9:** 6.

Ismail HM, Dorchies OM, Perozzo R, Strosova MK, Scapozza L, Ruegg UT (2013a). Inhibition of iPLA2 beta and of stretch-activated channels by doxorubicin alters dystrophic muscle function. *Br J Pharmacol* **169**(7)**:** 1537-1550.

.

Jiang J, Kang H, Song X, Huang S, Li S, Xu J (2013). A Model of Interaction between Nicotinamide Adenine Dinucleotide Phosphate (NADPH) Oxidase and Apocynin Analogues by Docking Method. *Int J Mol Sci* **14**(1)**:** 807-817.

Johnson DK, Schillinger KJ, Kwait DM, Hughes CV, McNamara EJ, Ishmael F*, et al.* (2002). Inhibition of NADPH oxidase activation in endothelial cells by ortho-methoxy-substituted catechols. *Endothelium* **9**(3)**:** 191-203.

Kanegae MP, Condino-Neto A, Pedroza LA, de Almeida AC, Rehder J, da Fonseca LM*, et al.* (2010). Diapocynin versus apocynin as pretranscriptional inhibitors of NADPH oxidase and cytokine production by peripheral blood mononuclear cells. *Biochem Biophys Res Commun* **393**(3)**:** 551-554.

Kanegae MP, da Fonseca LM, Brunetti IL, Silva SO, Ximenes VF (2007). The reactivity of ortho-methoxy-substituted catechol radicals with sulfhydryl groups: contribution for the comprehension of the mechanism of inhibition of NADPH oxidase by apocynin. *Biochem Pharmacol* **74**(3)**:** 457-464.

Khairallah RJ, Shi G, Sbrana F, Prosser BL, Borroto C, Mazaitis MJ*, et al.* (2012). Microtubules underlie dysfunction in duchenne muscular dystrophy. *Sci Signal* **5**(236)**:** ra56.

Kim JA, Neupane GP, Lee ES, Jeong BS, Park BC, Thapa P (2011). NADPH oxidase inhibitors: a patent review. *Expert Opin Ther Pat* **21**(8)**:** 1147-1158.

Kim JH, Kwak HB, Thompson LV, Lawler JM (2013). Contribution of oxidative stress to pathology in diaphragm and limb muscles with Duchenne muscular dystrophy. *J Muscle Res Cell M* **34**(1)**:** 1-13.

Kleniewska P, Piechota A, Skibska B, Goraca A (2012). The NADPH oxidase family and its inhibitors. *Arch Immunol Ther Exp (Warsz)* **60**(4)**:** 277-294.

Koenig M, Hoffman EP, Bertelson CJ, Monaco AP, Feener C, Kunkel LM (1987). Complete cloning of the Duchennne muscular dystrophy (DMD) cDNA and preliminary genomic organization of the DMD gene in normal and affected individuals. *Cell* **50:** 509-517.

Lindahl M, Backman E, Henriksson KG, Gorospe JR, Hoffman EP (1995). Phospolipase A_2 activity in dystrophinopathies. *Neuromuscul Disord* **5**(3)**:** 193-199.

Luchtefeld R, Luo R, Stine K, Alt ML, Chernovitz PA, Smith RE (2008). Dose formulation and analysis of diapocynin. *J Agric Food Chem* **56**(2)**:** 301-306.

Nakae Y, Dorchies OM, Stoward PJ, Zimmermann BF, Ritter C, Ruegg UT (2012). Quantitative evaluation of the beneficial effects in the mdx mouse of epigallocatechin gallate, an antioxidant polyphenol from green tea. *Histochem Cell Biol* **137**(6)**:** 811-827.

Petrof BJ, Shrager JB, Stedman HH, Kelly AM, Sweeney HL (1993). Dystrophin protects the sarcolemma from stresses developed during muscle contraction. *Proc Natl Acad Sci USA* **90**(8)**:** 3710-3714.

Prosser BL, Khairallah RJ, Ziman AP, Ward CW, Lederer WJ (2012). X-ROS signaling in the heart and skeletal muscle: Stretch-dependent local ROS regulates $[Ca^{2+}]_i$. *J Mol Cell Cardiol* **58:** 172-881.

Reggiani C (2008). Between channels and tears: aim at ROS to save the membrane of dystrophic fibres. *J Physiol* **586**(7)**:** 1779.

Reid MB (2001). Plasticity in skeletal, cardiac, and smooth muscle: Redox modulation of skeletal muscle contraction: what we know and what we don't. *J Appl Physiol* **90**(2)**:** 724-731.

Reutenauer-Patte J, Boittin FX, Patthey-Vuadens O, Ruegg UT, Dorchies OM (2012). Urocortins improve dystrophic skeletal muscle structure and function through both PKA- and Epac-dependent pathways. *Am J Pathol* **180**(2)**:** 749-762.

Rey FE, Cifuentes ME, Kiarash A, Quinn MT, Pagano PJ (2001). Novel competitive inhibitor of NAD(P)H oxidase assembly attenuates vascular O_2^- and systolic blood pressure in mice. *Circ Res* **89**(5)**:** 408-414.

Riganti C, Gazzano E, Polimeni M, Costamagna C, Bosia A, Ghigo D (2004). Diphenyleneiodonium inhibits the cell redox metabolism and induces oxidative stress. *J Biol Chem* **279**(46)**:** 47726-47731.

Ruegg UT, Shapovalov G, Jacobson K, Reutenauer-Patte J, Ismail HM, Dorchies OM*, et al.* (2012). Store-operated channels and Ca^{2+} handling in muscular dystrophy. In: *Store-operated Ca^{2+} entry (SOCE) pathways*, Groschner K, Graier WF, Romanin C (eds) Vol. 1, pp 449-457: SpringerWien.

Sakellariou GK, Vasilaki A, Palomero J, Kayani A, Zibrik L, McArdle A*, et al.* (2013). Studies of mitochondrial and nonmitochondrial sources implicate nicotinamide adenine dinucleotide phosphate oxidase(s) in the increased skeletal muscle superoxide generation that occurs during contractile activity. *Antioxid Redox Sign* **18**(6)**:** 603-621.

Selsby JT (2011). Increased catalase expression improves muscle function in mdx mice. *Exp Physiol* **96**(2)**:** 194-202.

Shkryl VM, Martins AS, Ullrich ND, Nowycky MC, Niggli E, Shirokova N (2009). Reciprocal amplification of ROS and Ca^{2+} signals in stressed mdx dystrophic skeletal muscle fibers. *Pflugers Arch* **458**(5)**:** 915-928.

Simons JM, Hart BA, Ip Vai Ching TR, Van Dijk H, Labadie RP (1990). Metabolic activation of natural phenols into selective oxidative burst agonists by activated human neutrophils. *Free Radic Biol Med* **8**(3)**:** 251-258.

Spurney CF, Knoblach S, Pistilli EE, Nagaraju K, Martin GR, Hoffman EP (2008). Dystrophin-deficient cardiomyopathy in mouse: expression of Nox4 and Lox are associated with fibrosis and altered functional parameters in the heart. *Neuromuscul Disord* **18**(5)**:** 371-381.

Tidball JG, Wehling-Henricks M (2007). The role of free radicals in the pathophysiology of muscular dystrophy. *J Appl Physiol* **102**(4)**:** 1677-1686.

Vejrazka M, Micek R, Stipek S (2005). Apocynin inhibits NADPH oxidase in phagocytes but stimulates ROS production in non-phagocytic cells. *Biochim Biophys Acta* **1722**(2)**:** 143-147.

Wang Q, Smith RE, Luchtefeld R, Sun AY, Simonyi A, Luo R*, et al.* (2008). Bioavailability of apocynin through its conversion to glycoconjugate but not to diapocynin. *Phytomedicine* **15**(6-7)**:** 496-503.

Weir EK, Wyatt CN, Reeve HL, Huang J, Archer SL, Peers C (1994). Diphenyliodonium inhibits both pottasium and calcium currents in isolated pulmonary-artery smooth-muscle cells. *J Appl Physiol* **76**(6)**:** 2611-2615.

Whitehead NP, Pham C, Gervasio OL, Allen DG (2008). N-Acetylcysteine ameliorates skeletal muscle pathophysiology in mdx mice. *J Physiol* **586**(7)**:** 2003-2014.

Whitehead NP, Streamer M, Lusambili LI, Sachs F, Allen DG (2006). Streptomycin reduces stretch-induced membrane permeability in muscles from mdx mice. *Neuromuscul Disord* **16**(12)**:** 845-854.

Whitehead NP, Yeung EW, Froehner SC, Allen DG (2010). Skeletal muscle NADPH oxidase is increased and triggers stretch-induced damage in the mdx mouse. *PLoS One* **5**(12)**:** e15354.

Wind S, Beuerlein K, Eucker T, Muller H, Scheurer P, Armitage ME*, et al.* (2010). Comparative pharmacology of chemically distinct NADPH oxidase inhibitors. *Br J Pharmacol* **161**(4)**:** 885-898.

Xia R, Webb JA, Gnall LL, Cutler K, Abramson JJ (2003). Skeletal muscle sarcoplasmic reticulum contains a NADH-dependent oxidase that generates superoxide. *Am J Physiol* **285**(1)**:** C215-221.

Yeung EW, Whitehead NP, Suchyna TM, Gottlieb PA, Sachs F, Allen DG (2005). Effects of stretch-activated channel blockers on $[Ca^{2+}]_i$ and muscle damage in the mdx mouse. *J Physiol* **562**(Pt 2)**:** 367-380.

Figure legends and figures

Figure 1

Diapocynin inhibits ROS production in dystrophic myotubes

ROS production in cultured dystrophic myotubes was monitored using DCFH-DA. Fluorescence increments over a period of 20 minutes were quantified in the presence of vehicle or test compounds. Diapocynin (Diapo) caused a concentration-dependent inhibition of ROS production amounting to about 40% at 300 µM, whereas apocynin (Apo) led to a 6-fold increase of fluorescence. The broad flavo-enzyme inhibitor, DPI, commonly used as NOX inhibitor, caused a similar inhibition as 300 µM diapocynin. Concentrations shown on the graph are in µM. ** $p \leq 0.01$, *** $p \leq 0.001$ (n = 3-7).

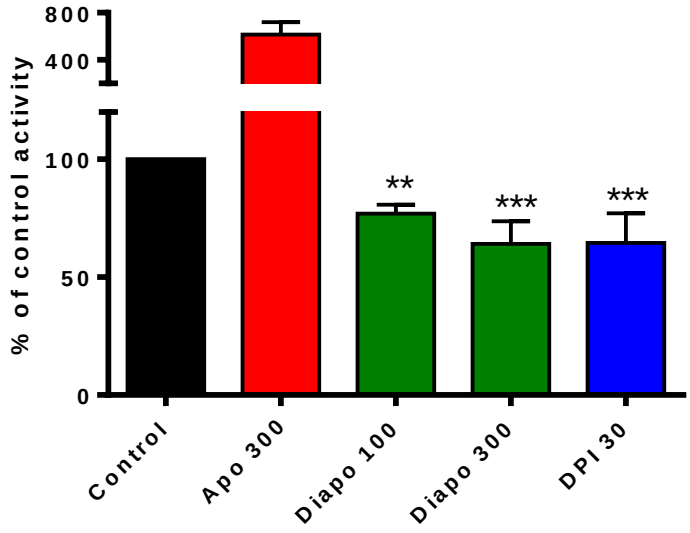
800
400
100
50
0
% of control activity
**
***
***
Control
Apo 300
Diapo 100
Diapo 300
DPI 30

Figure 1

Figure 2

Diapocynin displays potent inhibition of $iPLA_2$ in dystrophic myotubes

PED-6 was used as a probe to monitor $iPLA_2$ activity in myotubes. Cellular phospholipases cleave this probe to release the fluorescent BODIPY; the rate of formation of this moiety was monitored for 20 minutes. Experiments were performed in the absence of extracellular Ca^{2+} in order to facilitate the activity of $iPLA_2$ over other phospholipase isoforms. Diapocynin (Diapo) potently inhibited the $iPLA_2$ signal to levels similar to those of the suicide inhibitor, BEL. Note the absence of significant inhibition with DPI. Concentrations shown on the graph are in µM. *** $p \leq 0.001$ (n = 3-8).

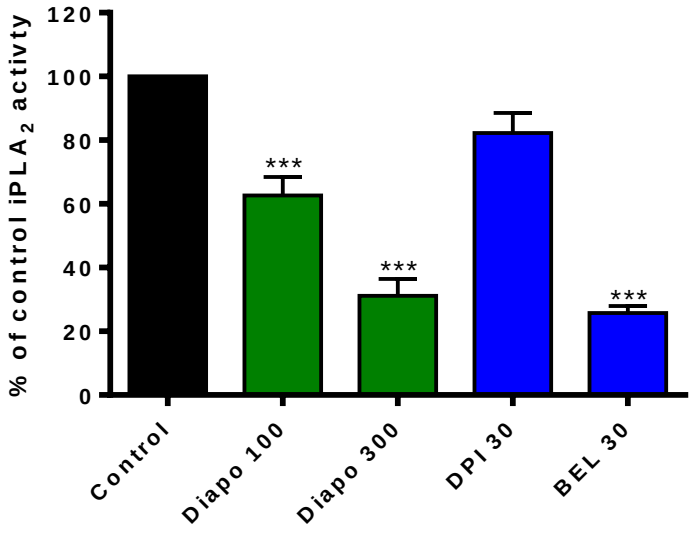
% of control iPLA2 activty
120
100
80
60
40
20
0
***
***
***
Control
Diapo 100
Diapo 300
DPI 30
BEL 30

Figure 2

Figure 3

Modulation of hypo-osmotic shock induced Ca^{2+}-influx in dystrophic myotubes

Exposing myotubes to a hypotonic PSS containing 1 µCi $^{45}Ca^{2+}$ induced a 3.7-fold increase in $^{45}Ca^{2+}$-influx compared to isotonic PSS. Diapocynin (Diapo) treatment resulted in a 30% inhibition of the stimulated influx, whereas DPI caused an inhibition to control levels. The SAC blockers, streptomycin (Strept) and Grammotoxin (GsMTx-4), or the microtubule disruptor, colchicine (Col), caused a similar inhibition of about 70%. Concentrations shown on the graph are in µM. *$p \leq 0.05$, ** $p \leq 0.01$, *** $p \leq 0.001$ (n = 4-7).

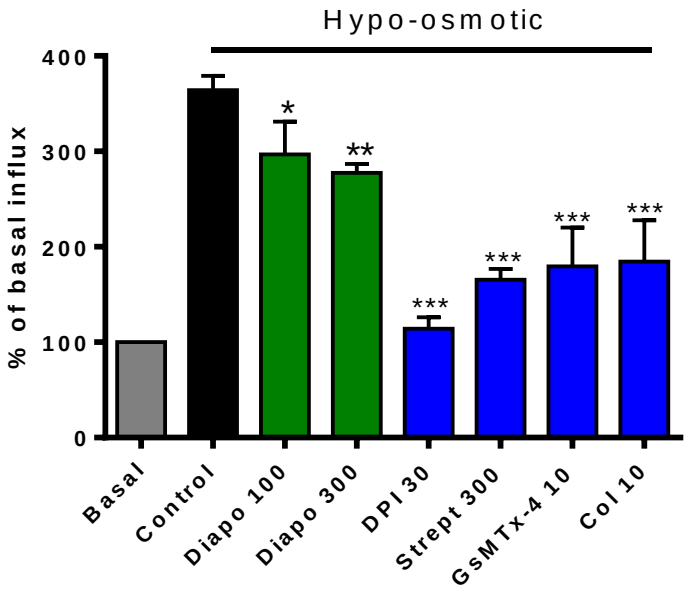
Hypo-osmotic
% of basal influx
400
300
200
100
0
*
**
***
***
***
***
Basal
Control
Diapo 100
Diapo 300
DPI 30
Strept 300
GsMTx-4 10
Col 10

Figure 3

Figure 4

Modulation of Ca^{2+} influx in dystrophic myotubes induced by store-depletion

Thapsigargin (5 µM) treatment was used to deplete the sarcoplasmic Ca^{2+} stores leading to activation of SOC influx. Re-addition of $^{45}Ca^{2+}$-containing buffer resulted in an almost 4-fold increase in $^{45}Ca^{2+}$-influx compared to non-treated cells. Diapocynin (Diapo) treatment had a small effect, whereas DPI showed a complete inhibition, similar to the one observed with BTP2, a commonly used SOC blocker, or BEL. Concentrations shown on the graph are in µM. *$p \leq 0.05$, *** $p \leq 0.001$ ($n = 3$-10).

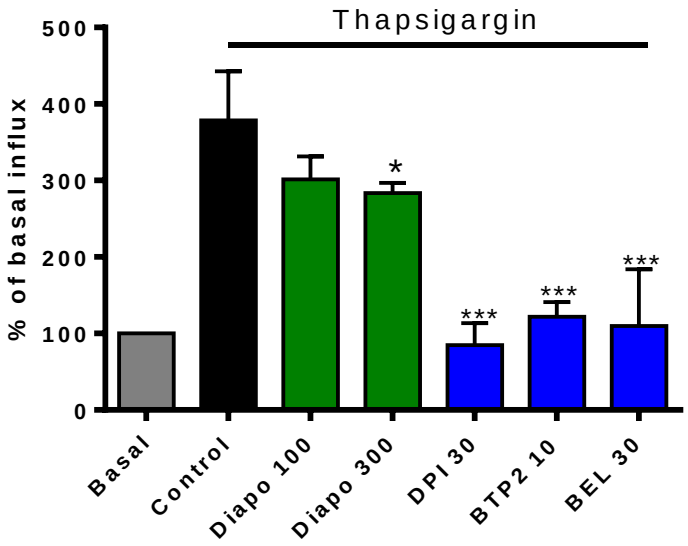
Thapsigargin
% of basal influx
500
400
300
200
100
0
*
***
***
***
Basal
Control
Diapo 100
Diapo 300
DPI 30
BTP2 10
BEL 30

Figure 4

Figure 5

Diapocynin abrogates force loss in eccentrically contracted EDL muscles whereas streptomycin promotes the recovery of force loss after a period of rest.

EDL muscles from wild-type (B6) and dystrophic mice were exposed to 10 eccentric contractions at 100 Hz lasting 400 ms during which they were stretched to a value of 109% of their optimal length. (A) Remaining force after 10 eccentric contractions. Note the increased force loss in dystrophic muscle (mdx) compared to wild type (B6) muscle. Of the tested compounds, only diapocynin (Diapo) abrogated the force loss seen in this assay while apocynin (Apo) failed to show such an effect. (B) Force recovered after 20 minutes of rest. Streptomycin (Strept) caused a marked recovery exceeding the one of wild-type muscles. Concentrations shown on the graph are in µM. *$p \leq 0.05$, ** $p \leq 0.01$ ($n = 4$-9).

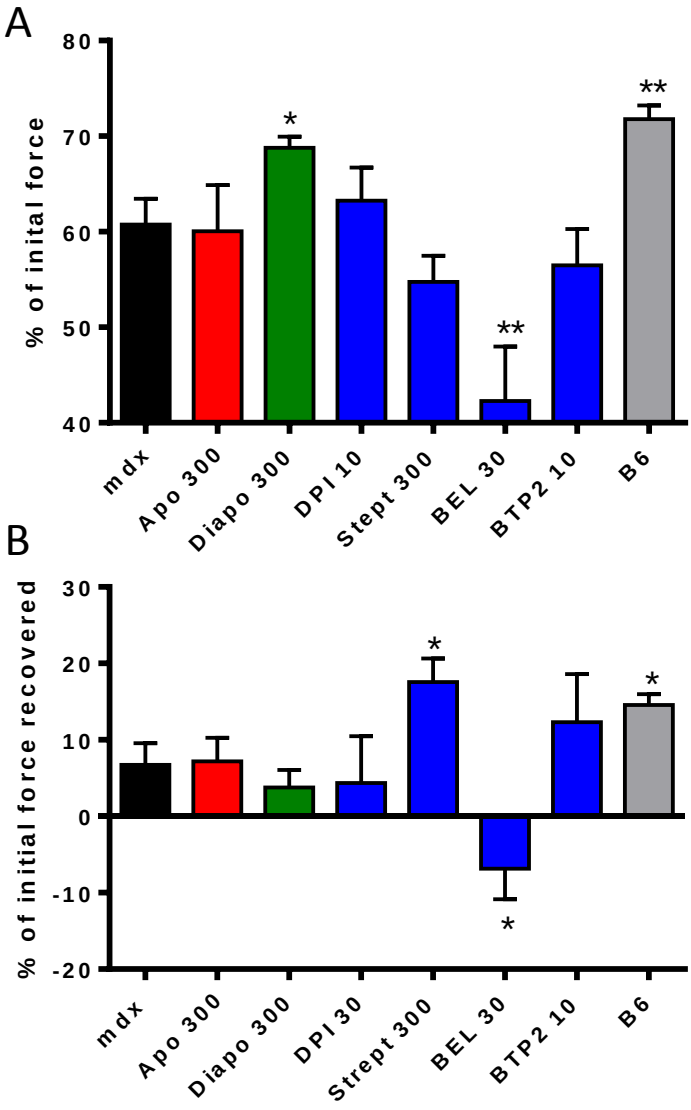
A
% of inital force
80
70
60
50
40
*
**
**
mdx
Apo 300
Diapo 300
DPI 10
Stept 300
BEL 30
BTP2 10
B6
B
% of initial force recovered
30
20
10
0
-10
-20
*
*
*
mdx
Apo 300
Diapo 300
DPI 30
Strept 300
BEL 30
BTP2 10
B6

Figure 5

Figure 6

Protection of sarcolemmal integrity by diapocynin in eccentrically contracted EDL muscles

Procion orange is a membrane-impermeable dye that enters only cells with damaged membranes. In this assay, EDL muscles were exposed to 10 eccentric contractions in physiological buffer containing 0.2% Procion orange. Muscles were subsequently rinsed twice in physiological buffer and embedded in tragacanth gum. Twenty micrometer thick sections were made around the mid-belly region of the muscles and the percentage of Procion orange-positive fibers were quantified. Representative section of wild type (A, left) and dystrophic (A, right) EDL muscles exposed to eccentric contractions in the presence of Procion orange. (B) Quantification of Procion orange-positive fibers in the experimental groups. Dystrophic muscle (mdx) displayed a 4-fold increase in dye uptake as compared to wild-type muscle (B6). Diapocynin (Diapo) or streptomycin (Strept) treatment protected the muscle from increased membrane damage, thus lowering the values of the stained fibers down to those of the non-dystrophic controls. Apocynin (Apo) did not offer a protection in this assay. Concentrations shown on the graph are in µM. ** $p \leq 0.01$, *** $p \leq 0.001$ ($n = 4$-8).

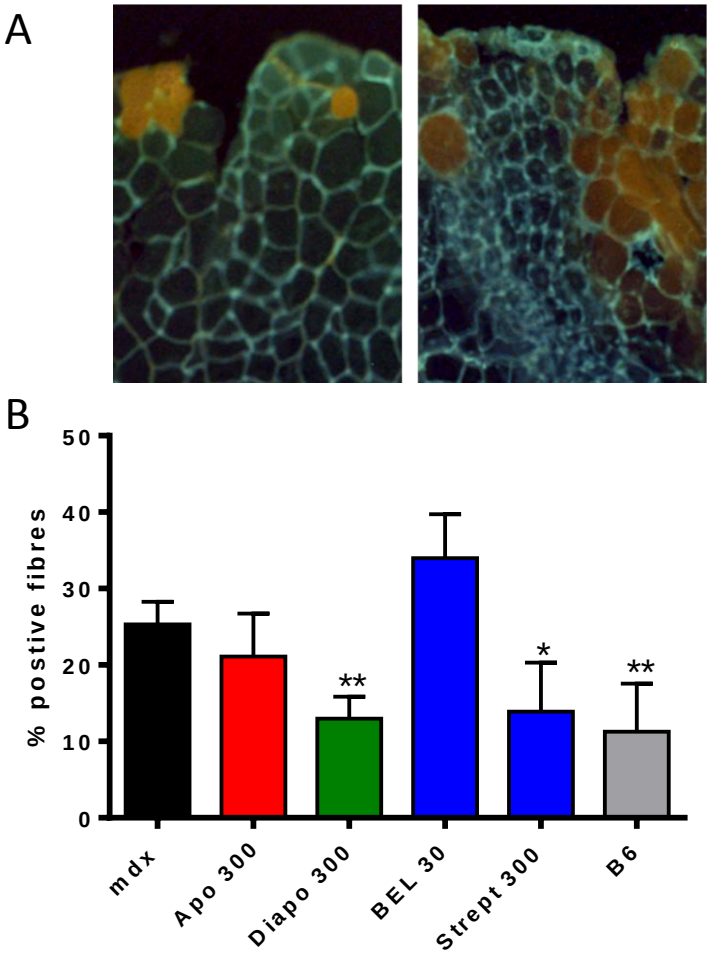
A
B
% postive fibres
50
40
30
20
10
0
**
*
**
mdx
Apo 300
Diapo 300
BEL 30
Strept 300
B6

Figure 6

Figure 7

Proposal for the cascade implicated in the force loss in eccentrically contracting dystrophic muscles

The illustration shows the cascade of events taking place in eccentrically contracting dystrophic muscle. Thick arrows highlight pathways reported to play a major role in muscle function, namely microtubules-NOX-SACs, $iPLA_2$-SOCs and membrane tears. Thin arrows point to suggested links between the main pathways involved. The blunted red arrows show the inhibitory effect of compounds used in the current study. The suggested cascade results in an elevation of intracellular Ca^{2+}, an event known to activate multiple downstream pathways playing a role in the dystrophic pathology.

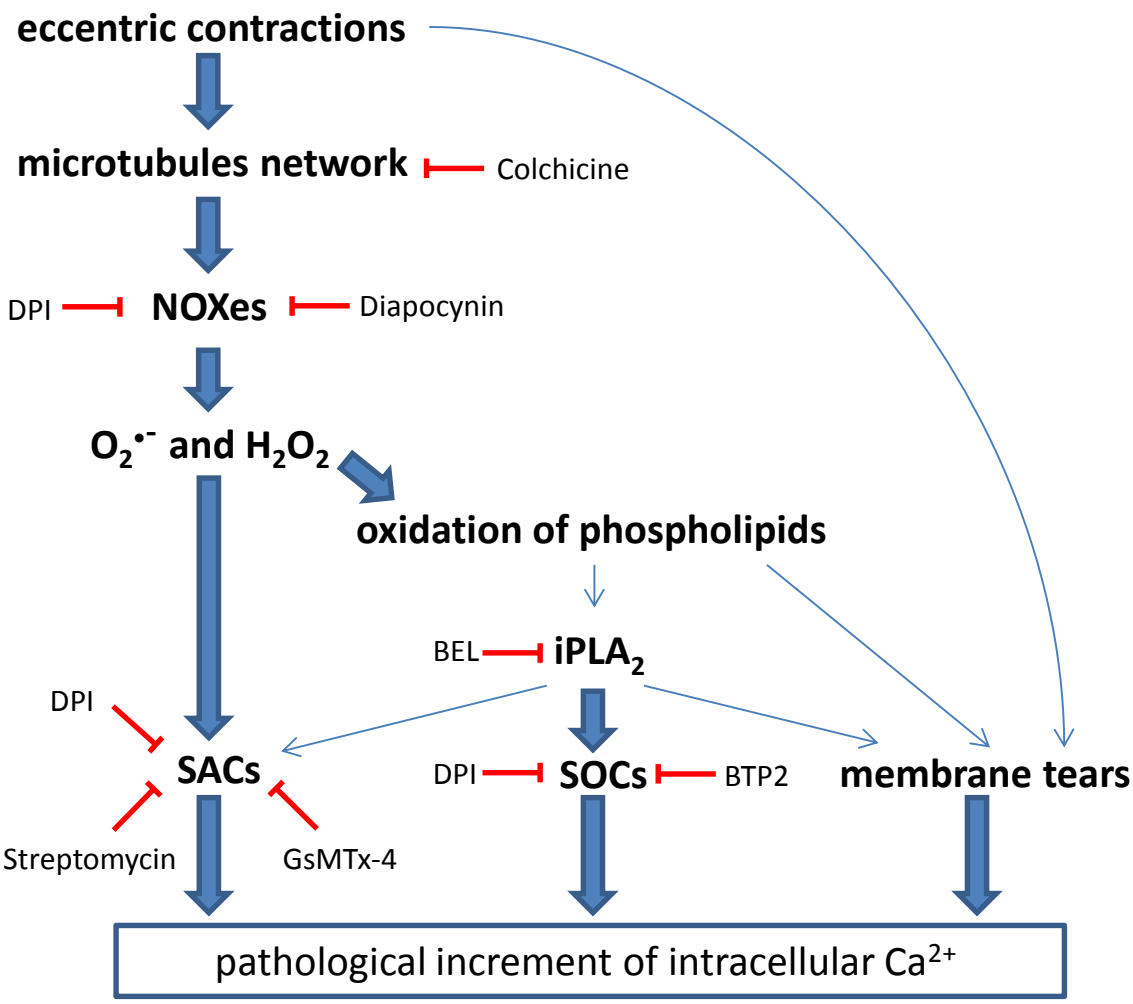
eccentric contractions
microtubules network
Colchicine
DPI
NOXes
Diapocynin
$O_2^{\bullet -}$ and H_2O_2
oxidation of phospholipids
BEL
iPLA$_2$
DPI
SACs
DPI
SOCs
BTP2
membrane tears
Streptomycin
GsMTx-4
pathological increment of intracellular Ca^{2+}

Figure 7

Chapter 4: Diapocynin, a putative NADPH oxidase inhibitor, ameliorates the phenotype of a mouse model of Duchenne muscular dystrophy

Manuscript in preparation

Preface

The following study is in preparation for submission before the end of 2013. Further experiments are being conducted to complete this manuscript. On-going work includes:

- In depth histological examination including necrotic surface determination and quantification of macrophages and other immune cell infiltration.
- Micro-arrays are being analysed in collaboration with Prof Eric Hoffmann at the Children's National Medical Center in Washington DC, USA. The results of this work will establish a full transcriptome of the treated mice deciphering the effects of the treatments on gene expression.
- Western blots using novel antibodies for NOXes.
- ELISA quantification of various cytokines including IL-1β, 6, 10.
- Quantification of apocynin and diapocynin in selected muscles and tissues.

Diapocynin, a putative NADPH oxidase inhibitor, ameliorates the phenotype of a mouse model of Duchenne muscular dystrophy

Hesham M. Ismail[1,2], Leonardo Scapozza[2], Urs T. Ruegg[1], Olivier M. Dorchies[1,2,3]

[1]Pharmacology; [2]Pharmaceutical Biochemistry, Geneva-Lausanne School of Pharmaceutical Sciences, University of Geneva and University of Lausanne, 30 Quai Ernest-Ansermet, Geneva 4, Switzerland; [3]Department of Cell Biology, University of Geneva, 30 Quai Ernest-Ansermet, Geneva 4, Switzerland.

Corresponding author: Olivier M. Dorchies, Olivier.dorchies@unige.ch

Abstract

Duchenne muscular dystrophy (DMD) is a severe X-linked muscular disease that causes premature death and for which no cure exists. We have shown previously that *in vitro* treatment of dystrophic myotubes and excised muscles with diapocynin, a dimer of the classically used NADPH oxidase inhibitor apocynin, ameliorated several molecular events involved in DMD pathogenesis, of which ROS production, phospholipase A_2 activity, Ca^{2+} influx and sarcolemmal integrity.

Here, we report on the *in vivo* effects of diapocynin and apocynin in mdx^{5Cv} dystrophic mice, a model of DMD. Apocynin (50 mg/kg/day) and diapocynin (10 and 100 mg/kg/day) were given orally to mdx^{5Cv} mouse pups, first via the lactating mothers from post-natal day 14 to 28 and subsequently directly to the weaned pups till post-natal day 35±1 or 60±3. Diapocynin but not apocynin enhanced spontaneous locomotor activity, rescued voluntary wheel running capabilities, and ameliorated diaphragm structure of dystrophic mice. Diapocynin and apocynin were equally potent at increasing the resistance to fatigue of triceps surae muscles exposed to repeated isometric contractions *in situ* and at preserving sarcolemmal integrity as evidenced by Evans blue dye uptake. Although apocynin and diapocynin had beneficial effects in dystrophic mice, diapocynin was superior in improving locomotion. Our findings suggest that diapocynin holds therapeutic potential for DMD.

Keywords

Apocynin, Duchenne muscular dystrophy, diapocynin, fatigue, mdx, muscle, NADPH oxidase

Introduction

Duchenne muscular dystrophy (DMD) is a rapidly progressive disease. In skeletal muscles of affected boys, lost muscle fibres are replaced with fat and fibrotic tissue. Patients are usually wheel-chaired by the age of 12. Adequate care and support has prolonged life expectancy to the early thirties. Most patients die because of respiratory failure or cardiomyopathy that become prominent in the late stages of the disease (Verhaert *et al.*, 2011). DMD is caused by mutations in the gene that encodes the protein dystrophin (Koenig *et al.*, 1987). In healthy skeletal muscles, dystrophin serves as an anchoring link between the cytoskeletal actin and the extracellular matrix through the dystrophin-glycoprotein complex. As a consequence of the lack of dystrophin, muscle fibres of DMD patient are sensitive to contraction-induced injury.

More than 25 years after the genetic cause of DMD has been identified (Koenig *et al.*, 1987), the molecular mechanisms leading to DMD remain incompletely understood. Increased Ca^{2+} was reported in muscle biopsies from DMD patients and in muscles of the mdx mice, a mouse model for DMD, implicating it to be a main driver of the pathology (Alderton & Steinhardt, 2000; Deconinck & Dan, 2007). Elevated Ca^{2+} influx through either store operated channels, stretch activated channels or sarcolemmal micro-ruptures were reported to be involved in this increase. Therapies targeting these subsets of channels have shown clear benefits in models of DMD yet proof of principle in DMD patients is still to be established (Ruegg *et al.*, 2012).

Oxidative stress has also been reported to be a major contributor to DMD pathology reviewed in Tidball and Wehling-Henricks (2007). Early studies have suggested that increased oxidative stress contribute to muscle damage and degeneration in dystrophic muscle. Markers of oxidative stress such as protein carbonyls and lipid peroxidation by-products were detected in muscles of DMD patients and mdx mice (Murphy & Kehrer, 1986; Ragusa *et al.*, 1997; Rodriguez & Tranopolsky, 2003). Lipid peroxidation products and increased expression of antioxidant enzymes have been detected in 3-week-old mdx mice before the onset of the disease, indicating an active role played by reactive oxygen species (ROS) in the pathogenesis (Disatnik *et al.*, 1998).

For a long time, mitochondria were thought to be the major source of pathological ROS in dystrophic muscles, however, in the last decade the focus on mitochondria decreased as evidences were accumulated for prevalent roles of NADPH oxidases (NOXes) in many ROS-mediated conditions including dystrophies (Quinn *et al.*, 2006; Sakellariou *et al.*, 2013a).

NOXes are transmembrane proteins that transport electrons across biological membranes to reduce oxygen to superoxide or H_2O_2. Many NOX isoforms exist that are expressed in a tissue-dependent manner and differ in their mode of activation. Of the NOXes whose mRNA is expressed in skeletal muscle, (Bedard & Krause, 2007). NOX4 is a constitutively active monomeric enzyme, whereas NOX2 requires the translocation of several regulatory subunits ($p22^{phox}$, $p47^{phox}$ and $p67^{phox}$) to the membrane-spanning subunit $gp91^{phox}$ to be active (Bedard & Krause, 2007).

It is becoming widely accepted that NOXes are major contributors of ROS production in both normal and dystrophic skeletal muscles (Jung *et al.*, 2008; Sakellariou *et al.*, 2013b; Xia *et al.*, 2003). In dystrophic muscle, noxious ROS can originate from NOXes expressed in the muscle fibres themselves as well as from infiltrated inflammatory cells (reviewed in (Lawler, 2011)). In fact, NOX2-generated ROS is a major cytotoxic mechanism of activated macrophages and lymphocytes. Reports have shown that NOX2 and all of its subunits, except $p22^{phox}$, are overexpressed in skeletal muscles from 19 days-old mice, just before the onset of necrosis (Whitehead *et al.*, 2010). NOX4 mRNA has been reported to be increased 5-fold in the left ventricles from 9-10 months old mdx mice (Spurney *et al.*, 2008).

To date, commercially available pharmacological compounds for efficient and selective NOX inhibition are lacking. One of the most popular compounds used for inhibiting NOX is apocynin. In fact, apocynin is a prodrug that undergoes dimerization into diapocynin by myeloperoxidases in phagocytic cells such as activated neutrophils and macrophages (Vejrazka *et al.*, 2005).

Using muscle cell cultures, which are unable to convert apocynin into active diapocynin, we have previously reported increased ROS production with apocynin. By contrast, providing synthetic diapocynin to the muscle cells markedly inhibited ROS production (Ismail *et al.*, 2013b). Diapocynin treatment also reduced Ca^{2+} influx and inhibited the activity of Ca^{2+}-independent phospholipase A_2 ($iPLA_2$), an enzyme that aggravates the dystrophic condition. Diapocynin also prevented force loss of dystrophic muscle subjected to eccentric contractions and preserved their membrane integrity as shown by reduced Procion orange dye uptake (Ismail *et al.*, 2013b). Collectively, our *in vitro* data were supporting diapocynin-mediated blockade of NOXes as an approach for the treatment of DMD. As a continuation of these encouraging findings, we report here on the evaluation of apocynin (50 mg/kg/day) and diapocynin (10 and 100 mg/kg/day) in vivo in mdx^{5Cv} mice.

No undesired effects were noticed with all treatment regimens. Diapocynin administration improved locomotor activity, normalized wheel running capability, increased resistance to fatigue induced by repeated contractions, improved sarcolemmal stability and protected diaphragm muscle form necrosis.

Materials and methods

Mice and treatment groups

All of the procedures involving animals were conducted in accordance with the Swiss Federal Veterinary Office's guidelines, based on Swiss Federal Law on Animal Welfare authorization number 106/3625/1. Colonies of dystrophic mdx^{5Cv} mice (The Jackson Laboratory, Bar Harbor, ME), and their genetically normal counterparts, C57BL/6J Charles River (Iffa Credo, Saint Germain sur l'Arbresle, France) were maintained at the Geneva-Lausanne School of Pharmaceutical Sciences. Animals were housed in plastic cages containing wood granule bedding, maintained with 12-hour dark/12-hour light cycles and unlimited access to food and water throughout the study. Apocynin (Sigma, Buchs, Switzerland) was used to synthesize diapocynin through an oxidative coupling reaction as described previously (Ismail *et al.*, 2013b; Wang *et al.*, 2008). Test compounds were mixed with crushed standard rodent chow and modified pellets were prepared (Provimi-Kliba, Kaiseraugst, Switzerland) to contain 0.1 g/kg and 1 g/kg of diapocynin, or 0.5 g/kg apocynin. Control diet consisted of drug-free pellets was prepared according to the same procedure. Because no data exist as to the stability of the compounds, control and modified diets were stored at -20°C in 0.5-kg vacuum-sealed bags and care was taken to provide the treated mice with small amounts of the diets 2-3 times per week.

Breeders were mated and pregnant females were housed in cages enriched with soft bedding material. Female pups were killed around post-natal day 2-3. Dams with 2-4 male dystrophic pups were randomly assigned to one of the following groups: low diapocynin (L-Dia group; 0.1 g/kg diet), high diapocynin (H-Dia group; 1 g/kg diet), apocynin (Apo group; 0.5 g/kg), or non-treated (Dys group; control diet). Male wild type mice fed control diet (wt group) were used for reference. Modified food pellets were provided to the feeding dams when the male pups were 14-15-days old (age 2 weeks). Modified food pellets were subsequently placed inside the cages (directly on the floor/bedding surface) when the pups were 17-18 days old (age 2.5 weeks), i.e. when they are old enough to start feeding themselves with solid chow. The male pups were weaned on post-natal day

28 (age 4 weeks). The treatments were continued to two end points, either 35±1 days post-natal (age 5 weeks) or 60±3 days post-natal (age 8-9 weeks) to evaluate the effects of the compounds on muscle necrosis and muscle regeneration, respectively.

A first set of 72 mice was used for measuring isometric force and collecting tissues for histology at 5 and 8-9 weeks of age (n = 6-8 mice per group). Treatments were repeated on another set of 57 8-weeks old mice dedicated to spontaneous wheel running (n = 11-12 mice per group). Finally, a third set of 27 mice was employed for assessing Evans blue dye uptake (n = 10-12 muscles per group). Body weight and food consumption was monitored every 3-4 days on all mice. Locomotor activity was measured on most 8-weeks old mice.

Spontaneous locomotor activity

Around post-natal day 52-60 (i.e. a few days before the end of the longest treatment period), spontaneous locomotor activity was measured as described (Nakae *et al.*, 2012). In brief, mice were isolated in a LOCOMO sensor system that utilizes a horizontal lattice of intersecting infrared beams (Melquest, Toyama, Japan). When a mouse crosses a beam, the setup records a single count. The locomotor activity was measured by periods of 10 min over a total duration of 48 hours. The activity of first day of measurement, during which the animals show high inter-individual variations, was excluded from the analysis. The locomotor activity was calculated from a 24-hours period starting at 10:00 a.m. on the second day of measurement.

Voluntary wheel running

Just after measurement of spontaneous locomotor activity, voluntary wheel running was assessed in a subset of mice (aged 8 weeks). Mice were housed individually for 7 days in cages equipped with free-turning stainless steel activity wheels (diameter 23 cm; lane width 5 cm) (Bioseb, Vitrolles, France). The wheel could be turned in either direction. The wheels were connected to a computer running dedicated software (Bioseb) and the distance travelled by each animal was automatically recorded by period of 5 minutes (Grounds *et al.*, 2008).

Evans blue dye uptake

Evans blue dye (Sigma) was used to evaluate the impact of the test compounds on membrane integrity essentially as described (Hamer *et al.*, 2002). At 8 weeks of age, mice received a single i.p injection of Evans blue dye (1% v/w, 10 mg/mL in 0.9 % NaCl, sterile filtered). Twenty-four hours

post injection, the mice were anaesthetized as described earlier and selected muscles (EDL, soleus, tibialis posterior, hemi-diaphragms) were dissected bilaterally and embedded in 1% tragacanth gum. Twenty µM sections were fixed in cold acetone at -20°C for 2 min and subsequently incubated for 1 h with 2 mg/mL wheat germ agglutinin conjugated to Alexa Fluor 488 (WGA-AF488; Molecular Probes, Invitrogen, Basel, Switzerland) in phosphate-buffered saline at room temperature to stain the extracellular matrix. Fluorescence images from the whole muscle surface were taken with an Axiocam camera fitted on a Mirax Midi scanner microscope (Zeiss, Feldbach, Switzerland). The quantity of Evans blue positive fibres were reported as percentage of the total fibres.

Isometric force measurement *in vivo*

At both the 5 and the 8 weeks end points, mice were anesthetized, and muscle responses to electrical stimulations were recorded isometrically in the right triceps surae as previously described (Dorchies *et al.*, 2013; Hibaoui *et al.*, 2011; Nakae *et al.*, 2012; Reutenauer-Patte *et al.*, 2012; Reutenauer *et al.*, 2008). Mice were anesthetized by an i.p. injection of a mixture of urethane (1.5 g/kg, Sigma) and diazepam (5 mg/kg, Roche, Basel, Switzerland). The knee joint was firmly immobilized, and the Achilles tendon was linked to a force transducer coupled to a LabView interface (National Instruments, Austin, TX). Two thin steel electrodes were inserted intramuscularly, and 0.5-ms pulses of controlled intensity and frequency were delivered. After manual settings of optimal muscle length (L_o) and optimal current intensity, five phasic twitches were recorded at a sampling rate of 3 kHz to determine the absolute peak twitch force (P_t), the time to peak twitch tension (TTP) and the time for half relaxation from peak twitch tension ($RT_{1/2}$). After a 3-minute pause, muscles were subjected to a force-frequency test: 200-ms long stimuli of increasing frequencies (10 to 100 Hz by increments of 10 Hz) were delivered at intervals of 30 seconds. When necessary, further stimulations at 120, 150, and 200 Hz were delivered to obtain the maximum response, which was taken as the absolute optimal tetanic tension (P_o). After another 3-minute pause, the resistance of the triceps to repeated tetani was assayed. Frequency was set at 100 Hz, and muscle tension was recorded while subjected to repeated stimulations, each contraction consisted of a 200-ms burst, repeated every 30 sec to deliver a total of 20 contractions. The responses were expressed as the percentage of the maximal tension. Absolute phasic and tetanic tensions were converted into specific tensions (in mN per mm^2 of muscle section) after normalization for the muscle cross-sectional area. The cross-sectional area values (in mm^2) were

determined by dividing the triceps surae muscle mass (in mg) by the product of the optimal muscle length (in mm) and the density of mammalian skeletal muscle (1.06 mg/mm^3).

Blood sampling and tissue collection

After the measurement of the muscle contractile properties, the thoracic cavity was opened, the mice received an intra-cardiac injection of heparin (30 µL; 3000 U/mL) and the aorta was cut. Whole blood was collected from the chest cavity in heparinized centrifuge tubes. The blood was centrifuged at 1000g for 10 min at 4°C, and plasma was stored at -80°C. Skeletal muscles and other selected organs were dissected and weighed.

Tissue extraction

Frozen gastrocnemius muscles were ground to a fine powder in liquid nitrogen-cooled mortars. Fractions of about 10 or 30 mg were rapidly weighed into liquid nitrogen-cooled microtubes. Powders were either used for RNA extraction prior to mRNA expression profiling, or for preparing muscle lysates for protein analysis. For Western-blot analysis, fractions of powdered muscles were lysed in 9 volumes (v/w) of Guba-Straub buffer (in mmol: 300 NaCl, 100 NaH_2PO_4, 50 Na_2HPO_4, 10 $Na_4P_2O_7$, 1 $MgCl_2$, and 10 EDTA at pH 6.5) containing 0.1% 2-mercaptoethanol and 0.2% protease inhibitor cocktail (Sigma). After incubation with gentle shaking for 45 minutes at 4°C, the samples were sonicated for 10 seconds, Triton X-100 (Applichem, Axonlab, Le Mont-sur-Lausanne, Switzerland) was added to a final concentration of 1%, and lysates were centrifuged at 12,000 *g* for 15 minutes at 4°C. The supernatants were collected, and protein content was determined using the Bradford method (Bio-Rad, Reinach, Switzerland). Lysates were diluted with reducing Laemmli buffer at a final protein concentration of 3 mg/mL before being used for immunoblotting.

Histologic examination of skeletal muscles

The *extensor digitorum longus* (EDL), *soleus* (Sol), from the right leg and the right hemi-diaphragm were embedded in tragacanth gum, frozen in liquid nitrogen-cooled isopentane, and stored at -80°C until processed further. Transverse sections 10 mm thick were stained with hematoxylin and eosin (H&E) according to standard procedures, and images covering the entire muscle sections were acquired with an Axiocam camera fitted on a Mirax Midi automated microscope (Dorchies *et al.*, 2013). In normal fibres, the nuclei are located close to the sarcolemma, whereas in regenerated fibres the nuclei remain internalized. On the basis of these morphologic features, both normal

fibres (showing peripheral nuclei) and regenerated fibres (presenting with centronucleation) were counted. Regenerated fibres are expressed as the percentage of the total muscle fibres.

Statistical analysis

GraphPad Prism software version 6 (GraphPad, San Diego, CA) was used for constructing the graphs and for performing the statistical analyses. One-way ANOVA analysis followed by Dunnett's multiple comparisons post-tests to assay the differences between treatment groups. Differences with P values ≤ 0.05 were considered significant.

Results

Apocynin and diapocynin treatments were well tolerated by dystrophic mice

Dystrophic mice treated orally with apocynin and diapocynin behaved normally throughout the course of the study. No toxicity was observed in any group and all the mice survived the whole treatment period. No treatment-dependent alteration in body weight was observed up to the 8 weeks of age (Figure 1A). Daily food intake was similar in all groups and slightly decreased from 0.196±0.011 to 0.157±0.012 g/g body weight/day during the course of the study (Figure 1B). On average, this corresponded to a daily drug intake of 87.5 mg/kg of apocynin in the Apo group, and 17.5 mg/kg and 175 mg/kg of diapocynin in the L-Dia and the H-Dia groups, respectively.

At the age of 5 weeks, no differences in the relative weight of any of the skeletal muscles examined were detected in any of the treatment groups. At the age of 8-9 weeks, both Apo and H-Dia caused a significant increase in the relative weight of the soleus (from 0.29±0.02 to 0.35±0.01 and 0.37± 0.01, respectively; not shown). The relative weight of the diaphragm was increased in Dys mice (2.6±0.07 mg/g) as compared to wt mice (1.9±0.02 mg/g), and all treatments normalized this hypertrophy (data not shown).

Diapocynin treatment transiently increased testes weight and diminished peri-epididymal white adipose tissue. At 8 weeks, the thymus weight was increased in all groups as compared to dystrophic controls (data not shown). These effects may be related to specific roles for NOXes in these tissues.

Diapocynin but not apocynin improves spontaneous locomotor activity

Mice were placed individually for 48 hours in a device that measures spontaneous activity in the horizontal plane. Data acquired during the second day of measurement, i.e. after mice got

acclimatized to their new environment are presented in Figure 2. Figure 2A shows actigrams that describes the evolution of the locomotor activity over 24 hours. Dys and wt mice were much more active during the dark phase than during the light phase and the treatments did not modify this overall behaviour. During the period of highest activity, Dys mice moved about 30% less than the wt mice (Figure 2B; 3302±200 vs. 5150±386 counts per 24h). Diapocynin at either dose completely normalized this decline in locomotor activity. Apocynin treatment failed in rescuing the activity deficit (Figure 2B).

Diapocynin but not apocynin restores voluntary wheel running capability

Mice were placed in cages equipped with freely rotating wheels for 7 days. Mice in all groups made spontaneous use of the wheel essentially in the dark phase. The running activity was presented as 2 major peaks, at the beginning and shortly before termination of the dark phase, respectively. This behaviour was not altered by any treatment. Mice from all groups spent about 35% of the time running in the wheels. The cumulative distance run by the mice during the 7-day period was strongly reduced in the Dys group as compared to the wt group (18.0±0.9 km vs. 30.4±1.6 km, respectively). This deficit in wheel running capability was improved by both doses of diapocynin but not by apocynin treatment. Other wheel running parameters, such as velocity and acceleration were not significantly different between the groups (Figure 3).

Diapocynin and apocynin prevented Evans blue dye uptake by muscle fibres

Sarcolemmal integrity is known to be compromised in dystrophic muscle. In order to evaluate the effects of apocynin and diapocynin on this feature, Evans blue dye, a membrane impermeable vital dye was injected i.p. to mice and dye uptake into muscle fibres was evaluated 24 hours afterwards in the soleus, diaphragm and tibialis posterior muscles. As illustrated in Figure 4A, EBD conferred a red fluorescence to the myofibres whose plasma membrane was damaged. In Dys mice, all tested muscles exhibited an enhanced EBD uptake amounting to 7.3±2.2% in the Sol, 15.7±2.2% in the diaphragm, and 28.1±3.1% in the tibialis posterior (Figure 4B). By contrast, EBD uptake was less than 1% in all wt muscles. Diapocynin and apocynin treatments reduced EBD uptake several-fold in all tested muscles to values close or even similar to that of wt mice (figure 4B).

Diapocynin and apocynin do not affect force generation but prevents muscle fatigue

Isometric force and resistance to fatigue of the triceps surae was evaluated *in situ* at both end points, i.e. at 5 and 8 weeks of age. Wt mice produced significantly higher phasic and tetanic forces

compared to their Dys counterparts at both end points. Treatment with either apocynin or diapocynin did not result in an improvement of any of the aforementioned parameters (Figure 5).

To evaluate the fatigue of the triceps surae, the muscle was submitted to repeated tetanic contractions (Figure 6). The procedure caused minimal force loss (5-7%) in wt mice but was much more deleterious in Dys mice, in which force dropped by about 25% at both end points. At 5 weeks of age, all treatments were equipotent and prevented force loss by about 50%. Overall, the protection from fatigue was similar at 8 weeks of age, However, L-Dia tended to be slightly less efficacious than in younger mice, resulting in a dose dependent protection from contraction-induced fatigue (Figure 6).

Diapocynin and apocynin improved diaphragm structure

The percentage of centrally nucleated fibres was determined in the EDL, soleus and diaphragm at 5 and 8 weeks of age. Neither diapocynin nor apocynin treatment altered the percentage of centrally nucleated fibres in the EDL and the soleus muscles. However centronucleation in the diaphragm decreased from about 50% in Dys mice to 38% in the Apo and H-Dia groups (n=6-16).

Discussion

The hypothesis on which the current work was based upon is that diapocynin would be superior in term of its pharmacokinetic profile as well as of its pharmacological efficacy compared to its prodrug apocynin, which requires myeloperoxidase expressed in neutrophils and activated macrophages to become a NOX inhibitor, namely diapocynin. Indeed, we found that diapocynin administration to mdx mice provided therapeutic benefits as judged by: 1) enhanced locomotor activity to levels of non-dystrophic controls, 2) amelioration of wheel running capabilities, 3) improved sarcolemmal stability as seen by prevention of Evans blue dye uptake, 4) increased resistance to fatigue and 5) improvement of diaphragm structure. Apocynin on the other hand was beneficial in some of the outcomes measured but did not ameliorate lost locomotor activity or reduced voluntary wheel running capability.

Diapocynin and apocynin treatment were well tolerated during the course of the study. Besides a small increase in the weight of the testes and reduced white adipose tissue at the 5 weeks end point, no other differences were observed at this time point. NOX activities have been implicated in fat deposition in mice receiving a fat rich diet and NOX inhibition was reported to inhibit diet-

induced obesity (Ronis *et al.*, 2013). Such an effect can explain the reduced white adipose tissue accumulation in mice seen by the treatments. At the 8 weeks end point, the weight of thymus was increased in all groups, which could be attributed to the immune modulatory effects of NOX inhibitors (Segal *et al.*, 2012). On the other hand, the weight of the Sol was increased whereas that of the diaphragm decreased. These weight changes are minimal and do not indicate a toxic effect.

Treatment of dystrophic mice with either dose of diapocynin or apocynin did not rescue the reduced force-generating ability as evidenced by *in situ* force measurement. This finding is supported by the histological results showing no structural improvements in the EDL or Sol muscles. However, a marked enhancement in the resistance to fatigue was observed in all treatment groups. Dystrophic muscles lost force in fatigue protocols in an aggravated manner compared to non-dystrophic controls. This observation is in agreement with previous reports from our lab (Dorchies *et al.*, 2013; Hibaoui *et al.*, 2011; Reutenauer-Patte *et al.*, 2012) although the protocol used here is less intense than the one used in previous studies. Fatigue is a multifactorial phenomenon with complicated regulation. Early reports suggested the involvement of ROS in fatigue regulation. Muscles produce ROS continuously, and the rate of which increases dramatically with exercise (reviewed in Reid (2008)). Downstream consequences of such radicals are multiple and include sarcolemmal function, myofilament interactions, mitochondrial metabolism and Ca^{2+} regulation (Reid, 2008). In an attempt to recapitulate the damage induced by ROS, brief exposure to hydrogen peroxide was shown to result in reduced force production without affecting tetanic Ca^{2+} transients and this effect was reversed by reducing agents (Moopanar & Allen, 2006). This leads to the conclusion that low ROS levels modulate fatigue by an effect on the myofilaments directly rather than by affecting Ca^{2+} regulation, which can be seen after higher and prolonged ROS exposure (Andrade *et al.*, 1998; Andrade *et al.*, 2001). This type of exposure is probably not the case in the low intensity fatigue employed in the current study. Supporting evidence for the involvement of ROS in skeletal muscle fatigue came from the protective effect rendered by anti-oxidant treatment of skeletal muscle. One of the most intensely studied anti-oxidants in skeletal muscle is *N*-acetylcysteine (NAC). Incubation of isolated muscles in buffers containing NAC delayed significantly the fatigue observed in these preparations (Shindoh *et al.*, 1990; Whitehead *et al.*, 2008). Clinical trials with NAC also reduced force loss in healthy volunteers undergoing NAC infusion (Reid *et al.*, 1994). However, other trials with different anti-oxidants were unsuccessful and their failure was attributed to the lack of specific targeting of the anti-oxidant therapies (reviewed in Kim *et al.*

(2013)). Diapocynin and apocynin inhibiting ROS production directly via NOXes should render dystrophic muscle more resistant to fatiguing stimulations. One has to consider that fatigue can be a protective mechanism, known as “muscle braking” (Reid, 2008). Moderate ROS levels act as a signal to prevent continuation of excessive workload, which eventually leads to an irreversible damage of the force-producing machinery. Another aspect to be investigated is whether a similar protection can be seen in non-dystrophic muscles treated with these compounds.

Other factors can contribute to the normalization of fatigue, wheel running capability and locomotor activity by NOX inhibitors such as vascular effects. Aberrant NOX expression and activity have been reported to be pathological inducers of various cardiovascular diseases including hypertension, atherosclerosis and cardiac failure and NOX inhibition to be cardio-protective after ischemia-reperfusion injury (Rodino-Janeiro *et al.*, 2013). In mdx mice, reduced tissue perfusion plays a role in the pathogenesis of this disease. In DMD, dystrophin absence causes signaling defects due to mislocalised and lowered production of NO, which results in reduced vasodilatation and inadequate tissue perfusion followed by functional ischemia (Ennen *et al.*, 2013). NOX inhibition by diapocynin or apocynin can provide functional improvements by ameliorating tissue perfusion.

The ameliorated muscle function seen in this study could also be due to the treatment-related histological improvement of the diaphragm, although it was marginal. A poster communication in 2009 established that mdx mice undergoing apocynin treatment showed an improvement of diaphragm structure and reduced fibrosis (Kim *et al.*, 2009). The authors reported that this protective effect was mediated through several pathways including matrix metalloproteinases 2 and 9, and tissue inhibitors of metalloproteinases (TIMP-1). The histological examination of the diaphragm in our study was limited to central nucleation at the two end points but a more detailed investigation including fibrotic markers and immune cell infiltration is ongoing to investigate the role played by NOXes, which seems to be of particular importance in the diaphragm.

Another target of excessive ROS production in mdx mice is the sarcolemma. Direct oxidation of membrane phospholipids or indirect effects initiated by increased ROS production can affect membrane fluidity, fragility and its response to mechanical stress (Allen & Whitehead, 2011). Diapocynin and apocynin by preventing excessive ROS production reduce oxidation of phospholipids and can improve membrane integrity; this is evidenced by decreased Evans blue dye

uptake seen in this study. This protection is in agreement with our results with Procion orange dye in isolated muscles exposed to repeated eccentric contractions, known to induce damage in dystrophic muscles (Ismail *et al.*, 2013b).

One has to consider that NOXes are strongly involved in immune response not only in the phagocytic respiratory burst but also in immune signaling and chemotaxis (Dupre-Crochet *et al.*, 2013). NOX inhibitors were reported to be anti-inflammatory (Ghosh *et al.*, 2012; Houser *et al.*, 2012), anti-fibrotic (Jarman *et al.*, 2013) and to have neuro-protective effects (Ghosh *et al.*, 2012; Sorce *et al.*, 2012). All of the above mentioned pharmacological effects of NOX inhibitors should convey a benefit to mdx mice suffering from a complex multifactorial pathology.

Diapocynin treatment was more potent than apocynin in the assays performed in this study as seen in the locomotor activity and wheel running tests. The original hypothesis upon which this work was constructed is the assumption that diapocynin administration would be therapeutically superior to apocynin, which requires activated macrophages for its bioconversion and these could not be available in all compartments. Diapocynin also has the advantage of being around 10 times more lipophilic compared to apocynin, which should improve its pharmacokinetic profile. Another consideration is the possibility that apocynin and diapocynin act as direct anti-oxidants through ROS scavenging. In such a case, diapocynin would be a better anti-oxidant due to the presence of 2 phenolic hydroxyl groups instead of one with apocynin.

In conclusion, we report here for the first time the therapeutic potential of diapocynin administration in mdx mice. Diapocynin administration improved locomotor activity and wheel running capability, increased resistance to fatigue and reduced sarcolemmal damage. Further investigations are needed to decipher the exact mechanism of action, to optimize dose as well as formulation and to decipher the contribution of exacerbated NOX activities in various dystrophic tissues.

Acknowledgments

This work was supported by grants from the Swiss National Science Foundation, the Association Française contre les myopathies (AFM, France) and the Duchenne Parent Project-The Netherlands (DPP-NL).

References

Alderton JM, Steinhardt RA (2000). Calcium influx through calcium leak channels is responsible for the elevated levels of calcium-dependent proteolysis in dystrophic myotubes. *J Biol Chem* **275**(13)**:** 9452-9460.

Allen DG, Whitehead NP (2011). Duchenne muscular dystrophy - What causes the increased membrane permeability in skeletal muscle? *Int J Biochem Cell* **43**(3)**:** 290-294.

Andrade FH, Reid MB, Allen DG, Westerblad H (1998). Effect of hydrogen peroxide and dithiothreitol on contractile function of single skeletal muscle fibres from the mouse. *J Physiol* **509 (Pt 2):** 565-575.

Andrade FH, Reid MB, Westerblad H (2001). Contractile response of skeletal muscle to low peroxide concentrations: myofibrillar calcium sensitivity as a likely target for redox-modulation. *FASEB J* **15**(2)**:** 309-311.

Bedard K, Krause KH (2007). The NOX family of ROS-generating NADPH oxidases: physiology and pathophysiology. *Physiol Rev* **87**(1)**:** 245-313.

Deconinck N, Dan B (2007). Pathophysiology of duchenne muscular dystrophy: current hypotheses. *Pediatr Neurol* **36**(1)**:** 1-7.

Disatnik MH, Dhawan J, Yu Y, Beal MF, Whirl MM, Franco AA*, et al.* (1998). Evidence of oxidative stress in mdx mouse muscle: studies of the pre-necrotic state. *J Neurol Sci* **161**(1)**:** 77-84.

Dorchies OM, Reutenauer-Patte J, Dahmane E, Ismail HM, Petermann O, Patthey- Vuadens O*, et al.* (2013). The anticancer drug tamoxifen counteracts the pathology in a mouse model of duchenne muscular dystrophy. *Am J Pathol* **182**(2)**:** 485-504.

Dupre-Crochet S, Erard M, Nubetae O (2013). ROS production in phagocytes: why, when, and where? *J Leukoc Biol*.

Ennen JP, Verma M, Asakura A (2013). Vascular-targeted therapies for Duchenne muscular dystrophy. *Skelet Muscle* **3**(1)**:** 9.

Ghosh A, Kanthasamy A, Joseph J, Anantharam V, Srivastava P, Dranka BP*, et al.* (2012). Anti-inflammatory and neuroprotective effects of an orally active apocynin derivative in pre-clinical models of Parkinson's disease. *J Neuroinflamm* **9:** 241.

Grounds MD, Radley HG, Lynch GS, Nagaraju K, De Luca A (2008). Towards developing standard operating procedures for pre-clinical testing in the mdx mouse model of Duchenne muscular dystrophy. *Neurobiol Dis* **31**(1)**:** 1-19.

Hamer PW, McGeachie JM, Davies MJ, Grounds MD (2002). Evans Blue Dye as an in vivo marker of myofibre damage: optimising parameters for detecting initial myofibre membrane permeability. *J Anat* **200**(1)**:** 69-79.

Hibaoui Y, Reutenauer-Patte J, Patthey-Vuadens O, Ruegg UT, Dorchies OM (2011). Melatonin improves muscle function of the dystrophic mdx5Cv mouse, a model for Duchenne muscular dystrophy. *J Pineal Res* **51**(2)**:** 163-171.

Houser KR, Johnson DK, Ishmael FT (2012). Anti-inflammatory effects of methoxyphenolic compounds on human airway cells. *J Inflamm (Lond)* **9:** 6.

Ismail HM, Scapozza L, Ruegg UT, Dorchies OM (2013). Diapocynin, a NADPH oxidase inhibitor, reduces ROS production and prevents force loss in eccentrically contracting dystrophic muscle. *PLoS One* **In revision**.

Jarman ER, Khambata VS, Cope C, Jones P, Roger J, Yun Ye L*, et al.* (2013). An Inhibitor of NADPH Oxidase-4 Attenuates Established Pulmonary Fibrosis in a Rodent Disease Model. *Am J Respir Cell Mol Biol*.

Jung C, Martins AS, Niggli E, Shirokova N (2008). Dystrophic cardiomyopathy: amplification of cellular damage by Ca^{2+} signalling and reactive oxygen species-generating pathways. *Cardiovasc Res* **77**(4)**:** 766-773.

Kim JH, H.B. K, Lawler JM (2009). The effects of a NAD(P)H oxidase inhibition on matrix metalloproteinases and TIMP-1 in the mdx diaphragm. *Int J Exerc Sci* **2**(1)**:** S36.

Kim JH, Kwak HB, Thompson LV, Lawler JM (2013). Contribution of oxidative stress to pathology in diaphragm and limb muscles with Duchenne muscular dystrophy. *J Muscle Res Cell M* **34**(1)**:** 1-13.

Koenig M, Hoffman EP, Bertelson CJ, Monaco AP, Feener C, Kunkel LM (1987). Complete cloning of the Duchennne muscular dystrophy (DMD) cDNA and preliminary genomic organization of the DMD gene in normal and affected individuals. *Cell* **50:** 509-517.

Lawler JM (2011). Exacerbation of pathology by oxidative stress in respiratory and locomotor muscles with Duchenne muscular dystrophy. *J Physiol* **589**(Pt 9)**:** 2161-2170.

Moopanar TR, Allen DG (2006). The activity-induced reduction of myofibrillar Ca^{2+} sensitivity in mouse skeletal muscle is reversed by dithiothreitol. *J Physiol* **571**(Pt 1)**:** 191-200.

Murphy ME, Kehrer JP (1986). Free radicals: a potential pathogenic mechanism in inherited muscular dystrophy. *Life Sci* **39**(24)**:** 2271-2278.

Nakae Y, Dorchies OM, Stoward PJ, Zimmermann BF, Ritter C, Ruegg UT (2012). Quantitative evaluation of the beneficial effects in the mdx mouse of epigallocatechin gallate, an antioxidant polyphenol from green tea. *Histochem Cell Biol* **137**(6)**:** 811-827.

Quinn MT, Ammons MC, Deleo FR (2006). The expanding role of NADPH oxidases in health and disease: no longer just agents of death and destruction. *Clin Sci (Lond)* **111**(1)**:** 1-20.

Ragusa RJ, Chow CK, Porter JD (1997). Oxidative stress as a potential pathogenic mechanism in an animal model of Duchenne muscular dystrophy. *Neuromuscul Disord* **7**(6-7)**:** 379-386.

Reid MB (2008). Free radicals and muscle fatigue: Of ROS, canaries, and the IOC. *Free Radic Biol Med* **44**(2)**:** 169-179.

Reid MB, Stokic DS, Koch SM, Khawli FA, Leis AA (1994). *N*-acetylcysteine inhibits muscle fatigue in humans. *J Clin Invest* **94**(6)**:** 2468-2474.

Reutenauer-Patte J, Boittin FX, Patthey-Vuadens O, Ruegg UT, Dorchies OM (2012). Urocortins improve dystrophic skeletal muscle structure and function through both PKA- and Epac-dependent pathways. *Am J Pathol* **180**(2)**:** 749-762.

Reutenauer J, Dorchies OM, Patthey-Vuadens O, Vuagniaux G, Ruegg UT (2008). Investigation of Debio 025, a cyclophilin inhibitor, in the dystrophic mdx mouse, a model for Duchenne muscular dystrophy. *Br J Pharmacol* **155**(4)**:** 574-584.

Rodino-Janeiro BK, Paradela-Dobarro B, Castineiras-Landeira MI, Raposeiras-Roubin S, Gonzalez-Juanatey JR, Alvarez E (2013). Current status of NADPH oxidase research in cardiovascular pharmacology. *Vasc Health Risk Manag* **9:** 401-428.

Rodriguez C, Tranopolsky MA (2003). Patients with dystrophinopathy show evidence of increased oxidative stress. *Free Radic. Biol. Med.* **34**(9)**:** 1217-1220.

Ronis MJ, Sharma N, Vantrease J, Borengasser SJ, Ferguson M, Mercer KE*, et al.* (2013). Female mice lacking p47phox have altered adipose tissue gene expression and are protected against high fat-induced obesity. *Physiol Genomics* **45**(9)**:** 351-366.

Ruegg UT, Shapovalov G, Jacobson K, Reutenauer-Patte J, Ismail HM, Dorchies OM*, et al.* (2012). Store-operated channels and Ca^{2+} handling in muscular dystrophy. In: *Store-operated Ca^{2+} entry (SOCE) pathways*, Groschner K, Graier WF, Romanin C (eds) Vol. 1, pp 449-457: SpringerWien.

Sakellariou GK, Jackson MJ, Vasilaki A (2013a). Redefining the major contributors to superoxide production in contracting skeletal muscle. The role of NAD(P)H oxidases. *Free Radic Res*.

Sakellariou GK, Vasilaki A, Palomero J, Kayani A, Zibrik L, McArdle A*, et al.* (2013b). Studies of mitochondrial and nonmitochondrial sources implicate nicotinamide adenine dinucleotide phosphate oxidase(s) in the increased skeletal muscle superoxide generation that occurs during contractile activity. *Antioxid Redox Sign* **18**(6)**:** 603-621.

Segal BH, Grimm MJ, Khan AN, Han W, Blackwell TS (2012). Regulation of innate immunity by NADPH oxidase. *Free Radic Biol Med* **53**(1)**:** 72-80.

Shindoh C, DiMarco A, Thomas A, Manubay P, Supinski G (1990). Effect of *N*-acetylcysteine on diaphragm fatigue. *J Appl Physiol* **68**(5)**:** 2107-2113.

Sorce S, Krause KH, Jaquet V (2012). Targeting NOX enzymes in the central nervous system: therapeutic opportunities. *Cell Mol Life Sci* **69**(14)**:** 2387-2407.

Spurney CF, Knoblach S, Pistilli EE, Nagaraju K, Martin GR, Hoffman EP (2008). Dystrophin-deficient cardiomyopathy in mouse: expression of Nox4 and Lox are associated with fibrosis and altered functional parameters in the heart. *Neuromuscul Disord* **18**(5)**:** 371-381.

Tidball JG, Wehling-Henricks M (2007). The role of free radicals in the pathophysiology of muscular dystrophy. *J Appl Physiol* **102**(4)**:** 1677-1686.

Vejrazka M, Micek R, Stipek S (2005). Apocynin inhibits NADPH oxidase in phagocytes but stimulates ROS production in non-phagocytic cells. *Biochim Biophys Acta* **1722**(2)**:** 143-147.

Verhaert D, Richards K, Rafael-Fortney JA, Raman SV (2011). Cardiac involvement in patients with muscular dystrophies: magnetic resonance imaging phenotype and genotypic considerations. *Circ Cardiovasc Imaging* **4**(1)**:** 67-76.

Wang Q, Smith RE, Luchtefeld R, Sun AY, Simonyi A, Luo R*, et al.* (2008). Bioavailability of apocynin through its conversion to glycoconjugate but not to diapocynin. *Phytomedicine* **15**(6-7)**:** 496-503.

Whitehead NP, Pham C, Gervasio OL, Allen DG (2008). *N*-Acetylcysteine ameliorates skeletal muscle pathophysiology in mdx mice. *J Physiol* **586**(7)**:** 2003-2014.

Whitehead NP, Yeung EW, Froehner SC, Allen DG (2010). Skeletal muscle NADPH oxidase is increased and triggers stretch-induced damage in the mdx mouse. *PLoS One* **5**(12)**:** e15354.

Xia R, Webb JA, Gnall LL, Cutler K, Abramson JJ (2003). Skeletal muscle sarcoplasmic reticulum contains a NADH-dependent oxidase that generates superoxide. *Am J Physiol* **285**(1)**:** C215-221.

Figure legends and figures

Figure 1

Diapocynin neither affected food intake nor body weight over a 9-week treatment period

Diapocynin was well tolerated as evidenced by the lack of effect on increase in body weight (A, n=12-26) or food intake (B, n=3-6). Food intake was calculated based on average food intake for a treatment cage and subsequently dividing the obtained value by the number of mice in the group.

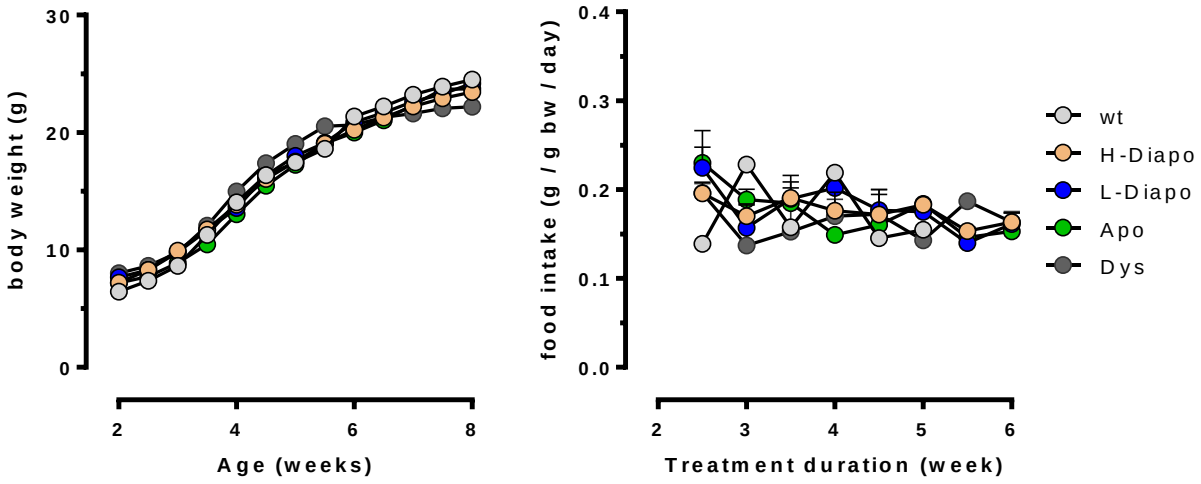
body weight (g)
30
20
10
0
2
4
6
8
Age (weeks)
food intake (g / g bw / day)
0.4
0.3
0.2
0.1
0.0
2
3
4
5
6
Treatment duration (week)
wt
H-Diapo
L-Diapo
Apo
Dys

Figure 1

Figure 2

Diapocynin treatment improves spontaneous locomotor activities to levels of non-dystrophic controls

After 9 weeks of treatment, mice were housed individually in cages covered with of lattice of infrared beams to detect and count mice movements. (A) An actigram showing the locomotion over a period of 24h. Mice move only in the dark phase of the day, with their activities culminating in the 6 hours period after dark followed by a quiescent period and finally another phase of activity just before the light phase. (B) A sum of total movements done in a 24-hour period shows the complete normalization by diapocynin of the lost spontaneous locomotion in dystrophic mdx mice (n=24-26). *p≤0.05, ** p≤0.01, *** p≤0.001

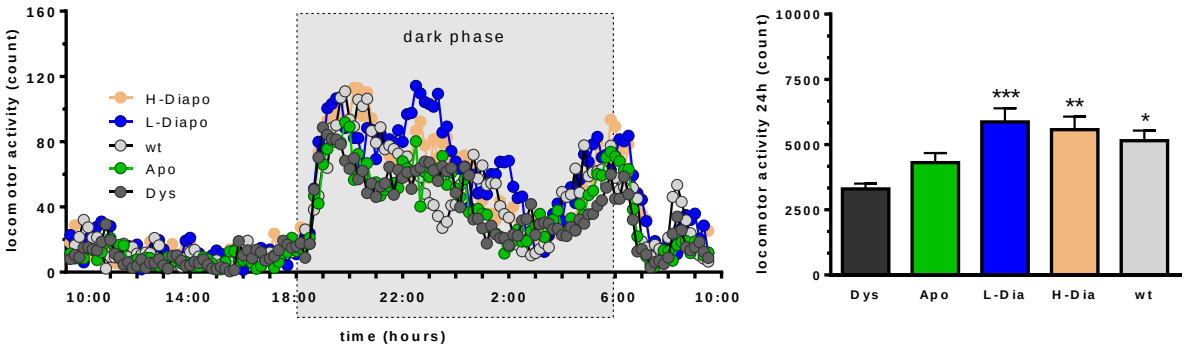
dark phase
H-Diapo
L-Diapo
wt
Apo
Dys
locomotor activity (count)
160
120
80
40
0
10:00
14:00
18:00
22:00
2:00
6:00
10:00
time (hours)
locomotor activity 24h (count)
10000
7500
5000
2500
0
***
**
*
Dys
Apo
L-Dia
H-Dia
wt

Figure 2

Figure 3

Diapocynin treatment improved wheel running capabilities in dystrophic mice

At the 8-weeks end point, mice were housed individually for 7 days in cages with access to freely rotating wheels in the cages. An actigram showing the mice activity in the 7th day is shown on the left and the evolution of the daily distance run is shown on the right (n=11-12). *p≤0.05, ** p≤0.01, *** p≤0.001

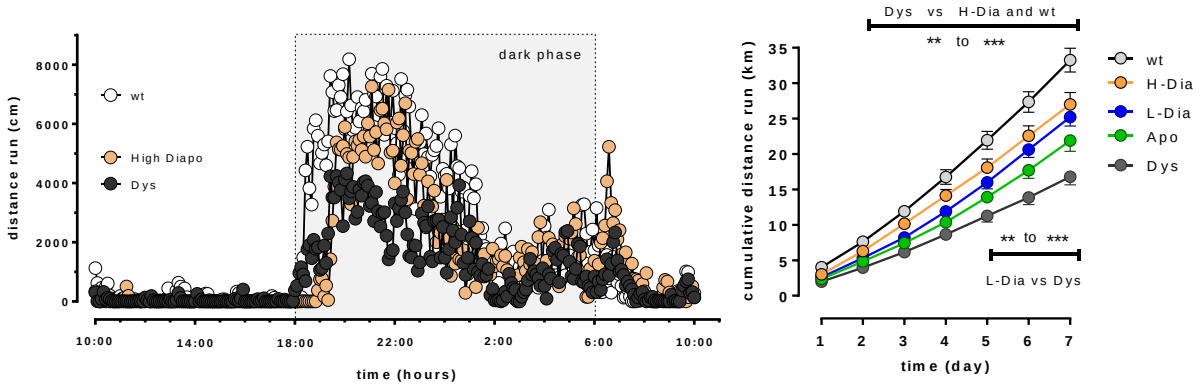
distance run (cm)
8000
6000
4000
2000
0
wt
High Diapo
Dys
dark phase
10:00
14:00
18:00
22:00
2:00
6:00
10:00
time (hours)
cumulative distance run (km)
35
30
25
20
15
10
5
0
Dys vs H-Dia and wt
** to ***
** to ***
L-Dia vs Dys
1
2
3
4
5
6
7
time (day)
wt
H-Dia
L-Dia
Apo
Dys

Figure 3

Figure 4

Enhancement of sarcolemmal integrity by diapocynin treatment

Evans blue dye was injected i.p. in mice at 8 weeks of age. Twenty-four hours later, mice were sacrificed and selected muscles dissected and sectioned to quantify percentage of damaged fiber with showing dye uptake. Tibialis posterior (TP) and the diaphragm (Dia) were the most affected muscles. Treatment with either diapocynin or apocynin managed to protect the muscles from enhanced dye uptake indicating improved sarcolemmal integrity (TP and Sol n=10-12, Dia n=5-6). *p≤0.05, **p≤0.01, *** p≤0.001

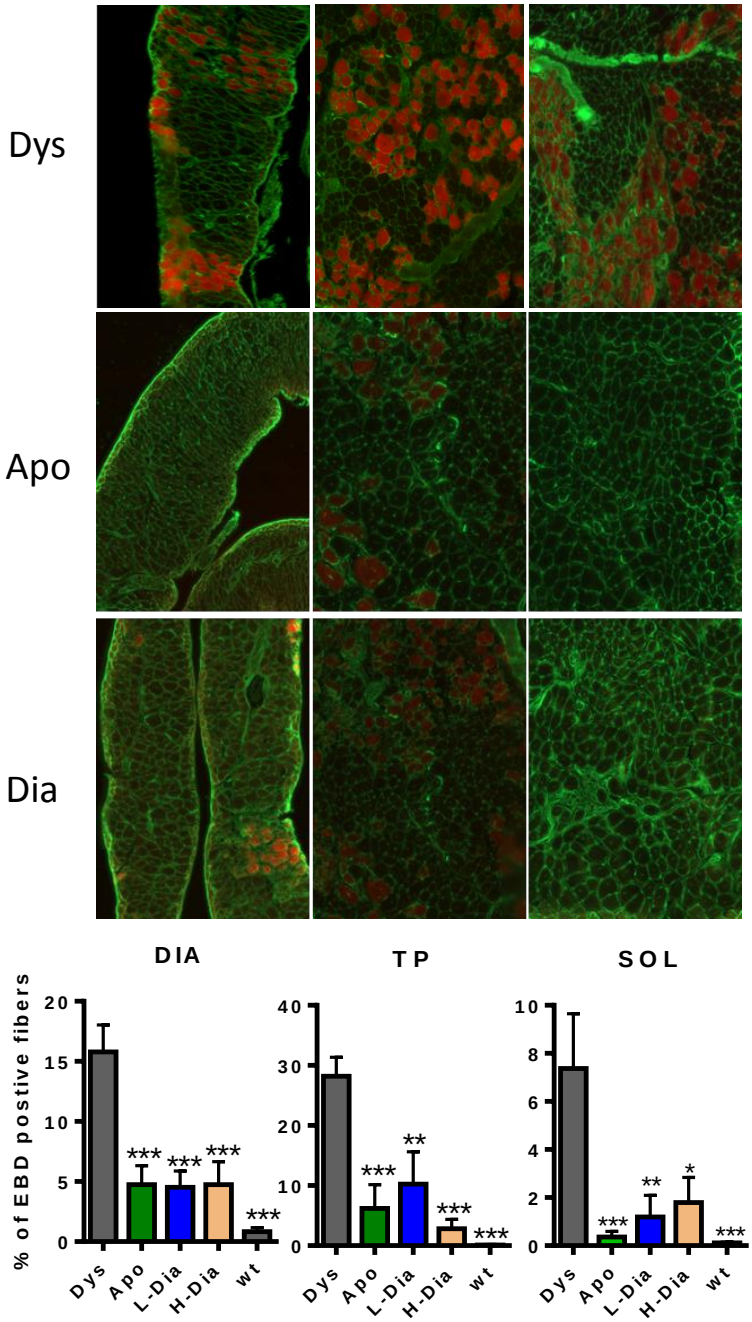
Dys
Apo
Dia
DIA
TP
SOL
% of EBD postive fibers
20
15
10
5
0
40
30
20
10
0
10
8
6
4
2
0
***
**
*
Dys
Apo
L-Dia
H-Dia
wt

Figure 4

Figure 5

Effects of apocynin and diapocynin on isometric phasic and tetanic tensions

Twitch and tetanic responses of the triceps muscle were elicited by intramuscular electrical stimulations under isometric conditions in mice aged 5 weeks (A to D) or 9 weeks (E to H)(n=6-8). The twitch responses are shown after normalization to the muscle cross-sectional area (A, E). In order to highlight the differences in the kinetics of contraction, the twitch responses were also expressed as percentage of the maximum peak value (B, F). The force-frequency relationships were determined by subjecting the triceps to 200ms stimulations of increasing frequency. They are shown after normalization to the muscle cross-sectional area (C, G) or to the maximum tetanic value (D, H). Treatment of dystrophic mice with apocynin and diapocynin for either 2 weeks or 6 weeks did not alter the twitch responses (A, E), the kinetics of contraction and relaxation (B, F), the maximum tetanic tension (C, G) and the behaviour of the triceps muscle towards increasing frequencies of stimulation (D, H).

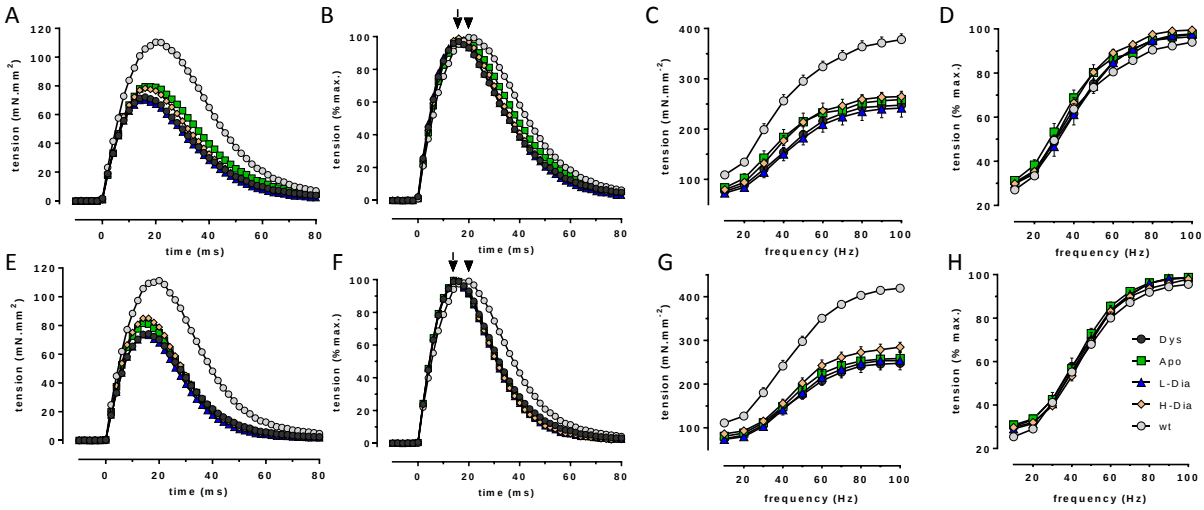
A
B
C
D
E
F
G
H
tension (mN.mm-2)
tension (% max.)
time (ms)
frequency (Hz)
Dys
Apo
L-Dia
H-Dia
wt

Figure 5

Figure 6

Effects of apocynin and diapocynin on muscle fatigue

Tetanic stimulations (200 ms at 100 Hz) were delivered to the triceps muscle every 30 sec resulting in a loss of tension output. A: from left to right, the average muscle response (n = 6-8) of 9-week old Dys, Apo, H-Dia, and wt mice are shown for tetani 1, 4, 7, 10 and 20. Muscle fatigue as a function of tetani number in mice aged 5 weeks (B) or 9 weeks (C). A force drop index was calculated as the average difference between every tetanic tension and the response elicited by the first tetanus in mice aged 5 weeks (D) or 9 weeks (E). Apocynin and diapocynin were equally potent at reducing muscle fatigue in dystrophic mice.

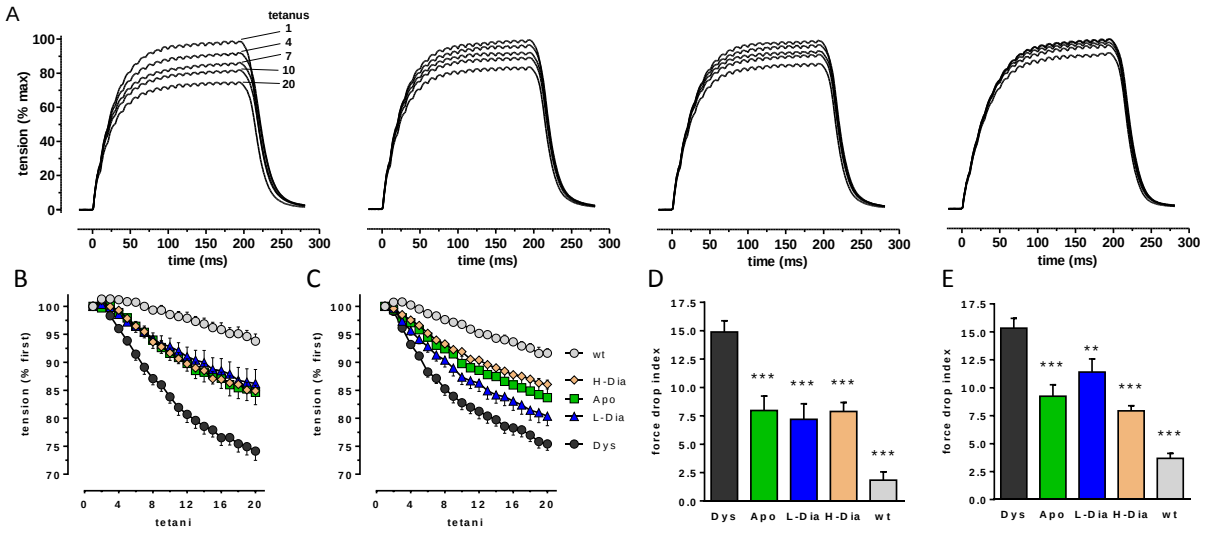
A
tetanus
1
4
7
10
20
tension (% max)
time (ms)
B
C
tension (% first)
tetani
wt
H-Dia
Apo
L-Dia
Dys
D
E
force drop index
Dys
Apo
L-Dia
H-Dia
wt

Figure 6

Chapter 5: General discussion and conclusions

To date, no cure for DMD exists. The only clinically authorized therapeutic interventions are corticosteroids, which retard the progression of the disease, provide limited improvement accompanied by an array of side effects that eventually lead to the refusal of the treatment by a subset of the patients. Nevertheless, the search for an efficient therapy of this disease continues and several clinical trials are now being carried out focused mainly on genetic and cellular therapies with the goal of reaching the patients within the next 5-10 years. Pharmaco-therapeutic agents still hold promise not only as a cure but also as combination therapies to the former two approaches. The last decade was very fruitful in the understanding of the pathophysiological changes occurring in DMD thus making the search for therapeutic interventions more realistic because of established targets. To this end, the aim of this thesis was to rationally select drug candidates with a proven efficacy for a validated target in DMD and to investigate its potential applicability.

Calcium dysregulation plays a central role in the pathogenesis of DMD. Aberrant Ca^{2+} influx through SOC, SAC and membrane tears are reported to be inducers of the damage observed in skeletal muscles of DMD patients. Due to the important role played by $iPLA_2$ in the regulation of Ca^{2+} influx through these pathways and due to the fact that the activity and expression of this enzyme is increased several fold in DMD muscle biopsies (Lindahl *et al.*, 1995), and mdx mice muscles (Boittin *et al.*, 2006; 2010), we considered it as a potential target in our search. The work by Sarvazyan and colleagues (McHowat *et al.*, 2001; 2004; Swift *et al.*, 2003, 2007) showing that doxorubicin strongly inhibits $iPLA_2$ in cardiomyocytes at clinically relevant concentrations, initiated the work of redirecting doxorubicin for use in DMD. Indeed, treating dystrophic myotubes with doxorubicin resulted in a concentration-dependent inhibition of $iPLA_2$. Secondary to this inhibition, a potent inhibition of SAC activity was observed. This was the first report of a SAC inhibitory action by doxorubicin. On another read-out, doxorubicin reduced enhanced Ca^{2+} entry into the subsarcolemmal space and mitochondria (data not shown) upon hypo-osmotic shock. Extending these findings to muscle function, doxorubicin treatment prevented force loss induced by eccentric contractions to which dystrophic muscle is particularly sensitive. Interpretation of the data obtained with doxorubicin was complicated by its biphasic effect on ROS production in muscle cells. Doxorubicin treatment resulted in an early phase in which ROS production increased followed by a concentration-dependent inhibition 10 min later. This bimodal effect was attributed to the ability of doxorubicin to undergo redox cycling on flavoenzymes with NOXes being among candidate targets. We have speculated that doxorubicin mediated SAC inhibition can occur through inhibition of

NOXes or Src kinases due to this phenomenon. Interestingly, authors of a recent paper (Nguyen *et al.*, 2013) showed that quinones can indeed modulate NOXes and that benzoquinones, with which doxorubicin is related, can inhibit NOX4 in a concentration range similar to the one used in our study. This finding reinforces the notion that part of the doxorubicin effect can be mediated by NOX inhibition.

Despite the fact that doxorubicin efficiently inhibited validated targets in DMD, a transition between *in vitro* results to an *in vivo* treatment protocol or to clinical trials is rather complicated. Doxorubicin treatment, shown to be potent in inhibiting $iPLA_2$ in humans (McHowat *et al.*, 2004), is associated with severe cardiomyopathy. In fact, acute administration of a high dose of doxorubicin is often used to induce cardiac toxicity in animal models (Teraoka *et al.*, 2000). DMD patients and mdx mice both show cardiac manifestations, including cardiomyopathy at the late stage of disease. Moreover, results of a study designed to evaluate whether dystrophin absence would affect the acutely induced doxorubicin cardiomyopathy, showed enhanced susceptibility and mortality rate compared to non-dystrophic mice (Deng *et al.*, 2007). For this reason, reduced non-cardiotoxic doses of doxorubicin should be carefully evaluated in mdx mice with the hope that the beneficial effects seen in cellular dystrophic models can be transferred to *in vivo* situations.

The understanding of the mechanism of action of doxorubicin on ROS, NOXes and SACs and the ways through which these players are interconnected drove the search for novel drug candidates. NOXes were the logical target due to their supposed upstream role in the pathogenic cascade of DMD. The lack of commercially available, non-toxic and bioavailable inhibitors, led us to choose the classic NOX inhibitor apocynin as positive control. A 6-fold increase in ROS production was observed upon apocynin treatment of dystrophic myotubes. Apocynin has been reported to exert such an effect in non-phagocytic cells (Vejrazka *et al.*, 2005); in order to become a NOX inhibitor, activation through oxidative coupling into its dimer, diapocynin, is required, which takes place in neutrophils and macrophages (Vejrazka *et al.*, 2005). Apocynin can therefore be considered a pro-drug. We were able to synthetize diapocynin in high purity and sufficient quantities to evaluate its effects in models of mdx mice. Diapocynin application to dystrophic myotubes resulted in an inhibition of ROS production. It was also potent in inhibiting $iPLA_2$ and to reduce Ca^{2+} influx through SAC and SOC, both reported to mediate the enhanced Ca^{2+} entry in dystrophic muscle cells (Ismail *et al.*, 2013b). When evaluated on isolated muscles, diapocynin abolished force loss induced by repeated

eccentric contractions even more strongly than previously reported with doxorubicin (Ismail *et al.*, 2013a; 2013b). Interestingly, it also prevented Procion orange dye uptake into mdx muscle indicating improved sarcolemmal integrity, which is highly compromised in mdx mice. Apocynin in this study had no beneficial effects on muscle function. The fact that the latter experiments were done *in vitro* and that the preparations are removed from their blood supply and the immune system, can explain the discrepancy with the *in vivo* results. However, the isolated muscles could still contain residual macrophages and immune cells to convert a portion of apocynin into diapocynin and thus their contribution should not be overlooked.

To evaluate whether diapocynin could be therapeutically useful, we investigated the effects of two doses of diapocynin (10 and 100 mg/kg/day) and one dose of apocynin (50 mg/kg/day) in mdx^{5Cv} mice. Since diapocynin has about double the molecular weight of apocynin, the higher diapocynin dose corresponds to the one used for apocynin on a molar basis. Indeed, both diapocynin doses resulted in normalization of spontaneous locomotor activity to levels of non-dystrophic controls, whereas apocynin failed to yield to an improvement. Diapocynin treatment also restored the lost wheel running capabilities, whereas apocynin was less efficacious. Neither apocynin nor diapocynin treatment led to improved force production of the triceps surae muscles, but both equally enhanced the resistance to fatigue. Also, both treatments enhanced sarcolemmal integrity to a similar extent as seen by the prevention of Evans blue dye uptake.

The hypothesis that diapocynin can be therapeutically more advantageous than apocynin was proven correct. We initially thought that the pool of activated immune cells needed for apocynin dimerization might be absent in mdx mice. But the similar responses in the fatigue protocol and in the Evans blue dye uptake test to the 2 compounds show that this is not the case. Yet, the effect on locomotor activity and wheel running capability indicate that diapocynin is superior. One has to consider that other differences between these two agents exist. Considering their anti-oxidant rather that NOX inhibiting potential, diapocynin is likely to be a stronger anti-oxidant due to the availability of 2 phenolic hydroxyl groups instead of one in apocynin (Figure 5.11). Also the enhanced lipophilicity of diapocynin compared to apocynin should render it more bioavailable and lead to tissue accumulation and higher on-target effects. An analytical tool is needed to evaluate the levels of apocynin and diapocynin present in muscles other tissues in our treatment groups. This would lead to the understanding of the conversion rate of apocynin in dystrophic tissue and

will clarify the potential of both compounds. Also the effects on the central nervous system reported recently for diapocynin (Ghosh *et al.*, 2012), might enhance the performance of mice in these assays. Putting together, all these qualities make diapocynin a superior therapeutic candidate with high potential for DMD and perhaps other diseases in which NOX are causally involved.

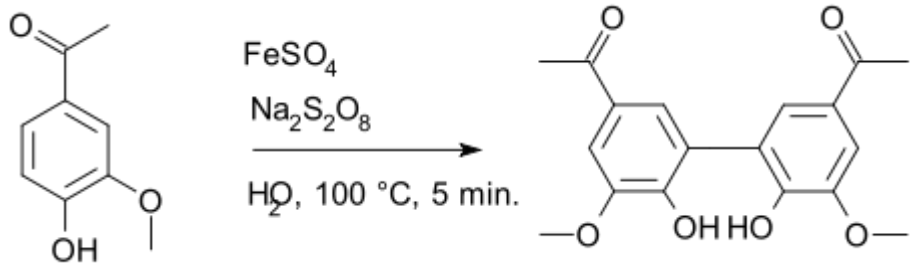

Figure 5-11 Conversion of apocynin into diapocynin

The reaction shown describes the method used to dimerize apocynin via an oxidative coupling reaction into diapocynin. Note the availability of 2 phenolic hydroxyl groups on diapocynin (Adapted from Luchtefeld *et al.* (2008)).

Several issues need to be addressed to understand the contribution of NOXes in dystrophy and in muscle function and are listed below:

- Verification the expression levels of NOXes in different muscle types at the mRNA and, more importantly, the protein levels. We have tested several antibodies to detect NOXes in mouse tissue, but upon analysis by SDS-PAGE, all of these showed non-specific bands and/or the putative specific bands were masked by co-migrating endogenous immunoglobulins. We have constructed pAAV plasmids to drive the overexpression of either NOX2 or NOX4 in mammalian cells and used them to construct positive controls. These plasmids were used to transfect HEK293 cells and drove efficient overexpression of either NOX2 or NOX4. Lysates of these cells were used as positive controls for our western blots together with tissue extracts from knock-out mice of either NOX isoform obtained from Prof Karl-Heinz Krause to be used as negative controls. However, the commercial antibodies showed clear bands in muscle extracts from mice with knocked-out NOXes. We will continue using these positive and negative controls for screening of more antibodies with the hope of reaching efficient ones.

- The availability of reliable assays to distinguish specifically ROS production by NOXes and not global ROS production in dystrophic skeletal muscles. The multinuclear nature of myotubes and muscle fibres is even complicated further by the central and peripheral localization of these nuclei due to the waves of necrosis and regeneration in DMD. This renders most available tools for detection ROS *in situ* difficult to interpret.
- Distinguishing the roles of NOX2 from that of NOX4 to understand the exact mechanisms by which these isoforms contribute to the DMD pathogenesis. This can be achieved by:
    - Driving muscle specific over-expression of either isoform using tools such as those developed in this study, the pAAV plasmids, to synthesize viral particles.
    - Using of isoform-specific NOX inhibitors, which to date are not commercially available but is foreseeable in the near future.
    - Generating mdx mice knocked out of either NOX2 or NOX4. However, the interpretation of the results from such mice should be carefully performed, due to the possibility of the involvement of vascular and immune components.
- An evaluation of the effect of NOX inhibition in healthy skeletal muscles is required to understand their contribution in normal muscle function and whether their inhibition could enhance fatigue tolerance.

In conclusion, although DMD is a monogenic disease, its aetiology remains multifactorial and treatment appears difficult. Pharmacotherapeutic agents, except those intended for pre-mature stop codon read-through or exon skipping, are so far considered as supportive or adjunct therapy, awaiting the delivery of novel genetic and cellular cures. The work presented here using mdx mice showed clear benefits by targeting NOXes, $iPLA_2$ and SACs, indicating an important role of these targets in DMD pathogenesis. However, more work is needed to decipher how they are arranged in the cascade that leads to the DMS phenotype. It appears that any potential treatment of DMD needs to be directed to several targets, requiring a combination therapy. Despite the complex nature of this devastating disease, our understanding of the pathology is increasing rapidly and a cure is foreseeable in the near future.

Chapter 6: References for all previous chapters

References

Aartsma-Rus A, Bremmer-Bout M, Janson AAM, den Dunnen JT, van Ommen GJB, van Deutekom JCT (2002). Targeted exon skipping as a potential gene correction therapy for Duchenne muscular dystrophy. *Neuromuscul Disord* **12**(Supplement 1)**:** S71-S77.

Ackermann EJ, Kempner ES, Dennis EA (1994). Calcium independent cytosolic phospholipase A_2 from macrophage-like P338D_1 cells - isolation and characterization. *J Biol Chem* **269**(12)**:** 9227-9233.

Ago T, Kuribayashi F, Hiroaki H, Takeya R, Ito T, Kohda D*, et al.* (2003). Phosphorylation of p47phox directs phox homology domain from SH3 domain toward phosphoinositides, leading to phagocyte NADPH oxidase activation. *Proc Natl Acad Sci U S A* **100**(8)**:** 4474-4479.

Ago T, Nunoi H, Ito T, Sumimoto H (1999). Mechanism for Phosphorylation-induced Activation of the Phagocyte NADPH Oxidase Protein p47phox. Triple replacmnet of Sserines 303, 304, AND 328 with aspartates disrupts the SH3 domain-mediated intramolecular interaction in p47phox, Therby activating the oxidase. *J Biol Chem* **274**(47)**:** 33644-33653.

Ahn AH, Kunkel LM (1993). The structural and functional diversity of dystrophin. *Nat Genet* **3**(4)**:** 283-291.

Alderton JM, Steinhardt RA (2000). Calcium influx through calcium leak channels is responsible for the elevated levels of calcium-dependent proteolysis in dystrophic myotubes. *J Biol Chem* **275**(13)**:** 9452-9460.

Allen DG, Gervasio OL, Yeung EW, Whitehead NP (2010). Calcium and the damage pathways in muscular dystrophy. *Can J Physiol Pharmacol* **88**(2)**:** 83-91.

Allen DG, Whitehead NP (2011). Duchenne muscular dystrophy - What causes the increased membrane permeability in skeletal muscle? *Int J Biochem Cell* **43**(3)**:** 290-294.

Allen DG, Whitehead NP, Yeung EW (2005). Mechanisms of stretch-induced muscle damage in normal and dystrophic muscle: role of ionic changes. *J Physiol* **567**(Pt 3)**:** 723-735.

Alter J, Lou F, Rabinowitz A, Yin H, Rosenfeld J, Wilton SD*, et al.* (2006). Systemic delivery of morpholino oligonucleotide restores dystrophin expression bodywide and improves dystrophic pathology. *Nat Med* **12**(2)**:** 175-177.

Amthor H, Macharia R, Navarrete R, Schuelke M, Brown SC, Otto A*, et al.* (2007). Lack of myostatin results in excessive muscle growth but impaired force generation. *Proc Natl Acad Sci U S A* **104**(6)**:** 1835-1840.

Andrade FH, Reid MB, Allen DG, Westerblad H (1998). Effect of hydrogen peroxide and dithiothreitol on contractile function of single skeletal muscle fibres from the mouse. *J Physiol* **509 (Pt 2):** 565-575.

Andrade FH, Reid MB, Westerblad H (2001). Contractile response of skeletal muscle to low peroxide concentrations: myofibrillar calcium sensitivity as a likely target for redox-modulation. *FASEB J* **15**(2)**:** 309-311.

Anthony K, Feng L, Arechavala-Gomeza V, Guglieri M, Straub V, Bushby K*, et al.* (2012). Exon skipping quantification by quantitative reverse-transcription polymerase chain reaction in Duchenne muscular dystrophy patients treated with the antisense oligomer eteplirsen. *Hum Gene Ther Methods* **23**(5)**:** 336-345.

Arahata K (2000). Muscular dystrophy. *Neuropathol* **20:** S34-S41.

Badalamente MA, Stracher A (2000). Delay of muscle degeneration and necrosis in mdx mice by calpain inhibition. *Muscle Nerve* **23**(1)**:** 106-111.

Balboa MA, Balsinde J (2002). Involvement of calcium-independent phospholipase A_2 in hydrogen peroxide-induced accumulation of free fatty acids in human U937 cells. *J Biol Chem* **277**(43)**:** 40384-40389.

Balboa MA, Balsinde J, Jones SS, Dennis EA (1997). Identity between the Ca^{2+}-independent phospholipase A_2 enzymes from $P388D_1$ macrophages and Chinese hamster ovary cells. *J Biol Chem* **272**(13)**:** 8576-8580.

Barbieri E, Sestili P (2012). Reactive oxygen species in skeletal muscle signaling. *J Sig Transd* **2012:** 982794.

Barton-Davis ER, Cordier L, Shoturma DI, Leland SE, Sweeney HL (1999). Aminoglycoside antibiotics restore dystrophin function to skeletal muscles of mdx mice. *J Clin Invest* **104**(4)**:** 375-381.

Bartoszek A (2002). Metabolic activation of adriamycin by NADPH-cytochrome P450 reductase; overview of its biological and biochemical effects. *Acta Biochimica Polonica* **49**(2)**:** 323-331.

Basset O, Boittin FX, Dorchies OM, Chatton JY, van Breemen C, Ruegg UT (2004). Involvement of inositol 1,4,5-trisphosphate in nicotinic calcium responses in dystrophic myotubes assessed by near-plasma membrane calcium measurement. *J Biol Chem* **279**(45)**:** 47092-47100.

Bedard K, Krause KH (2007). The NOX family of ROS-generating NADPH oxidases: physiology and pathophysiology. *Physiol Rev* **87**(1)**:** 245-313.

Beech DJ, Bahnasi YM, Dedman AM, Al-Shawaf E (2009). TRPC channel lipid specificity and mechanisms of lipid regulation. *Cell Calcium* **45**(6)**:** 583-588.

Béroud C, Tuffery-Giraud S, Matsuo M, Hamroun D, Humbertclaude V, Monnier N*, et al.* (2007). Multiexon skipping leading to an artificial DMD protein lacking amino acids from exons 45 through 55 could rescue up to 63% of patients with Duchenne muscular dystrophy. *Hum Mutat* **28**(2)**:** 196-202.

Bertorini TE, Palmieri GM, Griffin JW, Igarashi M, McGee J, Brown R*, et al.* (1988). Effect of chronic treatment with the calcium antagonist diltiazem in Duchenne muscular dystrophy. *Neurology* **38:** 609-613.

Beutner G, Sharma VK, Giovannucci DR, Yule DI, Sheu S (2001). Identification of a ryanodine receptor in rat heart mitochondria. *J Biol Chem* **276**(24)**:** 21482-21488.

Blake DJ, Weir A, Newey SE, Davies KE (2002). Function and genetics of dystrophin and dystrophin-related proteins in muscle. *Physiol Rev* **82**(2)**:** 291-329.

Boittin FX, Petermann O, Hirn C, Mittaud P, Dorchies OM, Roulet E*, et al.* (2006). Ca^{2+}-independent phospholipase A_2 enhances store-operated Ca^{2+} entry in dystrophic skeletal muscle fibers. *J Cell Sci* **119**(18)**:** 3733-3742.

Boittin FX, Shapovalov G, Hirn C, Ruegg UT (2010). Phospholipase A2-derived lysophosphatidylcholine triggers Ca^{2+} entry in dystrophic skeletal muscle fibers. *Biochem Biophys Res Commun* **391**(1)**:** 401-406.

Bolotina VM (2008). Orai, STIM1 and $iPLA_2$beta: a view from a different perspective. *J Physiol* **586**(13)**:** 3035-3042.

Bonifati MD, Ruzza G, Bonometto P, Berardinelli A, Gorni K, Orcesi S*, et al.* (2000). A multicenter, double-blind, randomized trial of deflazacort versus prednisone in Duchenne muscular dystrophy. *Muscle Nerve* **23**(9)**:** 1344-1347.

Brenman JE, Chao DS, Xia H, Aldape K, Bredt DS (1995). Nitric oxide synthase complexed with dystrophin and absent from skeletal muscle sarcolemma in Duchenne muscular dystrophy. *Cell* **82**(5)**:** 743-752.

Briguet A, Erb M, Courdier-Fruh I, Barzaghi P, Santos G, Herzner H*, et al.* (2008). Effect of calpain and proteasome inhibition on Ca^{2+}-dependent proteolysis and muscle histopathology in the mdx mouse. *FASEB J* **22**(12)**:** 4190-4200.

Brini M, Carafoli E (2000). Calcium signalling: a historical account, recent developments and future perspectives. *Cell Mol Life Sci* **57**(3)**:** 354-370.

Brooks SV, Faulkner JA (1988). Contractile properties of skeletal-muscles from young, adult and aged mice. *J Physiol* **404:** 71-82.

Buetler TM, Krauskopf A, Ruegg UT (2004). Role of superoxide as a signaling molecule. *News Physiol Sci* **19:** 120-123.

Buetler TM, Renard M, Offord EA, Schneider H, Ruegg UT (2002). Green tea extract decreases muscle necrosis in mdx mice and protects against reactive oxygen species. *Am J Clin Nutr* **75**(4)**:** 749-753.

Burkholder TJ (2009). Stretch-induced ERK2 phosphorylation requires PLA_2 activity in skeletal myotubes. *Biochem Biophys Res Commun* **386**(1)**:** 60-64.

Bushby K, Finkel R, Birnkrant DJ, Case LE, Clemens PR, Cripe L*, et al.* (2010a). Diagnosis and management of Duchenne muscular dystrophy, part 1: diagnosis, and pharmacological and psychosocial management. *Lancet Neurol* **9**(1)**:** 77-93.

Bushby K, Finkel R, Birnkrant DJ, Case LE, Clemens PR, Cripe L*, et al.* (2010b). Diagnosis and management of Duchenne muscular dystrophy, part 2: implementation of multidisciplinary care. *Lancet Neurol* **9**(2)**:** 177-189.

Buyse GM, Goemans N, Henricson E, Jara A, van den Hauwe M, Leshner R*, et al.* (2007). CINRG pilot trial of oxatomide in steroid-naïve Duchenne muscular dystrophy. *Eur J Paediatr Neurol* **11**(6)**:** 337-340.

Cahalan MD (2009). STIMulating store-operated Ca^{2+} entry. *Nat cell biol* **11**(6)**:** 669-677.

Calaghan S, White E (2004). Activation of Na^{+}-H^{+} exchange and stretch-activated channels underlies the slow inotropic response to stretch in myocytes and muscle from the rat heart. *J Physiol* **559**(1)**:** 205-214.

Campbell KP (1995). Three muscular dystrophies: loss of cytoskeleton-extracellular matrix linkage. *Cell* **80:** 675-679.

Campbell WG, Gordon SE, Carlson CJ, Pattison JS, Hamilton MT, Booth FW (2001). Differential global gene expression in red and white skeletal muscle. *Am J Physiol Cell Physiol* **280**(4)**:** C763-768.

Carafoli E (2003). Historical review: Mitochondria and calcium: ups and downs of an unusual relationship. *Trends Biochem Sci* **28**(4)**:** 175-181.

Carlson CG (1998). The dystrophinopathies: an alternative to the structural hypothesis. *Neurobiol Dis* **5**(1)**:** 3-15.

Castor LR, Locatelli KA, Ximenes VF (2010). Pro-oxidant activity of apocynin radical. *Free Radic Biol Med* **48**(12)**:** 1636-1643.

Catterall WA (1991). Excitation-contraction coupling in vertebrate skeletal muscle: a tale of two calcium channels. *Cell* **64**(5)**:** 871-874.

Chakraborty S, Berwick ZC, Bartlett PJ, Kumar S, Thomas AP, Sturek M*, et al.* (2011). Bromoenol lactone inhibits voltage-gated Ca^{2+} and transient receptor potential canonical channels. *J Pharmacol Exp Ther* **339**(2)**:** 329-340.

Childers MK, Bogan JR, Bogan DJ, Greiner H, Holder M, Grange RW*, et al.* (2011). Chronic administration of a leupeptin-derived calpain inhibitor fails to ameliorate severe muscle pathology in a canine model of duchenne muscular dystrophy. *Front Pharmacol* **2:** 89.

Cohn RD, Campbell KP (2000). Molecular basis of muscular dystrophies. *Muscle Nerve* **23**(10)**:** 1456-1471.

Cozzoli A, Capogrosso RF, Sblendorio VT, Dinardo MM, Jagerschmidt C, Namour F*, et al.* (2013). GLPG0492, a novel selective androgen receptor modulator, improves muscle performance in the exercised-mdx mouse model of muscular dystrophy. *Pharmacol Res* **72:** 9-24.

Danos O (2008). AAV vectors for RNA-based modulation of gene expression. *Gene Ther* **15**(11)**:** 864-869.

Davies KE, Nowak KJ (2006). Molecular mechanisms of muscular dystrophies: old and new players. *Nat Rev Mol Cell Biol* **7**(10)**:** 762-773.

Davies KJ, Doroshow JH (1986). Redox cycling of anthracyclines by cardiac mitochondria. I. Anthracycline radical formation by NADH dehydrogenase. *J Biol Chem* **261**(7)**:** 3060-3067.

Davies KJ, Maguire JJ, Brooks GA, Dallman PR, Packer L (1982). Muscle mitochondrial bioenergetics, oxygen supply, and work capacity during dietary iron deficiency and repletion. *Am J Physiol* **242**(6)**:** E418-427.

De Luca A (2012). Pre-clinical drug tests in the mdx mouse as a model of dystrophinopathies: an overview. *Acta Myol* **31**(1)**:** 40-47.

De Luca A, Nico B, Liantonio A, Didonna MP, Fraysse B, Pierno S*, et al.* (2005). A multidisciplinary evaluation of the effectiveness of cyclosporine A in dystrophic mdx mice. *Am J Pathol* **166**(2)**:** 477-489.

Deconinck N, Dan B (2007). Pathophysiology of duchenne muscular dystrophy: current hypotheses. *Pediatr Neurol* **36**(1)**:** 1-7.

Deng S, Kulle B, Hosseini M, Schluter G, Hasenfuss G, Wojnowski L*, et al.* (2007). Dystrophin-deficiency increases the susceptibility to doxorubicin-induced cardiotoxicity. *Eur J Heart Fail* **9**(10)**:** 986-994.

Dick DJ, Gardner-Medwin D, Gates PG, Gibson M, Simpson JM, T.J. W (1986). A trial of flunarizine in the treatment of Duchenne muscular dystrophy. *Muscle Nerve* **9**(4)**:** 349-354.

Disatnik MH, Dhawan J, Yu Y, Beal MF, Whirl MM, Franco AA*, et al.* (1998). Evidence of oxidative stress in mdx mouse muscle: studies of the pre-necrotic state. *J Neurol Sci* **161**(1)**:** 77-84.

Dogra C, Srivastava D, Kumar A (2008). Protein–DNA array-based identification of transcription factor activities differentially regulated in skeletal muscle of normal and dystrophin-deficient mdx mice. *Mol Cell Biochem* **312**(1)**:** 17-24.

Doran P, Wilton SD, Fletcher S, Ohlendieck K (2009). Proteomic profiling of antisense-induced exon skipping reveals reversal of pathobiochemical abnormalities in dystrophic mdx diaphragm. *Proteomics* **9**(3)**:** 671-685.

Dorchies OM, Reutenauer-Patte J, Dahmane E, Ismail HM, Petermann O, Patthey- Vuadens O*, et al.* (2013). The anticancer drug tamoxifen counteracts the pathology in a mouse model of duchenne muscular dystrophy. *Am J Pathol* **182**(2)**:** 485-504.

Dorchies OM, Wagner S, Buetler TM, Ruegg UT (2009). Protection of dystrophic muscle cells with polyphenols from green tea correlates with improved glutathione balance and increased expression of 67LR, a receptor for (-)-epigallocatechin gallate. *Biofactors* **35**(3)**:** 279-294.

Dorchies OM, Wagner S, Vuadens O, Waldhauser K, Buetler TM, Kucera P*, et al.* (2006). Green tea extract and its major polyphenol (-)-epigallocatechin gallate improve muscle function in a mouse model for Duchenne muscular dystrophy. *Am J Physiol-Cell Ph* **290**(2)**:** C616-C625.

Ducret T, Vandebrouck C, Cao ML, Lebacq J, Gailly P (2006). Functional role of store-operated and stretch-activated channels in murine adult skeletal muscle fibres. *J Physiol* **575**(Pt 3)**:** 913-924.

Duncan CJ, Jackson MJ (1987). Different mechanisms mediate structural-changes and intracellular enzyme efflux following damage to skeletal-muscle. *J Cell Sci* **87:** 183-188.

Dupre-Crochet S, Erard M, Nubetae O (2013). ROS production in phagocytes: why, when, and where? *J Leukoc Biol*.

Durbeej M, Campbell KP (2002). Muscular dystrophies involving the dystrophin-glycoprotein complex: an overview of current mouse models. *Curr Opin Genet Dev* **12**(3)**:** 349-361.

Emery AE (1977). Muscle histology and creatine kinase levels in the foetus in Duchenne muscular dystrophy. *Nature* **266**(5601)**:** 472-473.

Emery AEH (2002). The muscular dystrophies. *Lancet* **359**(9307)**:** 687-695.

Emery AEH, Skinner R, Howden LC, Matthews MB (1982). Verapamil in Duchenne Muscular Dystrophy. *Lancet* **319**(8271)**:** 559-559.

Engel AG, Yamamoto M, Fischbeck KH (1994). Dystrophinopathies. In: Engel AG, Franzini-Armstrong C (ed)^(eds). *Basic and Clinical Myology*, 2nd edn, Vol. 2. New York: McGraw-Hill, Inc. p^pp 1133-1187.

Ennen JP, Verma M, Asakura A (2013). Vascular-targeted therapies for Duchenne muscular dystrophy. *Skelet Muscle* **3**(1)**:** 9.

Ervasti JM, Campbell KP (1991). Membrane organization of the dystrophin-glycoprotein complex. *Cell* **66:** 1121-1131.

Estrada M, Cardenas C, Liberona JL, Carrasco MA, Mignery GA, Allen PD*, et al.* (2001). Calcium transients in 1B5 myotubes lacking ryanodine receptors are related to inositol trisphosphate receptors. *J Biol Chem* **276**(25)**:** 22868-22874.

Fanchaouy M, Polakova E, Jung C, Ogrodnik J, Shirokova N, Niggli E (2009). Pathways of abnormal stress-induced Ca^{2+} influx into dystrophic mdx cardiomyocytes. *Cell Calcium* **46**(2)**:** 114-121.

Fu J, Yamamoto K, Guan ZW, Kimura S, Iyanagi T (2004). Human neuronal nitric oxide synthase one-electron reduction of adriamycin: role can catalyze of flavin domain. *Arch Biochem Biophys* **427**(2)**:** 180-187.

Gailly P (2002). New aspects of calcium signaling in skeletal muscle cells: implications in Duchenne muscular dystrophy. *Biochim Biophys Acta - Proteins & Proteomics* **1600**(1-2)**:** 38-44.

Gaitanis A, Staal S (2010). Liposomal doxorubicin and nab-paclitaxel: nanoparticle cancer chemotherapy in current clinical use. *Method Mol Biol* **624:** 385-392.

Gervasio OL, Whitehead NP, Yeung EW, Phillips WD, Allen DG (2008). TRPC1 binds to caveolin-3 and is regulated by Src kinase - role in Duchenne muscular dystrophy. *J Cell Sci* **121**(Pt 13)**:** 2246-2255.

Ghosh A, Kanthasamy A, Joseph J, Anantharam V, Srivastava P, Dranka BP*, et al.* (2012). Anti-inflammatory and neuroprotective effects of an orally active apocynin derivative in pre-clinical models of Parkinson's disease. *J Neuroinflamm* **9:** 241.

Gilliam LAA, Ferreira LF, Bruton JD, Moylan JS, Westerblad H, Clair DKS*, et al.* (2009). Doxorubicin acts through tumor necrosis factor receptor subtype 1 to cause dysfunction of murine skeletal muscle. *J Appl Physiol* **107**(6)**:** 1935-1942.

Gilliam LAA, St Clair DK (2011). Chemotherapy-induced weakness and fatigue in skeletal muscle: The role of oxidative stress. *Antioxid Redox Sign* **15**(9)**:** 2543-2563.

Giorgio V, von Stockum S, Antoniel M, Fabbro A, Fogolari F, Forte M*, et al.* (2013). Dimers of mitochondrial ATP synthase form the permeability transition pore. *Proc Natl Acad Sci U S A* **110**(15)**:** 5887-5892.

Gordon AM, Homsher E, Regnier M (2000). Regulation of contraction in striated muscle. *Physiol Rev* **80**(2)**:** 853-924.

Griggs RC, Herr BE, Reha A, Elfring G, Atkinson L, Cwik V*, et al.* (2013). Corticosteroids in Duchenne muscular dystrophy: Major variations in practice. *Muscle Nerve* **48**(1)**:** 27-31.

Grounds MD, Radley HG, Lynch GS, Nagaraju K, De Luca A (2008). Towards developing standard operating procedures for pre-clinical testing in the mdx mouse model of Duchenne muscular dystrophy. *Neurobiol Dis* **31**(1)**:** 1-19.

Grounds MD, Torrisi JO (2004). Anti-TNFα (Remicade®) therapy protects dystrophic skeletal muscle from necrosis. *FASEB J* **18**(6)**:** 676-682.

Gunter TE, Buntinas L, Sparagna G, Eliseev R, Gunter K (2000). Mitochondrial calcium transport: mechanisms and functions. *Cell Calcium* **28**(5-6)**:** 285-296.

Gussoni E, Pavlath GK, Lanctot AM, Sharma KR, Miller RG, Steinman L*, et al.* (1992). Normal dystrophin transcripts detected in Duchenne muscular dystrophy patients after myoblast transplantation. *Nature* **356**(6368)**:** 435-438.

Gutierrez PL (2000). The metabolism of quinone-containing alkylating agents: Free radical production and measurement. *Front Biosci* **5:** D629-D638.

Gwozdz T, Dutko-Gwozdz J, Schafer C, Bolotina VM (2012). Overexpression of Orai1 and STIM1 proteins alters regulation of store-operated Ca^{2+} entry by endogenous mediators. *J Biol Chem* **287**(27)**:** 22865-22872.

Hain J, Nath S, Mayrleitner M, Fleischer S, Schindler H (1994). Phosphorylation modulates the function of the calcium release channel of sarcoplasmic reticulum from skeletal muscle. *Biophys J* **67**(5)**:** 1823-1833.

Hamada T, Sale DG, MacDougall JD, Tarnopolsky MA (2000). Postactivation potentiation, fiber type, and twitch contraction time in human knee extensor muscles. *J Appl Physiol* **88**(6)**:** 2131-2137.

Hamer PW, McGeachie JM, Davies MJ, Grounds MD (2002). Evans Blue Dye as an in vivo marker of myofibre damage: optimising parameters for detecting initial myofibre membrane permeability. *J Anat* **200**(1)**:** 69-79.

Hamill OP, McBride DW, Jr. (1996). The pharmacology of mechanogated membrane ion channels. *Pharmacol Rev* **48**(2)**:** 231-252.

Hammond SM, Wood MJ (2010). PRO-051, an antisense oligonucleotide for the potential treatment of Duchenne muscular dystrophy. *Curr Opin Mol Ther* **12**(4)**:** 478-486.

Harisseh R, Chatelier A, Magaud C, Deliot N, Constantin B (2013). Involvement of TRPV2 and SOCE in calcium influx disorder in DMD primary human myotubes with a specific contribution of alpha1-syntrophin and PLC/PKC in SOCE regulation. *Am J Physiol Cell Physiol* **304**(9)**:** C881-894.

Hazen SL, Zupan LA, Weiss RH, Getman DP, Gross RW (1991). Suicide inhibition of canine myocardial cytosolic calcium-independent phospholipase A_2. Mechanism-based discrimination between calcium-dependent and -independent phospholipases A_2. *J Biol Chem* **266**(11)**:** 7227-7232.

Hibaoui Y, Reutenauer-Patte J, Patthey-Vuadens O, Ruegg UT, Dorchies OM (2011). Melatonin improves muscle function of the dystrophic mdx5Cv mouse, a model for Duchenne muscular dystrophy. *J Pineal Res* **51**(2)**:** 163-171.

Hibaoui Y, Roulet E, Ruegg UT (2009). Melatonin prevents oxidative stress-mediated mitochondrial permeability transition and death in skeletal muscle cells. *J Pineal Res* **47**(3)**:** 238-252.

Hidalgo C, Donoso P, Carrasco MA (2005). The ryanodine receptors Ca^{2+} release channels: cellular redox sensors? *IUBMB Life* **57**(4-5)**:** 315-322.

Hnia K, Gayraud J, Hugon G, Ramonatxo M, De La Porte S, Matecki S*, et al.* (2008). L-arginine decreases inflammation and modulates the nuclear factor-kappaB/matrix metalloproteinase cascade in mdx muscle fibers. *Am J Pathol* **172**(6)**:** 1509-1519.

Hoffman EP, Brown RHJ, Kunkel LM (1987). Dystrophin: the protein product of the Duchenne muscular dystrophy locus. *Cell* **51:** 919-928.

Hoffman EP, Dressman D (2001). Molecular pathophysiology and targeted therapeutics for muscular dystrophy. *Trends Pharmacol Sci* **22**(9)**:** 465-470.

Hoffman EP, Schwartz L (1991). Dystrophin and disease. *Mol Aspects Med* **12**(3)**:** 175-194.

Holle AW, Engler AJ (2011). More than a feeling: discovering, understanding, and influencing mechanosensing pathways. *Curr Opin Biotech* **22**(5)**:** 648-654.

Hopf FW, Turner PR, Steinhardt RA (2007). Calcium misregulation and the pathogenesis of muscular dystrophy. *Sub-Cell Biochem* **45:** 429-464.

Houser KR, Johnson DK, Ishmael FT (2012). Anti-inflammatory effects of methoxyphenolic compounds on human airway cells. *J Inflamm (Lond)* **9:** 6.

Howl JD, Publicover SJ (1990). Permeabilzation of the sarcolemmal in mouse diaphragm exposed to BAY-K-8644 in vitro- time course, dependence on Ca^{2+} and effects of enzyme-inhibitors. *Acta Neuropathologica* **79**(4)**:** 438-443.

Hsu YH, Burke JE, Li S, Woods VL, Jr., Dennis EA (2009). Localizing the membrane binding region of Group VIA Ca^{2+}-independent phospholipase A_2 using peptide amide hydrogen/deuterium exchange mass spectrometry. *J Biol Chem* **284**(35)**:** 23652-23661.

Huxley AF, Niedergerke R (1954). Structural changes in muscle during contraction: Interference microscopy of living muscle fibres. *Nature* **173**(4412)**:** 971-973.

Huynh T, Uaesoontrachoon K, Quinn J, Tatem K, Heier C, Van Der Meulen J*, et al.* (2013). Selective modulation through the glucocorticoid receptor ameliorates muscle pathology in mdx mice. *J Pathol* **231**(2)**:** 223-235.

Inui M, Saito A, Fleischer S (1987). Purification of the ryanodine receptor and identity with feet structures of junctional terminal cisternae of sarcoplasmic reticulum from fast skeletal muscle. *J Biol Chem* **262**(4)**:** 1740-1747.

Ismail HM, Dorchies OM, Perozzo R, Strosova MK, Scapozza L, Ruegg UT (2013a). Inhibition of $iPLA_2$ beta and of stretch-activated channels by doxorubicin alters dystrophic muscle function. *Br J Pharmacol* **169**(7)**:** 1537-1550.

Ismail HM, Scapozza L, Ruegg UT, Dorchies OM (2013b). Diapocynin, a NADPH oxidase inhibitor, reduces ROS production and prevents force loss in eccentrically contracting dystrophic muscle. *PLoS One* **In revision**.

Iwata Y, Katanosaka Y, Arai Y, Shigekawa M, Wakabayashi S (2009). Dominant-negative inhibition of Ca^{2+} influx via TRPV2 ameliorates muscular dystrophy in animal models. *Hum Mol Genet* **18**(5)**:** 824-834.

Jaimovich E, Reyes R, Liberona JL, Powell JA (2000). IP_3 receptors, IP_3 transients, and nucleus-associated Ca^{2+} signals in cultured skeletal muscle. *Am J Physiol Cell Physiol* **278**(5)**:** C998-1010.

Jarman ER, Khambata VS, Cope C, Jones P, Roger J, Yun Ye L*, et al.* (2013). An Inhibitor of NADPH Oxidase-4 Attenuates Established Pulmonary Fibrosis in a Rodent Disease Model. *Am J Respir Cell Mol Biol*.

Jiang J, Kang H, Song X, Huang S, Li S, Xu J (2013). A Model of Interaction between Nicotinamide Adenine Dinucleotide Phosphate (NADPH) Oxidase and Apocynin Analogues by Docking Method. *Int J Mol Sci* **14**(1)**:** 807-817.

Johnson DK, Schillinger KJ, Kwait DM, Hughes CV, McNamara EJ, Ishmael F*, et al.* (2002). Inhibition of NADPH oxidase activation in endothelial cells by ortho-methoxy-substituted catechols. *Endothelium* **9**(3)**:** 191-203.

Jorgensen LH, Blain A, Greally E, Laval SH, Blamire AM, Davison BJ*, et al.* (2011). Long-term blocking of calcium channels in mdx mice results in differential effects on heart and skeletal muscle. *Am J Pathol* **178**(1)**:** 273-283.

Jung C, Martins AS, Niggli E, Shirokova N (2008). Dystrophic cardiomyopathy: amplification of cellular damage by Ca^{2+} signalling and reactive oxygen species-generating pathways. *Cardiovasc Res* **77**(4)**:** 766-773.

Jung D, Yang B, Meyer J, Chamberlain JS, Campbell KP (1995). Identification and characterization of the dystrophin anchoring site on beta-dystroglycan. *J Biol Chem* **270**(45)**:** 27305-27310.

Jung K, Reszka R (2001). Mitochondria as subcellular targets for clinically useful anthracyclines. *Adv Drug Deliver Rev* **49**(1-2)**:** 87-105.

Kanegae MP, Condino-Neto A, Pedroza LA, de Almeida AC, Rehder J, da Fonseca LM*, et al.* (2010). Diapocynin versus apocynin as pretranscriptional inhibitors of NADPH oxidase and cytokine production by peripheral blood mononuclear cells. *Biochem Biophys Res Commun* **393**(3)**:** 551-554.

Kanegae MP, da Fonseca LM, Brunetti IL, Silva SO, Ximenes VF (2007). The reactivity of ortho-methoxy-substituted catechol radicals with sulfhydryl groups: contribution for the comprehension of the mechanism of inhibition of NADPH oxidase by apocynin. *Biochem Pharmacol* **74**(3)**:** 457-464.

Kanter MM (1994). Free radicals, exercise, and antioxidant supplementation. *Int J Sport Nutr* **4**(3)**:** 205-220.

Khairallah RJ, Shi G, Sbrana F, Prosser BL, Borroto C, Mazaitis MJ*, et al.* (2012). Microtubules underlie dysfunction in duchenne muscular dystrophy. *Sci Signal* **5**(236)**:** ra56.

Kim JA, Neupane GP, Lee ES, Jeong BS, Park BC, Thapa P (2011). NADPH oxidase inhibitors: a patent review. *Expert Opin Ther Pat* **21**(8)**:** 1147-1158.

Kim JH, H.B. K, Lawler JM (2009). The effects of a NAD(P)H oxidase inhibition on matrix metalloproteinases and TIMP-1 in the mdx diaphragm. *Int J Exerc Sci* **2**(1)**:** S36.

Kim JH, Kwak HB, Thompson LV, Lawler JM (2013). Contribution of oxidative stress to pathology in diaphragm and limb muscles with Duchenne muscular dystrophy. *J Muscle Res Cell M* **34**(1)**:** 1-13.

Kim JH, Lawler JM (2012). Amplification of proinflammatory phenotype, damage, and weakness by oxidative stress in the diaphragm muscle of mdx mice. *Free Radic Biol Med* **52**(9)**:** 1597-1606.

Kirschner J, Schessl J, Schara U, Reitter B, Stettner GM, Hobbiebrunken E*, et al.* (2010). Treatment of Duchenne muscular dystrophy with ciclosporin A: a randomised, double-blind, placebo-controlled multicentre trial. *Lancet Neurol* **9**(11)**:** 1053-1059.

Kleniewska P, Piechota A, Skibska B, Goraca A (2012). The NADPH oxidase family and its inhibitors. *Arch Immunol Ther Exp (Warsz)* **60**(4)**:** 277-294.

Koenig M, Hoffman EP, Bertelson CJ, Monaco AP, Feener C, Kunkel LM (1987). Complete cloning of the Duchennne muscular dystrophy (DMD) cDNA and preliminary genomic organization of the DMD gene in normal and affected individuals. *Cell* **50:** 509-517.

Koenig M, Monaco AP, Kunkel LM (1988). The complete sequence of dystrophin predicts a rod-shaped cytoskeletal protein. *Cell* **53:** 219-226.

Konieczny P, Swiderski K, Chamberlain JS (2013). Gene and cell-mediated therapies for muscular dystrophy. *Muscle Nerve* **47**(5)**:** 649-663.

Koren A, Sauber C, Sentjurc M, Schara M (1983). Free radicals in tetanic activity of isolated skeletal muscle. *Comp Biochem Physiol B* **74**(3)**:** 633-635.

Korge P, Byrd SK, Campbell KB (1993). Functional coupling between sarcoplasmic-reticulum-bound creatine kinase and Ca^{2+}-ATPase. *Eur J Biochem* **213**(3)**:** 973-980.

Law PK, Yap JL (1979). New muscle transplant method produces normal twitch tension in dystrophic muscle. *Muscle Nerve.* **2**(5)**:** 356-363.

Lawler JM (2011). Exacerbation of pathology by oxidative stress in respiratory and locomotor muscles with Duchenne muscular dystrophy. *J Physiol* **589**(Pt 9)**:** 2161-2170.

Leberer E, Pette D (1986). Immunochemical quantification of sarcoplasmic reticulum Ca-ATPase, of calsequestrin and of parvalbumin in rabbit skeletal muscles of defined fiber composition. *Eur J Biochem* **156**(3)**:** 489-496.

Leijendekker WJ, Passaquin AC, Metzinger L, Ruegg UT (1996). Regulation of cytosolic calcium in skeletal muscle cells of the *mdx* mouse under conditions of stress. *Br J Pharmacol* **118**(3)**:** 611-616.

Li ZB, Kollias HD, Wagner KR (2008). Myostatin directly regulates skeletal muscle fibrosis. *J Biol Chem* **283**(28)**:** 19371-19378.

Lindahl M, Backman E, Henriksson KG, Gorospe JR, Hoffman EP (1995). Phospolipase A_2 activity in dystrophinopathies. *Neuromuscul Disord* **5**(3)**:** 193-199.

Louis M, Raymackers JM, H. D, Lebacq J, Francaux M (2004). Effect of creatine supplementation on skeletal muscle of mdx mice. *Muscle Nerve* **29**(5)**:** 687-692.

Luchtefeld R, Luo R, Stine K, Alt ML, Chernovitz PA, Smith RE (2008). Dose formulation and analysis of diapocynin. *J Agric Food Chem* **56**(2)**:** 301-306.

McHowat J, Swift LM, Arutunyan A, Sarvazyan N (2001). Clinical concentrations of doxorubicin inhibit activity of myocardial membrane-associated, calcium-independent phospholipase A_2. *Cancer Res* **61**(10)**:** 4024-4029.

McHowat J, Swift LM, Crown KN, Sarvazyan NA (2004). Changes in phospholipid content and myocardial calcium-independent phospholipase A_2 activity during chronic anthracycline administration. *J Pharmacol Exp Ther* **311**(2)**:** 736-741.

McNeil PL, Khakee R (1992). Disruptions of muscle fiber plasma membranes. Role in exercise-induced damage. *Am J Pathol* **140**(5)**:** 1097-1109.

Mendell JR, Kissel JT, Amato AA, King W, Signore L, Prior TW*, et al.* (1995). Myoblast transfer in the treatment of Duchenne's muscular dystrophy. *N Engl J Med* **333**(13)**:** 832-838.

Meregalli M, Farini A, Parolini D, Maciotta S, Torrente Y (2010). Stem cell therapies to treat muscular dystrophy: progress to date. *BioDrugs* **24**(4)**:** 237-247.

Mesa LE, Dubrovsky AL, Corderi J, Marco P, Flores D (1991). Steroids in Duchenne muscular dystrophy--deflazacort trial. *Neuromuscul Disord* **1:** 261-266.

Metzinger L, Passaquin AC, Leijendekker WJ, Poindron P, Ruegg UT (1995). Modulation by prednisolone of calcium handling in skeletal muscle cells. *Br J Pharmacol* **116**(7)**:** 2811-2816.

Millay DP, Goonasekera SA, Sargent MA, Maillet M, Aronow BJ, Molkentin JD (2009). Calcium influx is sufficient to induce muscular dystrophy through a TRPC-dependent mechanism. *Proc Natl Acad Sci USA* **106**(45)**:** 19023-19028.

Mofarrahi M, Brandes RP, Gorlach A, Hanze J, Terada LS, Quinn MT*, et al.* (2008). Regulation of proliferation of skeletal muscle precursor cells by NADPH oxidase. *Antioxid Redox Signal* **10**(3)**:** 559-574.

Moizard MP, Toutain A, Fournier D, Berret F, Raynaud M, Billard C*, et al.* (2000). Severe cognitive impairment in DMD: obvious clinical indication for Dp71 isoform point mutation screening. *Eur J Hum Genet* **8**(7)**:** 552-556.

Monaco AP, Kunkel LM (1988). Cloning of the Duchenne/Becker muscular dystrophy locus. *Adv Hum Genet.* **17:** 61-98.

Monet M, Gkika D, Lehen'kyi V, Pourtier A, Vanden Abeele F, Bidaux G*, et al.* (2009). Lysophospholipids stimulate prostate cancer cell migration via TRPV2 channel activation. *Biochim Biophys Acta* **1793**(3)**:** 528-539.

Moopanar TR, Allen DG (2006). The activity-induced reduction of myofibrillar Ca^{2+} sensitivity in mouse skeletal muscle is reversed by dithiothreitol. *J Physiol* **571**(Pt 1)**:** 191-200.

Moxley RT, Brooke MH, Fenichel GM, Mendell JR, Griggs RC, Miller JP*, et al.* (1987). Clinical investigation in Duchenne dystrophy. VI. Double-blind controlled trial of nifedipine. *Muscle Nerve* **10:** 22-33.

Murphy ME, Kehrer JP (1986). Free radicals: a potential pathogenic mechanism in inherited muscular dystrophy. *Life Sci* **39**(24)**:** 2271-2278.

Nakae Y, Dorchies OM, Stoward PJ, Zimmermann BF, Ritter C, Ruegg UT (2012). Quantitative evaluation of the beneficial effects in the mdx mouse of epigallocatechin gallate, an antioxidant polyphenol from green tea. *Histochem Cell Biol* **137**(6)**:** 811-827.

Nguyen MV, Lardy B, Rousset F, Hazane-Puch F, Zhang L, Trocme C*, et al.* (2013). Quinone compounds regulate the level of ROS production by the NADPH oxidase Nox4. *Biochem Pharmacol* **85**(11)**:** 1644-1654.

Niebroj-Dobosz I, Hausmanowa-Petrusewicz I (2005). The involvement of oxidative stress in determining the severity and progress of pathological processes in dystrophin-deficient muscles. *Acta Biochim Pol* **52**(2)**:** 449-452.

Odom GL, Gregorevic P, Chamberlain JS (2007). Viral-mediated gene therapy for the muscular dystrophies: Successes, limitations and recent advances. *Biochim Biophys Acta* **1772**(2)**:** 243-262.

Orrenius S, Zhivotovsky B, Nicotera P (2003). Regulation of cell death: the calcium-apoptosis link. *Nat Rev Mol Cell Biol* **4**(7)**:** 552-565.

Pan Y, Chen C, Shen Y, Zhu CH, Wang G, Wang XC*, et al.* (2008). Curcumin alleviates dystrophic muscle pathology in mdx mice. *Mol Cells* **25**(4)**:** 531-537.

Paolini C, Fessenden JD, Pessah IN, Franzini-Armstrong C (2004). Evidence for conformational coupling between two calcium channels. *Proc Natl Acad Sci USA* **101**(34)**:** 12748-12752.

Parekh AB, Putney JW, Jr. (2005). Store-operated calcium channels. *Physiol Rev* **85**(2)**:** 757-810.

Partridge TA, Morgan JE, Coulton GR, Hoffman EP, Kunkel LM (1989). Conversion of mdx myofibres from dystrophin-negative to -positive by injection of normal myoblasts. *Nature* **337**(6203)**:** 176-179.

Passaquin A, Renard M, Kay L, Challet C, Mokhtarian A, Wallimann T*, et al.* (2002). Creatine supplementation reduces skeletal muscle degeneration and enhances mitochondrial function in mdx mice. *Neuromuscul Disord* **12**(2)**:** 174-182.

Passaquin AC, Lhote P, Ruegg UT (1998). Calcium influx inhibition by steroids and analogs in C2C12 skeletal muscle cells. *Br J Pharmacol* **124**(8)**:** 1751-1759.

Patel K, Amthor H (2005). The function of Myostatin and strategies of Myostatin blockade-new hope for therapies aimed at promoting growth of skeletal muscle. *Neuromuscul Disord* **15**(2)**:** 117-126.

Petrof BJ, Shrager JB, Stedman HH, Kelly AM, Sweeney HL (1993). Dystrophin protects the sarcolemma from stresses developed during muscle contraction. *Proc Natl Acad Sci USA* **90**(8)**:** 3710-3714.

Pinset C, Mulle C, Benoit P, Changeux JP, Chelly J, Gros F*, et al.* (1991). Functional adult acetylcholine receptor develops independently of motor innervation in Sol 8 mouse muscle cell line. *EMBO J* **10**(9)**:** 2411-2418.

Pozzan T, Rizzuto R (2000). High tide of calcium in mitochondria. *Nat Cell Biol* **2:** 25-27.

Prosser BL, Khairallah RJ, Ziman AP, Ward CW, Lederer WJ (2012). X-ROS signaling in the heart and skeletal muscle: Stretch-dependent local ROS regulates $[Ca^{2+}]_i$. *J Mol Cell Cardiol* **58:** 172-881.

Quinn MT, Ammons MC, Deleo FR (2006). The expanding role of NADPH oxidases in health and disease: no longer just agents of death and destruction. *Clin Sci (Lond)* **111**(1)**:** 1-20.

Rabkin SW, Sunga P (1987). The effect of doxorubicin (adriamycin) on cytoplasmic microtubule system in cardiac cells. *J Mol Cell Cardiol* **19**(11)**:** 1073-1083.

Radley HG, Davies MJ, Grounds MD (2008). Reduced muscle necrosis and long-term benefits in dystrophic mdx mice after cV1q (blockade of TNF) treatment. *Neuromuscul Disord* **18**(3)**:** 227-238.

Ragusa RJ, Chow CK, Porter JD (1997). Oxidative stress as a potential pathogenic mechanism in an animal model of Duchenne muscular dystrophy. *Neuromuscul Disord* **7**(6-7)**:** 379-386.

Rasola A, Bernardi P (2007). The mitochondrial permeability transition pore and its involvement in cell death and in disease pathogenesis. *Apoptosis* **12**(5)**:** 815-833.

Reddy PA, Anandavalli TE, Anandaraj MP (1986). Calcium activated neutral proteases (milli- and micro-CANP) and endogenous CANP inhibitor of muscle in Duchenne muscular dystrophy (DMD). *Clin Chim Acta* **160**(3)**:** 281-288.

Reggiani C (2008). Between channels and tears: aim at ROS to save the membrane of dystrophic fibres. *J Physiol* **586**(7)**:** 1779.

Reid MB (2008). Free radicals and muscle fatigue: Of ROS, canaries, and the IOC. *Free Radic Biol Med* **44**(2)**:** 169-179.

Reid MB (2001). Plasticity in skeletal, cardiac, and smooth muscle: Redox modulation of skeletal muscle contraction: what we know and what we don't. *J Appl Physiol* **90**(2)**:** 724-731.

Reid MB, Stokic DS, Koch SM, Khawli FA, Leis AA (1994). *N*-acetylcysteine inhibits muscle fatigue in humans. *J Clin Invest* **94**(6)**:** 2468-2474.

Renganathan M, Messi ML, Delbono O (1998). Overexpression of IGF-1 Exclusively in Skeletal Muscle Prevents Age-related Decline in the Number of Dihydropyridine Receptors. *J Biol Chem* **273**(44)**:** 28845-28851.

Reutenauer-Patte J, Boittin FX, Patthey-Vuadens O, Ruegg UT, Dorchies OM (2012). Urocortins improve dystrophic skeletal muscle structure and function through both PKA- and Epac-dependent pathways. *Am J Pathol* **180**(2)**:** 749-762.

Reutenauer J, Dorchies OM, Patthey-Vuadens O, Vuagniaux G, Ruegg UT (2008). Investigation of Debio 025, a cyclophilin inhibitor, in the dystrophic mdx mouse, a model for Duchenne muscular dystrophy. *Br J Pharmacol* **155**(4)**:** 574-584.

Rey FE, Cifuentes ME, Kiarash A, Quinn MT, Pagano PJ (2001). Novel competitive inhibitor of NAD(P)H oxidase assembly attenuates vascular O_2^- and systolic blood pressure in mice. *Circ Res* **89**(5)**:** 408-414.

Riganti C, Gazzano E, Polimeni M, Costamagna C, Bosia A, Ghigo D (2004). Diphenyleneiodonium inhibits the cell redox metabolism and induces oxidative stress. *J Biol Chem* **279**(46)**:** 47726-47731.

Rios E, Brum G (1987). Involvement of dihydropyridine receptors in excitation–contraction coupling in skeletal muscle. *Nature* **325**(6106)**:** 717-720.

Rizzuto R, Simpson AW, Brini M, Pozzan T (1992). Rapid changes of mitochondrial Ca^{2+} revealed by specifically targeted recombinant aequorin. *Nature* **358**(6384)**:** 325-327.

Rodino-Janeiro BK, Paradela-Dobarro B, Castineiras-Landeira MI, Raposeiras-Roubin S, Gonzalez-Juanatey JR, Alvarez E (2013). Current status of NADPH oxidase research in cardiovascular pharmacology. *Vasc Health Risk Manag* **9:** 401-428.

Rodriguez C, Tranopolsky MA (2003). Patients with dystrophinopathy show evidence of increased oxidative stress. *Free Radic. Biol. Med.* **34**(9)**:** 1217-1220.

Ronis MJ, Sharma N, Vantrease J, Borengasser SJ, Ferguson M, Mercer KE*, et al.* (2013). Female mice lacking p47phox have altered adipose tissue gene expression and are protected against high fat-induced obesity. *Physiol Genomics* **45**(9)**:** 351-366.

Rossi AM, Eppenberger HM, Volpe P, Cotrufo R, Wallimann T (1990). Muscle-type MM creatine kinase is specifically bound to sarcoplasmic reticulum and can support Ca^{2+} uptake and regulate local ATP/ADP ratios. *J Biol Chem* **265**(9)**:** 5258-5266.

Ruegg JC (1992). Calcium in muscle contraction: cellular and molecular physiology. 2nd edn. Springer-Verlag: Berlin.

Ruegg UT (2013). Pharmacological prospects in the treatment of Duchenne muscular dystrophy. *Curr Opin Neurol* **26**(5)**:** 577-584.

Ruegg UT, Shapovalov G, Jacobson K, Reutenauer-Patte J, Ismail HM, Dorchies OM*, et al.* (2012). Store-operated channels and Ca^{2+} handling in muscular dystrophy. In: *Store-operated Ca^{2+} entry (SOCE) pathways*, Groschner K, Graier WF, Romanin C (eds) Vol. 1, pp 449-457: SpringerWien.

Sakellariou GK, Jackson MJ, Vasilaki A (2013a). Redefining the major contributors to superoxide production in contracting skeletal muscle. The role of NAD(P)H oxidases. *Free Radic Res* **In press**.

Sakellariou GK, Vasilaki A, Palomero J, Kayani A, Zibrik L, McArdle A*, et al.* (2013b). Studies of mitochondrial and nonmitochondrial sources implicate nicotinamide adenine dinucleotide phosphate oxidase(s) in the increased skeletal muscle superoxide generation that occurs during contractile activity. *Antioxid Redox Sign* **18**(6)**:** 603-621.

Schiaffino S, Reggiani C (1996). Molecular diversity of myofibrillar proteins: gene regulation and functional significance. *Physiol Rev* **76**(2)**:** 371-423.

Segal BH, Grimm MJ, Khan AN, Han W, Blackwell TS (2012). Regulation of innate immunity by NADPH oxidase. *Free Radic Biol Med* **53**(1)**:** 72-80.

Selsby JT (2011). Increased catalase expression improves muscle function in mdx mice. *Exp Physiol* **96**(2)**:** 194-202.

Serysheva II, Hamilton SL, Chiu W, Ludtke SJ (2005). Structure of Ca^{2+} release channel at 14 A resolution. *J Mol Biol* **345**(3)**:** 427-431.

Shin JH, Pan X, Hakim CH, Yang HT, Yue Y, Zhang K*, et al.* (2013). Microdystrophin ameliorates muscular dystrophy in the canine model of duchenne muscular dystrophy. *Mol Ther* **21**(4)**:** 750-757.

Shindoh C, DiMarco A, Thomas A, Manubay P, Supinski G (1990). Effect of N-acetylcysteine on diaphragm fatigue. *J Appl Physiol* **68**(5)**:** 2107-2113.

Shkryl VM, Martins AS, Ullrich ND, Nowycky MC, Niggli E, Shirokova N (2009). Reciprocal amplification of ROS and Ca^{2+} signals in stressed mdx dystrophic skeletal muscle fibers. *Pflugers Arch* **458**(5)**:** 915-928.

Simons JM, Hart BA, Ip Vai Ching TR, Van Dijk H, Labadie RP (1990). Metabolic activation of natural phenols into selective oxidative burst agonists by activated human neutrophils. *Free Radic Biol Med* **8**(3)**:** 251-258.

Sorce S, Krause KH, Jaquet V (2012). Targeting NOX enzymes in the central nervous system: therapeutic opportunities. *Cell Mol Life Sci* **69**(14)**:** 2387-2407.

Sparagna GC, Gunter KK, Sheu S, Gunter TE (1995). Mitochondrial calcium uptake from physiological-type pulses of calcium. A description of the rapid uptake mode. *J Biol Chem* **270**(46)**:** 27510-27515.

Spencer MJ, Croall DE, Tidball JG (1995). Calpains are activated in necrotic fibers from mdx dystrophic mice. *J Biol Chem* **270**(18)**:** 10909-10914.

Spencer MJ, Mellgren RL (2002). Overexpression of a calpastatin transgene in mdx muscle reduces dystrophic pathology. *Hum Mol Genet* **11**(21)**:** 2645-2655.

Spurney CF, Knoblach S, Pistilli EE, Nagaraju K, Martin GR, Hoffman EP (2008). Dystrophin-deficient cardiomyopathy in mouse: expression of Nox4 and Lox are associated with fibrosis and altered functional parameters in the heart. *Neuromuscul Disord* **18**(5)**:** 371-381.

Spurney CF, Rocha CT, Henricson E, Florence J, Mayhew J, Gorni K*, et al.* (2011). CINRG pilot trial of coenzyme Q10 in steroid-treated Duchenne muscular dystrophy. *Muscle Nerve* **44**(2)**:** 174-178.

St-Pierre SJ, Chakkalakal JV, Kolodziejczyk SM, Knudson JC, Jasmin BJ, Megeney LA (2004). Glucocorticoid treatment alleviates dystrophic myofiber pathology by activation of the calcineurin/NF-AT pathway. *FASEB J* **18**(15)**:** 1937-1939.

Strehler EE, Zacharias DA (2001). Role of alternative splicing in generating isoform diversity among plasma membrane calcium pumps. *Physiol Rev* **81**(1)**:** 21-50.

Suzuki A, Yoshida M, Hayashi K, Mizuno Y, Hagiwara Y, Ozawa E (1994). Molecular organization at the glycoprotein-complex-binding site of dystrophin. Three dystrophin-associated proteins bind directly to the carboxy-terminal portion of dystrophin. *Eur J Biochem* **220**(2)**:** 283-292.

Swift L, McHowat J, Sarvazyan N (2007). Anthracycline-induced phospholipase A_2 inhibition. *Cardiovasc Toxicol* **7**(2)**:** 86-91.

Swift L, McHowat J, Sarvazyan N (2003). Inhibition of membrane-associated calcium-independent phospholipase A_2 as a potential culprit of anthracycline cardiotoxicity. *Cancer Res* **63**(18)**:** 5992-5998.

Talon S, Vallot O, Huchet-Cadiou C, Lompre A, Leoty C (2002). IP_3-induced tension and IP_3-receptor expression in rat soleus muscle during postnatal development. *Am J Physiol Regul Integr Comp Physiol* **282**(4)**:** R1164-1173.

Tarnopolsky MA, Roy BD, MacDonald JR (1997). A randomized, controlled trial of creatine monohydrate in patients with mitochondrial cytopathies. *Muscle Nerve* **20**(12)**:** 1502-1509.

Teraoka K, Hirano M, Yamaguchi K, Yamashina A (2000). Progressive cardiac dysfunction in adriamycin-induced cardiomyopathy rats. *Eur J Heart Fail* **2**(4)**:** 373-378.

Tidball JG, Wehling-Henricks M (2007). The role of free radicals in the pathophysiology of muscular dystrophy. *J Appl Physiol* **102**(4)**:** 1677-1686.

Turner PR, Fong PY, Denetclaw WF, Steinhardt RA (1991). Increased calcium influx in dystrophic muscle. *J Cell Biol* **115**(6)**:** 1701-1712.

Van Norren K, van Helvoort A, Argiles JM, van Tuijl S, Arts K, Gorselink M*, et al.* (2009). Direct effects of doxorubicin on skeletal muscle contribute to fatigue. *Br J Cancer* **100**(2)**:** 311-314.

Vandebrouck A, Ducret T, Basset O, Sebille S, Raymond G, Ruegg U*, et al.* (2006). Regulation of store-operated calcium entries and mitochondrial uptake by minidystrophin expression in cultured myotubes. *FASEB J* **20**(1)**:** 136-138.

Vejrazka M, Micek R, Stipek S (2005). Apocynin inhibits NADPH oxidase in phagocytes but stimulates ROS production in non-phagocytic cells. *Biochim Biophys Acta* **1722**(2)**:** 143-147.

Verhaert D, Richards K, Rafael-Fortney JA, Raman SV (2011). Cardiac involvement in patients with muscular dystrophies: magnetic resonance imaging phenotype and genotypic considerations. *Circ Cardiovasc Imaging* **4**(1)**:** 67-76.

Vetter SW, Leclerc E (2003). Novel aspects of calmodulin target recognition and activation. *Eur J Biochem* **270**(3)**:** 404-414.

Wagner K, Hamed S, Hadley D, Gropman A, Burstein A, Escolar D*, et al.* (2001). Gentamicin treatment of Duchenne and Becker muscular dystrophy due to nonsense mutations. *Ann Neurol* **49**(6)**:** 706-711.

Wagner KR, Liu X, Chang X, Allen RE (2005). Muscle regeneration in the prolonged absence of myostatin. *Proc Natl Acad Sci USA* **102**(7)**:** 2519-2524.

Wagner S, Dorchies OM, Stoeckel H, Warter JM, Poindron P, Takeda K (2003). Functional maturation of nicotinic acetylcholine receptors as an indicator of murine muscular differentiation in a new nerve-muscle co-culture system. *Pflugers Arch* **447**(1)**:** 14-22.

Wang Q, Smith RE, Luchtefeld R, Sun AY, Simonyi A, Luo R*, et al.* (2008). Bioavailability of apocynin through its conversion to glycoconjugate but not to diapocynin. *Phytomedicine* **15**(6-7)**:** 496-503.

Weir EK, Wyatt CN, Reeve HL, Huang J, Archer SL, Peers C (1994). Diphenyliodonium inhibits both pottasium and calcium currents in isolated pulmonary-artery smooth-muscle cells. *J Appl Physiol* **76**(6)**:** 2611-2615.

Welch EM, Barton ER, Zhuo J, Tomizawa Y, Friesen WJ, Trifillis P*, et al.* (2007). PTC124 targets genetic disorders caused by nonsense mutations. *Nature* **447**(7140)**:** 87-91.

Whitehead NP, Pham C, Gervasio OL, Allen DG (2008). N-Acetylcysteine ameliorates skeletal muscle pathophysiology in mdx mice. *J Physiol* **586**(7)**:** 2003-2014.

Whitehead NP, Streamer M, Lusambili LI, Sachs F, Allen DG (2006). Streptomycin reduces stretch-induced membrane permeability in muscles from mdx mice. *Neuromuscul Disord* **16**(12)**:** 845-854.

Whitehead NP, Yeung EW, Froehner SC, Allen DG (2010). Skeletal muscle NADPH oxidase is increased and triggers stretch-induced damage in the mdx mouse. *PLoS One* **5**(12)**:** e15354.

Wilton SD, Fletcher S (2008). Exon skipping and Duchenne muscular dystrophy: Hope, hype and how feasible? *Neurol India* **56**(3)**:** 254-262.

Wind S, Beuerlein K, Eucker T, Muller H, Scheurer P, Armitage ME*, et al.* (2010). Comparative pharmacology of chemically distinct NADPH oxidase inhibitors. *Br J Pharmacol* **161**(4)**:** 885-898.

Winstead MV, Balsinde J, Dennis EA (2000). Calcium-independent phospholipase A(2): structure and function. *Biochim Biophys Acta* **1488**(1-2)**:** 28-39.

Wolf MB, Baynes JW (2006). The anti-cancer drug, doxorubicin, causes oxidant stress-induced endothelial dysfunction. *Biochim Biophys Acta* **1760**(2)**:** 267-271.

Wuytack F, Raeymaekers L, De Smedt H, Eggermont JA, Missiaen L, Van Den Bosch L*, et al.* (1992). Ca^{2+}-Transport ATPases and Their Regulation in Muscle and Brain. *Ann N Y Acad Sci* **671**(Ion-Motive ATPases: Structure, Function, and Regulation)**:** 82-91.

Xia R, Webb JA, Gnall LL, Cutler K, Abramson JJ (2003). Skeletal muscle sarcoplasmic reticulum contains a NADH-dependent oxidase that generates superoxide. *Am J Physiol* **285**(1)**:** C215-221.

Yano K, Zarain-Herzberg A (1994). Sarcoplasmic reticulum calsequestrins: structural and functional properties. *Mol Cell Biochem* **135**(1)**:** 61-70.

Yasuda S, Townsend D, Michele DE, Favre EG, Day SM, Metzger JM (2005). Dystrophic heart failure blocked by membrane sealant poloxamer. *Nature* **436**(7053)**:** 1025-1029.

Yeung EW, Whitehead NP, Suchyna TM, Gottlieb PA, Sachs F, Allen DG (2005). Effects of stretch-activated channel blockers on $[Ca^{2+}]_i$ and muscle damage in the mdx mouse. *J Physiol* **562**(Pt 2)**:** 367-380.

Yin C, Blayney LM, Anthony Lai F (2005). Physical coupling between ryanodine receptor-calcium release channels. *J Mol Biol* **349**(3)**:** 538-546.

Yoshida M, Ozawa E (1990). Glycoprotein complex anchoring dystrophin to sarcolemma. *J Biochem* **108**(5)**:** 748-752.

Zhang BT, Whitehead NP, Gervasio OL, Reardon TF, Vale M, Fatkin D*, et al.* (2012). Pathways of Ca^{2+} entry and cytoskeletal damage following eccentric contractions in mouse skeletal muscle. *J Appl Physiol* **112**(12)**:** 2077-2086.

Zhang BT, Yeung SS, Allen DG, Qin L, Yeung EW (2008). Role of the calcium-calpain pathway in cytoskeletal damage after eccentric contractions. *J Appl Physiol* **105**(1)**:** 352-357.

Zhi G, Ryder JW, Huang J, Ding P, Chen Y, Zhao Y*, et al.* (2005). Myosin light chain kinase and myosin phosphorylation effect frequency-dependent potentiation of skeletal muscle contraction. *Proc Natl Acad Sci USA* **102**(48)**:** 17519-17524.

Zitt C, Strauss B, Schwarz EC, Spaeth N, Rast G, Hatzelmann A*, et al.* (2004). Potent inhibition of Ca^{2+} release-activated Ca^{2+} channels and T-lymphocyte activation by the pyrazole derivative BTP2. *J Biol Chem* **279**(13)**:** 12427-12437.